

FIXED -  $u$  FINITE - ENERGY  
SUM RULE CALCULATIONS FOR  $\pi$ N SCATTERING  
USING REALISTIC SPECTRAL FUNCTIONS

Thesis for the Degree of Ph. D.

MICHIGAN STATE UNIVERSITY

LAURENCE J. SOWASH

1971

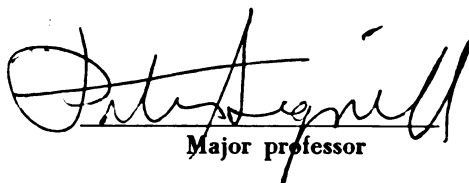


This is to certify that the  
thesis entitled  
FIXED-uFINITE-ENERGY SUM RULE  
CALCULATIONS FOR  $\pi$ N SCATTERING  
USING REALISTIC SPECTRAL FUNCTIONS  
presented by

Laurence J. Sowash

has been accepted towards fulfillment  
of the requirements for

Ph.D. degree in Physics

  
Major professor

Date 3/15/71

## ABSTRACT

### FIXED-u FINITE-ENERGY SUM RULE CALCULATIONS FOR $\pi N$ SCATTERING USING REALISTIC SPECTRAL FUNCTIONS

By

Laurence J. Sowash

Realistic spectral functions have been used to calculate fixed-u Finite Energy Sum Rules (FESR) for  $\pi N$  scattering. The FESR equate positive integral moments of the Regge and low-energy scattering amplitudes. The fixed-u FESR isolate baryon Regge amplitudes which dominate high-energy backward scattering. The generation of realistic spectral functions involves detailed consideration of t-channel threshold properties. Regge convergence properties implicit in the sum rules are used to choose between available sets of direct channel phase shifts. The FESR are used to fit coupling constants for  $J=0, 1$  mesons. The calculations are extended to higher moments than possible in previous calculations.

FIXED-u FINITE-ENERGY SUM RULE  
CALCULATIONS FOR  $\pi$ N SCATTERING  
USING REALISTIC SPECTRAL FUNCTIONS

By

Laurence J. <sup>10-2-71</sup>Sowash

A THESIS

Submitted to  
Michigan State University  
in partial fulfillment of the requirements  
for the degree of

DOCTOR OF PHILOSOPHY

Department of Physics

1971

## ACKNOWLEDGMENTS

My special thanks go to Professor Peter Signell for suggesting this project and encouraging and guiding these efforts. Professors Jules Kovacs, Joseph Kubis and Dr. Jonas Holdeman were especially helpful.

## TABLE OF CONTENTS

I. INTRODUCTION	1
II. THE FORMAL DESCRIPTION OF $\pi N$ SCATTERING	6
A. Notation and Kinematics	6
B. The Invariant T-Matrix	7
C. Cross Sections	9
D. Partial Wave Amplitudes	10
E. Crossing Symmetry	11
F. Kinematics of Cross-Channel Processes	12
G. The Mandelstam Plane	14
III. $\pi N$ DYNAMICS AND FINITE ENERGY SUM RULES	19
A. The Mandelstam Representation	19
B. The Finite Energy Sum Rules	25
C. The Concept(s) of Duality	28
IV. THE SPECTRAL FUNCTIONS	33
A. The Regge Amplitudes	33
B. The s-channel Spectral Function	38
C. The t-channel Spectral Function	41
D. The Preliminary Spectral Functions	49
E. Transforming the Partial Wave Series	59
V. RESULTS AND DISCUSSION	71
A. The Finite Energy Sum Rules	71
B. The $N_{\pi}$ and $N_{\pi}$ FESR	72
C. The $\Delta$ FESR	78

D. The Cutkosky-Deo Scheme	78
APPENDICES	
A. Generalized Spinor Invariants for $\pi N$ Scattering	81
B. Isotopology of $\pi N$ Scattering	84
C. Invariants in Terms of Partial Waves	88
D. Partial Wave Amplitudes for $\pi\pi \rightarrow N\bar{N}$	93
REFERENCES	97

## LIST OF TABLES

Table	Page
1. The baryon trajectories and their quantum numbers.	36
2. Quantum numbers and coupling constants of the zero-width mesons.	46
3. Quantum numbers and parameters of the finite-width mesons.	50



## LIST OF FIGURES

Figure	Page
1. The Mandelstam diagram for $\pi N$ scattering.	15
2. The cut $\cos\phi$ Plane for $\pi N$ scattering.	17
3. The region of integration for the FESR.	37
4. The $F_+^N(X,u)$ spectral function near $X = X_0$ .	42
5. The $F_+^A(X,u)$ spectral function near $X = X_0$ .	43
6. The $F_-^N(X,u)$ spectral function at $u = 0$ .	52
7. The $F_-^A(X,u)$ spectral function at $u = 0$ .	53
8. The $F_-^N(X,u)$ spectral function at $u = 1.0 \text{ GeV}^2$ .	54
9. The $F_+^N(X,u)$ spectral function at $u = 1.0 \text{ GeV}^2$ .	55
10. The $F_-^A(X,u)$ spectral function at $u = 1.0 \text{ GeV}^2$ .	56
11. The $F_+^A(X,u)$ spectral function at $u = 1.0 \text{ GeV}^2$ .	57
12. Intersection of the Lehmann Ellipse and the Mandelstam plane.	61
13. Graph of $x$ versus $z$ at $W = 1.1 \text{ GeV}$ . in the $s$ channel.	66
14. Graph of $x$ versus $z$ at $W = 1.8 \text{ GeV}$ . in the $s$ channel.	66
15. Graph of $x$ versus $z$ in the $t$ channel at $t = 4.125$ .	66
16. The $F_+^N(X,z)$ spectral function at $u = 1.0 \text{ GeV}^2$ . generated from transformed partial wave amplitudes.	68
17. The $F_+^N(X,z)$ spectral function at $u = 1.0 \text{ GeV}^2$ generated by expanding $x$ in terms of polynomials in $z$ .	70
18. The $n = 1$ $N_{\alpha}$ and $N_{\beta}$ FESR.	73
19. The $n = 3$ $N_{\alpha}$ and $N_{\beta}$ FESR.	74

20. The $n=5$ $N_{u\bar{u}}$ , and $N_{d\bar{d}}$ FESR.	75
21. The contributions of each of Barger's zero-width mesons to the $n=1$ $N_{u\bar{u}}$ FESR.	77
22. The low-energy terms for the $n=0, 1, 2, \Delta_8$ FESR.	79
23. The low-energy terms for the $n=3, 4, 5, \Delta_8$ FESR.	79

## INTRODUCTION

Finite energy sum rules are a development of the description of strong interaction processes by integral equations for scattering amplitudes. This description is derived from Quantum Field Theory as embodied in perturbation theory and Feynman graph techniques.

Mandelstam demonstrated that perturbation theory as applied to two-particle interactions was equivalent to a two-dimensional integral representation of the scattering amplitude. This representation is not complete since only a few basic properties of the spectral function (the integrand of the two-dimensional integral) can be established a priori. For this reason one cannot speak of 'solutions' to the Mandelstam representation (nor, as we shall see, to finite energy sum rules). However, these equations do serve as very strong constraints on the form the scattering amplitude can take.

The Mandelstam representation exhibits the scattering amplitude in the form of an integral which explicitly satisfies the Pauli principle and Crossing symmetry. It is one of the basic features of S-matrix theory that the scattering amplitude is viewed as an analytic function of energy and momentum-transfer variables, defined by its analytic structure and basic symmetry considerations rather than through any connection with underlying 'fields'.

In the Mandelstam representation the scattering amplitude describing some process  $a + b \rightarrow c + d$  has singularities (poles or branch cuts) at

the allowed physical energies of any initial or final state in each of its respective 'channels', as well as poles corresponding to intermediate bound states. The separate channels of a reaction are generated by interchanging an initial and final state particle. Interchanged particles become antiparticles and vice versa. The respective channels are labeled by the appropriate Mandelstam variables corresponding to the center of mass energy squared for that channel.

In  $\pi N$  scattering we consider three channels:

$$\pi + N \longrightarrow \pi + N \quad \text{'s-channel'}$$

$$N + \bar{N} \longrightarrow \bar{\pi} + \pi \quad \text{'t-channel'}$$

$$\bar{\pi} + N \longrightarrow \pi + N \quad \text{'u-channel'}$$

The self-conjugate property of the pion reduces the u-channel to a reaction identical to the s-channel but having a branch cut in a different variable. Crossing symmetry states that these three reactions are described by the same analytic function continued to the appropriate value of s, t, u.

Four scattering amplitudes are in fact required to describe  $\pi N$  scattering, since there are two allowed spin states and two allowed isotopic spin states in each channel. Each of these amplitudes has its separate Mandelstam representation. The details of these spin and isospin complications will be dealt with in chapters II and III. For the present we shall speak of a single 'scalar' amplitude  $F(s,t,u)$ , neglecting spin and isospin. The Mandelstam representation of  $F(s,t,u)$  has the form

$$F(s,t,u) = \frac{1}{\pi^2} \int_{(m+\mu)^2}^{\infty} d\epsilon' \int_{4\mu^2}^{\infty} dt' \frac{\alpha_1(\epsilon', t')}{(\epsilon' - s)(t' - t)} + \frac{1}{\pi^2} \int_{4\mu^2}^{\infty} dt' \int_{(m+\mu)^2}^{\infty} du' \frac{\alpha_2(t', u')}{(t' - t)(u' - u)} \quad (1.1)$$

$$+ \frac{1}{\pi} \int_{(m+\mu)^2}^{\infty} ds' \int_{(m+\mu)^2}^{\infty} du' \frac{d_2(s', u')}{(s'-s)(u'-u)}$$

We have omitted the pole at the nucleon mass from  $F(s, t, u)$ . Further, assuming that  $F(s, t, u)$  has even rather than odd parity under Crossing, Eq. (1.1) could be reduced to

$$F(s, t, u) = \frac{1}{\pi} \int_{(m+\mu)^2}^{\infty} ds' \operatorname{Im} F(s', t) \left\{ \frac{1}{s'-s} + \frac{1}{s'-u} \right\} ds' + \frac{1}{\pi} \int_{4\mu^2}^{\infty} dt' \operatorname{Im} F(t', s) \frac{1}{t'-t} \quad (1.2)$$

This is the so-called one-dimensional form of the Mandelstam representation, the form used in most calculations.

As required, the cuts in  $s$  and  $u$  obviously extend from  $(m+\mu)^2$  to infinity and the cut in  $t$  extends from  $4\mu^2$  to infinity, even though the process  $N\bar{N} \rightarrow \pi\pi$  cannot physically occur on the low energy portion of the cut  $4\mu^2 \leq t \leq 4m^2$ . This unphysical cut has received a great deal of attention in the context of the Mandelstam representation. This attention was warranted by the connection between the process  $N\bar{N} \rightarrow \pi\pi$  and the electromagnetic structure of the nucleon. The nucleon isovector form factors  $F_{1,2}^V(t)$  (the 'structure constants' for electron-nucleon scattering) can be represented in the form of dispersion relations as

$$F_{1,2}^V(t) = \frac{1}{\pi} \int_{4\mu^2}^{\infty} \frac{\operatorname{Im} F_{1,2}^V(t')}{t'-t} dt' \quad (1.3)$$

The spectral functions  $\operatorname{Im} F_{1,2}^V(t)$  contain linear combinations of  $J = 1$   $N\bar{N} \rightarrow \pi\pi$  partial wave amplitudes and are proportional to the pion form factor. One of the earliest successes of the Mandelstam

representation was to help establish the existence of the rho-meson by combining equations similar to (1.2) and (1.3) with information on nucleon resonances and data on the form factors. Similar calculations also yield information on  $\pi\pi$  elastic scattering phase shifts.

Lack of complete knowledge on the high energy behavior of scattering amplitudes has limited attempts to apply the Mandelstam representation over any very wide range of energies. This difficulty is enhanced by the fact that the energy denominators in (1.2) suppress the effects of the high-energy states. Further, cuts extending to infinity often make it impossible to evaluate the contributions of terms in the amplitude which do not converge rapidly at high energy.

Alternate forms of integral constraints on the scattering amplitude have been proposed recently. One form which avoids the mathematical difficulties inherent in the Mandelstam representation while still serving many of the same purposes is the so-called Finite Energy Sum Rule (FESR). The FESRs we have investigated were first studied by Barger, Michael, and Phillips, and take the form of moments of the scattering amplitude

$$\int_{-x_0}^{x_0} X^n \operatorname{Im} F_{\text{Regge}}(X, u) dX = \int_{-x_0}^{x_0} X^n \operatorname{Im} F(X, u) dX$$

In this equation  $F_{\text{Regge}}(X, u)$  is the asymptotic form of the amplitude  $F(X, u)$  beyond the energy at which the amplitude becomes Reggeized.

$X_0$  is the value of the coordinate  $X$  at which this 'matching' takes place. The coordinate  $X$  is defined such that high-energy states occur at large positive and negative values of  $X$ . Thus the FESR enhances the effects of high-energy terms (near  $\pm X_0$ ). In chapter III we show that these equations can at least be understood (if not derived) in the context

of the Mandelstam representation despite their radically different appearance.

The Regge amplitudes which appear in these fixed-u FESR are generated by baryon Regge exchange. Baryon exchange describes  $\pi N$  scattering in the backward direction at high energies just as meson Regge exchange describes high energy  $\pi N$  scattering in the forward direction as energy increases along lines of fixed  $t$ .

We will not be concerned with the ambiguities which still remain in determining the continuation of baryon Regge amplitudes to low energy, but will simply use forms appropriate to high energy data analysis.

Part of our approach to implementing the FESR is to develop a parameterization of the meson resonances which is more realistic than the simple zero-width pole approximation frequently encountered in dispersion relations. We take resonance widths and threshold properties into account in as realistic a fashion as possible so as to generate a continuous  $t$ -channel amplitude whose relation to the Regge amplitude near  $X_0$  can be examined in detail. This is an improvement over previous calculations which did not generate a continuous spectral function. In addition we examine the behavior of the  $s$ -channel amplitude near  $X_0$  in order to select the best set of phase shifts to describe the process. This approach allows us to satisfy higher moments of the sum rules in cases in which previous calculations were reasonable only for the lowest ( $n=0$  or  $1$ ) moments.

THE FORMAL DESCRIPTION OF  $\pi$ -N SCATTERINGA. Notation and Kinematics

Pion and nucleon mass will be labeled  $\mu$  ( $\approx .1396$  GeV) and  $m$  ( $\approx .9382$  GeV) respectively<sup>(1)</sup>. Initial and final states will be subscripted 1, 2 respectively. Pion and nucleon 4-momenta are denoted by  $q$  and  $p$ . Momentum-energy conservation in the process  $\pi_1 + N_1 \rightarrow \pi_2 + N_2$  is then expressed

$$q_1 + p_1 = q_2 + p_2 \quad (2.1)$$

In general we will operate in the center of mass system, in which

$$\begin{aligned} \vec{q}_1 &= -\vec{p}_1 = \vec{k} \\ \vec{q}_2 &= -\vec{p}_2 = \vec{k}' \\ |\vec{k}| &= |\vec{k}'| \equiv k \end{aligned}$$

Now, letting any 3-momentum  $\vec{k}$  define a coordinate axis, all 4-momenta are determined by specifying  $k$ , the "C. M. momentum" and  $\cos \theta \equiv \vec{k} \cdot \vec{k}' / k^2$  the "scattering angle".

If we wish to specify the scattering amplitude which describes the interaction as a function  $F(q_1, q_2, p_1, p_2)$  it is sufficient to regard it as a function of the two variables  $k, \cos \theta$  or any equivalent set. In order to define a Lorentz-invariant scattering amplitude it is customary to construct the invariants<sup>(2)</sup>



$$s \equiv -(p_1 + q_1)^2 = +2\mu^2 + 2m^2 - t - u = W^2 \quad (2.2)$$

$$t \equiv -(q_1 - q_2)^2 = -2k^2(1 - \cos\theta) \quad (2.3)$$

$$u \equiv -(p_2 - q_2)^2 = (E_k - \omega_k)^2 - 2k^2(1 + \cos\theta) \quad (2.4)$$

where:  $E_k \equiv \sqrt{k^2 + m^2}$  = initial and final nucleon energy,

$\omega_k \equiv \sqrt{k^2 + \mu^2}$  = initial and final pion energy,

$W$  = center of mass total energy.

Only two of these variables can be regarded as independent since

$$s + t + u = 2m^2 + 2\mu^2 \quad (2.5)$$

### B. The Invariant T-matrix

To determine the most general scalar invariant form of the scattering operator in nucleon spinor space we could write,

$$\begin{aligned} F = & f_0(k, \cos\theta) + \sum_i \gamma \cdot p_i f_i(k, \cos\theta) + \gamma \cdot q_i g_i(k, \cos\theta) \\ & + \sum_{i,j} \gamma \cdot p_i \gamma \cdot q_j f_{ij}(k, \cos\theta) \\ & + \dots \end{aligned}$$

forming an infinite set of spinor operators by constructing all possible higher-ordered products. The Dirac equation:

$$(\gamma \cdot p + m) u(p) = 0$$

can be used to eliminate the terms linear in nucleon momentum. This

fact, together with Eq. (2.1), shows that the terms linear in pion momentum are not independent. The quadratic and higher-ordered terms can all be shown to be equivalent to a spinor-independent function plus a term linear in either pion momentum (Appendix A). The conventional choice is:

$$F(k, \cos\theta) = -F_0(k, \cos\theta) + i \gamma \cdot Q F_1(k, \cos\theta)$$

where 
$$Q \equiv \frac{1}{2}(q_1 + q_2)$$

The invariant T-matrix can thus be written:

$$T = -A(k, \cos\theta) + i \gamma \cdot Q B(k, \cos\theta) \quad (2.6)$$

T is related to the S-matrix by:

$$S_{fi} = \delta_{fi} - (2\pi)^4 i \delta(q_1 + p_1 - q_2 - p_2) \left( \frac{m_1}{\tau_1 \tau_2 \omega_1 \omega_2} \right)^{\frac{1}{2}} \bar{u}_2 T u_1 \quad (2.7)$$

where:  $\bar{u}_2, u_1$  are nucleon spinors for initial and final nucleons.

$\delta_{fi}$  is the 'no scattering' Delta-function, f and i denoting final and initial states.

A and B are also matrices in isotopic-spin space. In the so-called 'numbered' pion representation,

$$A = A^{(\alpha)}(\Delta, t, u) \delta_{\alpha\beta} + \frac{1}{2} [\tau_u, \tau_\beta] A^{(\alpha)}(\Delta, t, u) \quad (2.8)$$

$$B = B^{(\alpha)}(\Delta, t, u) \delta_{\alpha\beta} + \frac{1}{2} [\tau_u, \tau_\beta] B^{(\alpha)}(\Delta, t, u)$$

where:  $\alpha, \beta = 1, 2, 3$  are the final and initial pion labels.

$\tau_u, \tau_p$  are the nucleon isospin operators.

The details of constructing this representation and relating A and B to matrix elements corresponding to good isospin  $I = 1/2, 3/2$  and the physical scattering processes of  $\pi^+ p$ ,  $\pi^- p$  elastic scattering and charge exchange ( $\pi^+ p \rightarrow \pi^0 n$ ) are presented in Appendix B.

The major results are:

$$\begin{aligned}
 A^{\pi^0 p} &= A^{(+)} - A^{(-)} = A^{(3/2)} \\
 A^{\pi^- p} &= A^{(+)} + A^{(-)} \\
 A^{cex} &= -\sqrt{2} A^{(-)}
 \end{aligned}
 \tag{2.9}$$

$$\begin{aligned}
 A^{1/2} &= A^{(+)} + 2A^{(-)} \\
 A^{3/2} &= A^{(+)} - A^{(-)}
 \end{aligned}
 \tag{2.10}$$

The same relations held for the B amplitudes.

### C. Cross Sections

The cross-section for any process is commonly written

$$\frac{d\sigma}{d\Omega} = |F(k, \cos\theta)|^2
 \tag{2.11}$$

where  $F(k, \cos\theta)$  is the 'scattering amplitude'. The connection between  $F$  and the T-matrix for boson-fermion scattering is

$$F(k, \cos\theta) = -\frac{16\pi^5 m}{W} T(k, \cos\theta)
 \tag{2.12}$$

To compute the elastic cross-section for some isospin state it is necessary to sum (2.11) over initial and final spin states properly normalized. The details are presented in Gasiorowicz<sup>(3)</sup>. The result is,<sup>(4)</sup>

$$\sigma_{\text{total}} = (K^2 - \mu^2)^{-\frac{1}{2}} \text{Im } A'(k, \cos\theta)
 \tag{2.13}$$

$$\frac{d\sigma}{d\Omega} = \frac{m^2}{16\pi^5 k} \left\{ \left(1 - \frac{t}{4m^2}\right) \times |A'(k, \cos\theta)|^2 + \frac{t}{4m^2} \left(1 - \frac{(m+K)^2}{1 - \frac{t}{4m^2}}\right) |B(k, \cos\theta)|^2 \right\}$$

where:

$$A'(k, \cos\theta) = A(k, \cos\theta) + (K + t/4m^2)(1 - t/4m^2)^{-1} B(k, \cos\theta)$$

$$K = (1 - m^2 - \mu^2)/(2m)$$

Here as in (2.11) and (2.12) isospin labels have been suppressed.

#### D. Partial Wave Amplitudes

In order to relate  $A^{(\pm)}$  and  $B^{(\pm)}$  to amplitudes for good  $j, l$  ( $j, l \neq \frac{1}{2}$ ) first define

$$\begin{aligned} f_1^T(k, \cos \theta) &= \sum_{l=0}^{\infty} f_l^T(k) P_{l+1}'(\cos \theta) - \sum_{l=2}^{\infty} f_l^T(k) P_{l-1}'(\cos \theta) \\ f_2^T(k, \cos \theta) &= \sum_{l=1}^{\infty} \{ f_l^T(k) - f_{l-1}^T(k) \} P_l'(\cos \theta) \end{aligned} \quad (2.14)$$

where

$$P_l'(\cos \theta) \equiv \frac{d}{d(\cos \theta)} P_l(\cos \theta)$$

$$f_l^T(k) = \frac{-1}{2k} \{ \eta_l^T e^{2i\delta_l^T} \} \quad \text{are the partial wave amplitudes}$$

for isospin T and  $j = l \pm \frac{1}{2}$ .

Then A, B are related to  $f_1$ ,  $f_2$  by

$$f_1 = \frac{E+m}{8\pi W} \{ A + (W-m)B \} \quad (2.15)$$

$$f_2 = \frac{E-m}{8\pi W} \{ -A + (W+m)B \}$$

The details are presented in Appendix C.

Partial waves can be calculated in terms of invariants by inverting Eq. (2.14), giving,

$$\begin{aligned} f_l^T(k) &= \frac{1}{2} \int_{-1}^1 \{ f_1^T(k, \cos \theta) P_l(\cos \theta) \\ &\quad + f_2^T(k, \cos \theta) P_{l+1}'(\cos \theta) \} d(\cos \theta) \end{aligned} \quad (2.16)$$

### E. Crossing Symmetry

The basic idea of crossing symmetry as applied to pion-nucleon scattering is that the scattering amplitude possesses well-defined properties under the interchange of initial and final nucleons or initial and final pions. In particular, it is observed that under the interchange  $q_1 \leftrightarrow -q_2$  the scattering amplitude<sup>(5)</sup> has the property

$$F(q, p, q, p_2) = F(-q_2 p_1, -q, p_2)$$

While this relation does not relate the amplitude for physical processes (note that the pion energies are negative on the right-hand side), this relation implies that the process

$$\pi_1 + N_1 \rightarrow \pi_2 + N_2$$

is not independent of the process

$$\pi_2 + N_1 \rightarrow \pi_1 + N_2$$

In the foregoing discussion the implicit assumption was made that all quantum numbers of  $\pi_1$  and  $\pi_2$  were interchanged in addition to the initial and final pion momenta. An exact statement of Crossing Symmetry is that the T-matrix must be invariant under the transformation generated by the product of Charge Conjugation and G-parity operators. This imposes on  $A^{(\pm)}$  and  $B^{(\pm)}$  the symmetry requirements,

$$\begin{aligned} A^{(\pm)}(s, t, u) &= \pm A^{(\pm)}(u, t, s) \\ B^{(\pm)}(s, t, u) &= \mp B^{(\pm)}(u, t, s) \end{aligned} \quad (2.17)$$

since the replacements  $q_1 \leftrightarrow -q_2$  and  $p_1 \leftrightarrow -p_2$  each effect the transformation  $s \leftrightarrow u$ ,  $t$  being unchanged (see Eqs. (2.2) - (2.4)).

The square of the Center of Mass total energy of the reaction  $\pi_2 + N_1 \rightarrow \pi_1 + N_2$  is just the Mandelstam variable  $u$ . This leads to the designation 'u-channel process' for the reactions produced from

the direct interaction ('s-channel process') by applying the Crossing relations.

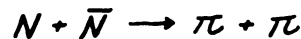
#### F. Kinematics of Cross-Channel Processes

One could begin the analysis of pion-nucleon scattering by labeling the direct channel energy-square 'u' and construct the s-channel amplitudes, if necessary, from Eq. (2.17). Partial wave amplitudes as functions of u-channel momentum  $k_u$  could also be extracted as in equations (2.6) through (2.16), with  $\cos\theta$  replaced by  $\cos\theta_u$ .

However, other processes than those related by the Crossing relations will also be of interest. In particular, consider the reaction generated by interchanging  $q_1$  and  $-p_2$ . Conservation of energy-momentum,

$$p_1 - p_2 = q_2 - q_1$$

now describes the reaction,



It is possible to express the T-matrix in terms of t-channel variables (for this reaction t is the C.M. energy square) as an alternative to (2.14) - (2.16).

To do this first express s, t, u in terms of t-channel variables

$$s = -p^2 - q^2 + 2pq \cos\phi$$

$$t = 4E^2 = 4(p^2 + m^2) = 4(q^2 + \mu^2)$$

$$u = -p^2 - q^2 - 2pq \cos\phi$$

where:  $p$  = magnitude of Nucleon C.M. momentum

$q$  = magnitude of pion C.M. momentum

$\phi$  = t-channel scattering angle.

In terms of  $p$ ,  $q$ ,  $\cos\phi$  we have<sup>(6)</sup>

$$A^{(\pm)}(z, \cos \phi) = \frac{8\pi}{p^2} \sum_j (1 \pm j)(pq)^j \left\{ \frac{m}{\sqrt{j(j+1)}} f_{-}^{(\pm)j}(z) \cos \phi P_j'(\cos \phi) - f_{+}^{(\pm)j}(z) P_j(\cos \phi) \right\} \quad (2.19)$$

$$B^{(\pm)}(z, \cos \phi) = 8\pi \sum_j \frac{(j \pm \frac{1}{2})}{\sqrt{j(j+1)}} (pq)^{j-1} f_{-}^{(\pm)j}(z) P_j'(\cos \phi)$$

The amplitudes  $f_{\pm}^{(\pm)j}(z)$  describe states of total angular momentum  $j$ ; the subscripts  $\pm$  refer to  $N\bar{N}$  states of identical, +, helicity or opposite, -, helicity. The superscripts  $(\pm)$  label amplitudes proportional to states of good t-channel isospin, since

$$A^{(+)} = \frac{1}{\sqrt{2}} A^{(0)} \quad A^{(-)} = \frac{1}{2} A^{(1)} \quad (2.20)$$

These relations hold for  $B^{(\pm)}$  amplitudes as well.

The Pauli principle requires that the (+) isospin amplitudes contain only states of even  $j$  and the (-) amplitudes only states of odd  $j$ .

Equation (2.19) can be inverted to give;

$$f_{+}^{(\pm)j}(z) = \frac{1}{8\pi} \left\{ -\frac{p^2}{(pq)^j} A_j^{(\pm)}(z) + \frac{m}{(2j+1)(pq)^{j-1}} \left[ (j+1) B_{j+1}^{(\pm)}(z) + j B_{j-1}^{(\pm)}(z) \right] \right\} \quad (2.21)$$

$$f_{-}^{(\pm)j}(z) = \frac{1}{8\pi} \frac{\sqrt{j(j+1)}}{2j+1} \frac{1}{(pq)^{j-1}} \left\{ B_{j-1}^{(\pm)}(z) - B_{j+1}^{(\pm)}(z) \right\}$$

where:

$$[A_j^{(\pm)}; B_j^{(\pm)}] \equiv \int_{-1}^{+1} [A^{(\pm)}(z, \cos \phi); B^{(\pm)}(z, \cos \phi)] P_j(\cos \phi) d(\cos \phi)$$

It is convenient for later applications to express  $A^{(\pm)}$ ,  $B^{(\pm)}$  in terms of t-channel partial wave amplitudes  $f_{\ell}^{(\pm)j}(z)$  as well as the helicity amplitudes  $f_{\pm}^{(\pm)j}(z)$ . Here  $\ell$  denotes the orbital angular momentum of the  $N\bar{N}$  system (for the pions,  $s=0$  so that  $j=\ell$ ). The details of the calculation are presented in Appendix D. The major result is;

$$\begin{aligned}
 f_+^{(2)j}(z) &= \frac{1}{\sqrt{2}} \left( \frac{z-1}{2j+1} \right)^{\frac{1}{2}} f_{j-1}^{(2)j}(z) - \frac{1}{\sqrt{2}} \left( \frac{z+1}{2j+1} \right)^{\frac{1}{2}} f_{j+1}^{(2)j}(z) \\
 f_-^{(2)j}(z) &= \frac{1}{\sqrt{2}} \left( \frac{z+1}{2j+1} \right)^{\frac{1}{2}} f_{j-1}^{(2)j}(z) + \frac{1}{\sqrt{2}} \left( \frac{z-1}{2j+1} \right)^{\frac{1}{2}} f_{j+1}^{(2)j}(z)
 \end{aligned} \tag{2.22}$$

Note that no singlet  $N\bar{N}$  states contribute. This is due to parity conservation which in this case requires that  $\ell = j \neq 1$  for the  $N\bar{N}$  states.

#### G. The Mandelstam Plane

The singularity structure of  $\pi N$  scattering can be conveniently represented in 2-dimensional graphic form by using the sides of an equilateral triangle for  $s$ ,  $t$ ,  $u$  axes as in Figure 1. The median is scaled to be of length  $2m^2 + 2\mu^2$  so that the constraint  $s + t + u = 2m^2 + 2\mu^2$  is satisfied.

The  $s$ ,  $t$ ,  $u$ -channel physical regions are labeled. The symmetry of the diagram about the mid-line is just one consequence of Crossing symmetry. Note that the  $t$ -channel threshold for two pions is  $4\mu^2$ , while for two nucleons it is  $4m^2$ . Thus we can think of the  $t$ -channel singularities as extending down to  $4\mu^2$  in the sense that an external state of the  $t$ -channel exists in the region  $4\mu^2 \leq t \leq 4m^2$  even though the process  $\pi\pi \rightarrow N\bar{N}$  cannot physically occur in this region.

The only stable particle intermediate state available to any channel is the nucleon itself, which can appear in the  $s$ - or  $u$ -channel. Such fixed-energy singularities appear as lines in the Mandelstam plane as seen in Figure 1. Note that each nucleon pole occurs below the threshold of its respective channel.

Physical regions for scattering processes are limited not only by energy considerations but also by the physical limits on scattering angles.



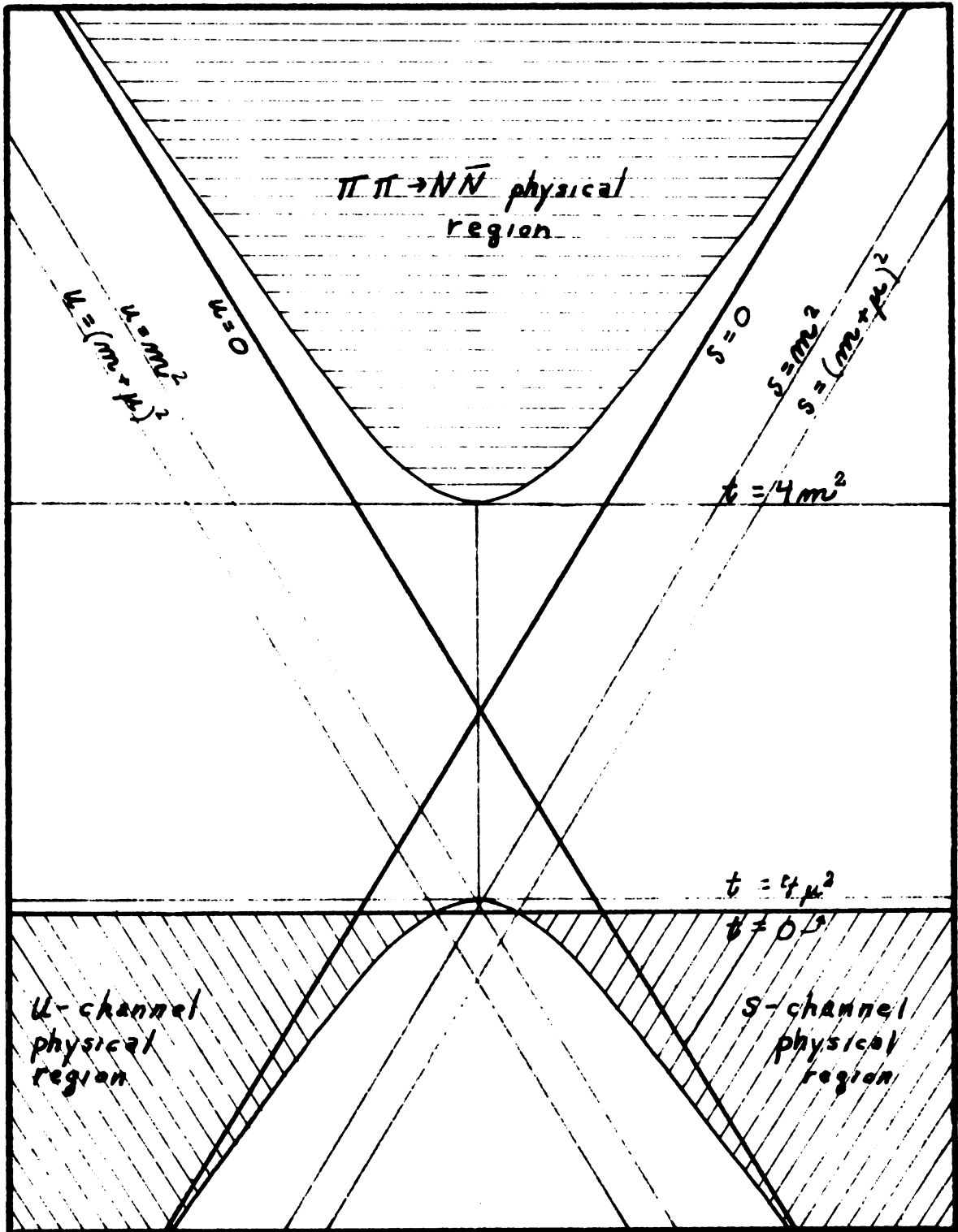


Figure 1. The Mandelstam plane showing the basic cut structure of  $\pi N$  scattering.

The line  $t=0$  corresponds to forward scattering in both  $s$  and  $u$ -channels. Backward scattering in these channels is limited by the curves  $su = (m^2 - \mu^2)^2$ . This curve also limits the  $t$ -channel scattering angle in both the forward and backward directions.

The delineation of the region of physical scattering angle for  $4\mu^2 \leq t \leq 4m^2$  is complicated by the fact that it does not lie exclusively in the Mandelstam plane. In this range of  $t$ , pion momentum  $q$  is real but nucleon momentum  $p$  is pure imaginary. Then the  $t$ -channel scattering angle

$$\cos \phi = \frac{s + p^2 + q^2}{4pq} = -\frac{u^2 + p^2 + q^2}{4pq}$$

can be seen to be pure imaginary for real  $s, u$  (i.e., points in the Mandelstam plane), except for the locus  $s + p^2 + q^2 = 0$  which is the line  $s=u$  in the Mandelstam plane.

In the region  $4\mu^2 \leq t \leq 4m^2$  the condition  $-1 \leq \cos \phi \leq 1$  is equivalent to  $su \leq (m^2 - \mu^2)^2$ . Further, since  $s$  and  $u$  are complex conjugates of one another in this region, this latter inequality is equivalent to  $|s| \leq m^2 - \mu^2$ . The physical region in  $\cos \phi$  then is limited to the interior of a circle of radius  $m^2 - \mu^2$  centered on the origin in the complex  $s$ -plane as shown in Figure 2. The physical regions of  $s, t, u$  channel processes project onto the real axis in the complex  $s$ -plane as shown.

The point behind this detailed discussion of locating physical regions in both energy and angle on the Mandelstam plane should be clear; the evaluation of the scattering amplitude for some arbitrary choice of kinematic variables is typically limited by the fact that no experimental information regarding the process may exist at the corresponding location

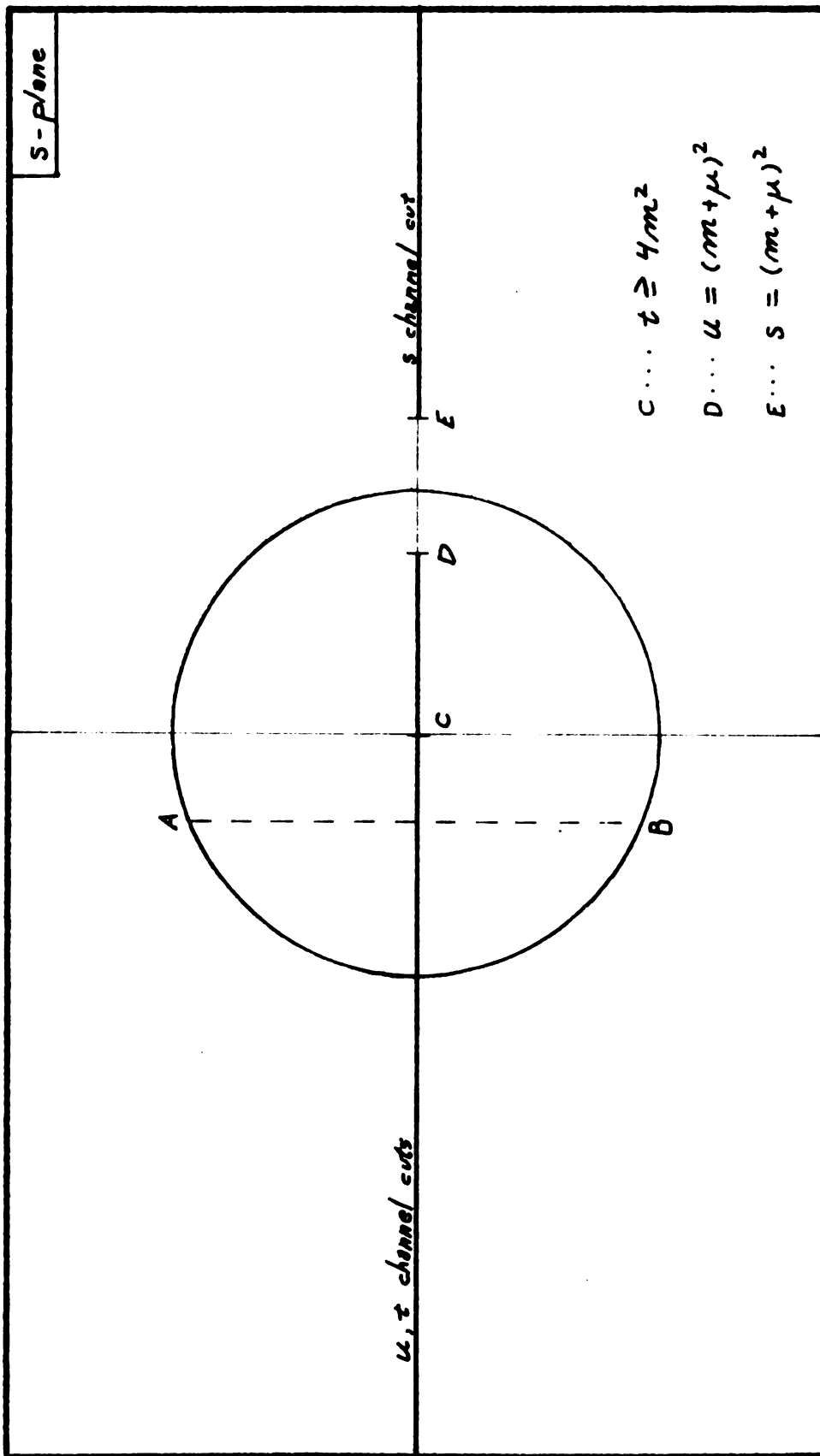


Figure 2. The physical  $\cos \phi$  region for  $4\mu^2 \leq t \leq 4m^2$ . Note that varying  $\cos \phi$  between  $+1$  and  $-1$  describes the line segment AB at fixed  $t$ .

in the Mandelstam plane except as an extrapolation from some (hopefully nearby) experimentally accessible region. Just as strong a caveat is to be observed as regards extrapolation in angle as in energy. This is particularly true in the case of input data parameterized as partial waves in some channel. The partial wave series is necessarily truncated after some infinite number of terms, typically when the error estimate on some high angular momentum phases makes them consistent with zero. For increasingly large values of  $\cos\theta$  outside the physical region the Legendre polynomials diverge like  $(\cos\theta)^L$ . Obviously, even a very small coefficient of some high- $L$  Legendre polynomial will dominate the lower terms in the series if this extrapolation is carried too far in  $\cos\theta$ . This fact causes serious problems even before the limits of convergence of the partial wave series (the Lehmann Ellipse) are reached, as we shall see.

# $\pi N$ DYNAMICS AND FINITE ENERGY SUM RULES

## A. The Mandelstam Representation

Before the advent of Duality and Finite Energy Sum Rules the basic language of dispersion relations was the Mandelstam representation. A brief review will provide a context in which Finite Energy Sum Rules can be discussed.

Assuming that the amplitude to be calculated possessed the singularity structure of field theoretic perturbation theory, Mandelstam<sup>(7)</sup> was able to write down a two-dimensional integral representation which the amplitude in question was required to satisfy. For  $\pi N$  scattering the Mandelstam representation has the form:

$$\begin{aligned} A^{(\pm)}(s, t, u) = & \frac{1}{\pi} \int_{(m+\mu)^2}^{\infty} ds' \int_{(m+\mu)^2}^{\infty} du' \frac{\alpha_{s'u'}^{(\pm)}(s', u')}{(s'-s)(u'-u)} \\ & + \frac{1}{\pi} \int_{(m+\mu)^2}^{\infty} du' \int_{4\mu^2}^{\infty} dt' \frac{\alpha_{u't'}^{(\pm)}(u', t')}{(u'-u)(t'-t)} \\ & + \frac{1}{\pi} \int_{4\mu^2}^{\infty} dt' \int_{(m+\mu)^2}^{\infty} ds' \frac{\alpha_{t's'}^{(\pm)}(t', s')}{(t'-t)(s'-s)} \end{aligned} \quad (3.1)$$

$$B^{(\pm)}(s, t, u) = g^2 \left( \frac{1}{m^2-s} \mp \frac{1}{m^2-u} \right)$$

+ similar terms.

It can be seen that the integral over each integration variable covers the range of that variable appropriate to physical values of the energy-square in that channel. Of particular note is the t-channel integration which begins at the 2-pion threshold  $t=4\mu^2$  rather than the

$\bar{N}\bar{N}$  threshold  $t = 4m^2$ .

Crossing symmetry is then translated into a set of symmetry relations on the spectral functions  $\alpha_{s,u}, \alpha_{s,t}, \alpha_{t,u}$  so that the Mandelstam representation explicitly satisfies the conditions of Eq. (2.17). Since an a priori knowledge of the structure of the spectral functions is not contained in the Mandelstam representation it does not serve as the sole basis for determining the amplitudes  $A^{(\pm)}(s,t,u)$ ,  $B^{(\pm)}(s,t,u)$  although at the same time it does determine their analyticity properties and also serves as a strong constraint or consistency requirement on any proposed solution.

To transform the Mandelstam representation into a useful calculation tool it is convenient to reduce it to one-dimensional form. By formally evaluating one integration in each of the double integrals and exploiting the symmetry of the spectral functions  $\alpha_{ij}$ , Eq. (3.1) can be reduced<sup>(8)</sup> to

$$\begin{aligned}
 A^{(\pm)}(s,t,u) &= \frac{1}{\pi} \int_{(m+\mu)^2}^{\infty} ds' A_1^{(\pm)}(s';t) \left( \frac{1}{s'-s} \pm \frac{1}{s'-u} \right) \\
 &\quad + \frac{1}{\pi} \int_{4\mu^2}^{\infty} dt' A_2^{(\pm)}(t';s) \frac{1}{t'-t} \\
 B^{(\pm)}(s,t,u) &= \frac{1}{\pi} \int_{(m+\mu)^2}^{\infty} ds' B_1^{(\pm)}(s';t) \left( \frac{1}{s'-s} \mp \frac{1}{s'-u} \right) \\
 &\quad + \frac{1}{\pi} \int_{4\mu^2}^{\infty} dt' B_2^{(\pm)}(t';s) \frac{1}{t'-t} \\
 &\quad + g^2 \left( \frac{1}{m^2-s} \mp \frac{1}{m^2-u} \right)
 \end{aligned} \tag{3.2}$$

In the equations one is guaranteed only that  $A_i^{(\pm)}$ ,  $B_i^{(\pm)}$ , the 1-dimensional spectral functions, are real. This fact allows us to separate out the real and imaginary parts of each side of the equations. We will use  $A^{(\pm)}(s,t,u)$  as an example although  $B^{(\pm)}(s,t,u)$  also satisfies the same

conditions. Let  $s, t, u$  have values such that only the term  $\frac{1}{s'-s}$  becomes singular. Then Eq. (3.2) has real and imaginary parts

$$\begin{aligned}
 \operatorname{Re} A^{(2)}(s, t, u) &= \frac{1}{\pi} \mathcal{P} \int_{(m+\mu)^2}^{\infty} ds' A_1^{(2)}(s', t) \frac{1}{s'-s} \\
 &\quad \pm \frac{1}{\pi} \int_{(m+\mu)^2}^{\infty} ds' A_2^{(2)}(s', t) \frac{1}{s'-u} \\
 &\quad + \frac{1}{\pi} \int_{\frac{4\mu^2}{4\mu^2}}^{\infty} dt' A_2^{(2)}(t', s) \frac{1}{t'-t} \\
 \operatorname{Im} A^{(2)}(s, t, u) &= A_1(s, t)
 \end{aligned} \tag{3.3}$$

The second equation allows us to identify the spectral functions unambiguously. Substituting this relation into the first of Eq. (3.3) gives

$$\begin{aligned}
 \operatorname{Re} A^{(2)}(s, t, u) &= \frac{1}{\pi} \int_{(m+\mu)^2}^{\infty} \frac{\operatorname{Im} A^{(2)}(s', t)}{s'-s} ds' \\
 &\quad + \frac{1}{\pi} \int_{(m+\mu)^2}^{\infty} \frac{\operatorname{Im} A^{(2)}(u', t)}{u'-u} du' \\
 &\quad + \frac{1}{\pi} \int_{\frac{4\mu^2}{4\mu^2}}^{\infty} \frac{\operatorname{Im} A^{(2)}(t', s)}{t'-t} dt'
 \end{aligned} \tag{3.4}$$

We have replaced the dummy variables  $s'$  by  $u'$  to get the second term and have implicitly carried out the procedure used in obtaining Eq. (3.3) for each channel. Thus, one of the terms in this equation may be thought of as a Principal value integral depending on the values of  $s, t, u$  selected. Also, if  $s, t, u$  are all simultaneously outside their respective physical regions none of the integrals is singular and hence the amplitude is pure real (except for the Nucleon pole terms at  $s=m^2$  or  $u=m^2$  in  $B^{(\pm)}(s, t, u)$ ). The imaginary part of any amplitude should thus be required to vanish outside the physical energy region of any given channel.

The Mandelstam representation explicitly exhibits the real part of the amplitude in terms of contributions from the imaginary part in each channel, but in order to calculate the real part, the spectral functions

(imaginary parts) are assumed to be stable against cross-channel contributions. This implies that the integrand in each term possesses the threshold properties and high energy convergence (or divergence!) properties of the particular channel over which it is to be integrated. For example, the imaginary part of  $A^{(\pm)}(s,t,u)$  is assumed to contain only contributions from non-strange Isotopic spin 1/2 or 3/2 Baryon intermediate states for s- or u-channel integrations and the t-channel term is assumed to be calculable in terms of non-strange Isotopic spin 0 or 1 meson intermediate states.

One of the most persistent difficulties in the path of using the Mandelstam representation, even on the modest scale outlined here, before the advent of Regge theory, was the fact that the integration in Eq. (3.4) extended to infinite energy in each channel while only a few low energy resonances were known. This led to truncating the integrations at a point above which little was known about the spectral functions<sup>(9)</sup> as well as the use of subtractions<sup>(10)</sup> and the introduction of phenomenological constants<sup>(11)</sup> to account for 'higher-states', to mention only a few of the more popular responses to an unsatisfactory situation.

While these approaches all relied on the obvious fact that nearby singularities ought to influence the amplitude at a particular point more than those farther away in the Mandelstam plane none is as intrinsically satisfying as the possibility of taking high-energy behavior into account more or less analytically via Regge poles and/or cuts.

The subtraction approach provides a sufficient number of similarities to the philosophy of Finite Energy Sum Rules that a few words about this method are in order.

Suppose one was presented with the dispersion relation of the form



$$\operatorname{Re} f(x) = \frac{1}{\pi} \int \frac{\operatorname{Im} f(x')}{x' - x} dx'$$

Without detailed information about the high-energy behavior of  $\operatorname{Im} f(x)$  it is advantageous to also write

$$\operatorname{Re} f(0) = \frac{1}{\pi} \int \frac{\operatorname{Im} f(x')}{x'} dx'$$

so that the difference of the two equations appears as a subtracted dispersion relation:

$$\operatorname{Re} f(x) = \operatorname{Re} f(0) + \frac{x}{\pi} \int \frac{\operatorname{Im} f(x')}{x'(x' - x)} dx'$$

The integral appearing in this equation now is of smaller magnitude than previously and also converges more rapidly. Of course the price paid for this improved property is that a new piece of input data has been introduced, or another phenomenological constant has been introduced.

Looked at in another way, this equation can be interpreted as having replaced the problem of evaluating the function  $\operatorname{Re} f(x)$  by the problem of evaluating the difference  $\Delta(x) \equiv \operatorname{Re}(f(x) - f(0))$ .

One could extend the subtraction approach by performing more than one subtraction or by evaluating the derivative of  $\operatorname{Re} f(x)$ , although the price to be paid for minimizing the effect of the high- $x$  behavior would be the introduction of a successively greater amount of input data or a host of phenomenological constants. However, if one can regard the high-energy behavior of the spectral functions for a suitably<sup>(12)</sup> chosen amplitude as essentially known, all of these problems could be avoided. This is the basic point of view underlying Finite Energy Sum Rules.

Suppose, for example, that the Regge parameterization of  $A^{(\pm)}(s, t, u)$  satisfied the Mandelstam representation as expressed in Eq. (3.4). Then,

writing Eq. (3.4) for  $A^{(\pm)}(s, t, u)$  as well as for its Regge-asymptotic parameterization  $A_{\text{Regge}}^{(\pm)}(w, t, u)$  and subtracting these two equations one has

$$\begin{aligned} \text{Re } \Delta^{(\pm)}(s, t, u) = & \frac{1}{\pi} \int_{(m+\mu)^2}^{\infty} \frac{\text{Im } \Delta^{(\pm)}(s', t)}{s' - s} ds' \\ & \pm \frac{1}{\pi} \int_{(m+\mu)^2}^{\infty} \frac{\text{Im } \Delta^{(\pm)}(u', t)}{u' - u} du' \\ & + \frac{1}{\pi} \int_{\mu^2}^{\infty} \frac{\text{Im } \Delta^{(\pm)}(t', s)}{t' - t} dt' \end{aligned} \quad (3.5)$$

where  $\Delta^{(\pm)}(s, t, u) \equiv A^{(\pm)}(s, t, u) - A_{\text{Regge}}^{(\pm)}(s, t, u)$

Now, since the amplitude  $A^{(\pm)}(s, t, u)$  must of necessity approach the Regge amplitude as energy increases, the function  $\Delta^{(\pm)}(s, t, u)$  must vanish beyond that point. Therefore we are in a position to analytically truncate the integration of Eq. (3.5) at some finite energy in each channel. Equation (3.5) can then be cast in the form

$$\text{Re } \Delta^{(\pm)}(s, t, u) = \frac{1}{\pi} \int_{(m+\mu)^2}^{s_0} \frac{\text{Im } \Delta^{(\pm)}(s', t)}{s' - s} ds' + \frac{1}{\pi} \int_{(m+\mu)^2}^{u_0} \frac{\text{Im } \Delta^{(\pm)}(u', t)}{u' - u} du' + \frac{1}{\pi} \int_{\mu^2}^{t_0} \frac{\text{Im } \Delta^{(\pm)}(t', s)}{t' - t} dt' \quad (3.6)$$

In this equation  $s_0$ ,  $t_0$ ,  $u_0$  are the values of the energy-squared in each channel above which the difference  $\Delta^{(\pm)}(s, t, u)$  is required to vanish (the limits of the 'Regge' region in each channel). If we were to evaluate (3.6) at some point well above the 'Regge limit' in each channel, the left-hand side would be zero. One could then expand the denominators on the right-hand side to obtain

$$\begin{aligned} 0 = \sum_{n=0}^{\infty} B_n \left\{ s^{-n-1} \int_{(m+\mu)^2}^{s_0} s'^n \text{Im } \Delta^{(\pm)}(s', t) ds' \right. \\ \left. + u^{-n-1} \int_{(m+\mu)^2}^{u_0} u'^n \text{Im } \Delta^{(\pm)}(u', t) du' \right. \end{aligned} \quad (3.7)$$

$$+ t^{-n-1} \int_{\frac{1}{4}\mu^2}^{t_0} \lambda_n(s') ds' \Delta^{(2)}(t', s) ds'$$

In this equation,  $B_n$  are the coefficients of the binomial expansion.

Equation (3.7) could naively be assumed to require that the coefficients of each power of the energy-square  $s, t, u$  vanish identically. However, since only two of the variables  $s, t, u$  are independent these coefficients are likewise not independent. One could, however, expand one of the terms ( $t^{-n-1}$  say) in terms of  $s, u$  and reduce Eq. (3.7) to the form

$$\begin{aligned} 0 = \sum_{n=0}^{\infty} B_n \left\{ s^{-n-1} \left[ \int_{\frac{1}{4}\mu^2}^{t_0} \lambda_n(s') ds' \Delta^{(2)}(s', t) ds' \right. \right. \\ \left. \left. + \int_{\frac{1}{4}\mu^2}^{t_0} \lambda_n(t') ds' \Delta^{(2)}(s', u) ds' \right] \right. \\ \left. + u^{-n-1} \left[ \int_{\frac{1}{4}\mu^2}^{u_0} \lambda_n(u') ds' \Delta^{(2)}(u', t) ds' \right. \right. \\ \left. \left. + \int_{\frac{1}{4}\mu^2}^{t_0} \lambda_n(t') ds' \Delta^{(2)}(t', u) ds' \right] \right\} \end{aligned}$$

The weight functions  $\lambda_n(u')$  is a simple polynomial in terms of positive powers of  $u'$ . However, one could now require that the coefficients of powers of  $s, u$  vanish identically. Such a relation has the form of a "Finite Energy Sum Rule".

We have deliberately been rather unspecific about a number of points in this development of Finite Energy Sum Rules (FESR), precisely because although the Mandelstam representation forms the background for introducing the concept, the FESR as actually used cannot be rigorously derived from it. Our interest in these relations stems more from the fact that they seem to be obeyed by  $\pi N$  scattering amplitudes than that they can be derived in some rigorous fashion from the Mandelstam representation.

## B. The Finite Energy Sum Rules

The FESR as we actually use them were first introduced by Barger,

Michael and Phillips<sup>(13)</sup>. They derive from the work of Dolen, Horn, and Schmid<sup>(14)</sup> and subsequent investigations of Chiu and DerSarkissian<sup>(15)</sup>. They can be extracted more or less from the Mandelstam representation as expressed in Eq. (3.5) if the u-channel term on the right-hand side is first eliminated. That is, let us rewrite (3.5) as

$$\text{Re } \Delta^{(\pm)}(s, t, u) = \frac{1}{\pi} \int_{(m+\mu)^2}^{s_0} \frac{dm' \Delta^{(\pm)}(s', u)}{s' - s} ds' + \frac{1}{\pi} \int_{\mu^2}^{t_0} \frac{dm' \Delta^{(\pm)}(s', u)}{t' - t} dt' \quad (3.9)$$

We will examine the motivation for neglecting the u-channel terms shortly. Note that both terms on the right hand side have been written as fixed-u integrals although they did not appear in quite that form in the Mandelstam representation. Further, the amplitudes  $\Delta^{(\pm)}$  are to be considered as written in terms of either  $A^{(\pm)}(s, t, u)$ ,  $B^{(\pm)}(s, t, u)$  or any of a fairly wide range of linear combinations of these amplitudes. This is to allow for the writing of FESR in terms of amplitudes which can be saturated by some small number of Regge pole contributions at high energies. For the same reason we will also write the FESR in terms of u-channel isospin, rather than the t-channel isospin indicated by the superscripts  $(\pm)$  which have been carried along to this point only because of their convenience in expressing the Crossing relations (2.17).

It is convenient to write (3.9) in terms of the variable X defined as

$$X \equiv \frac{1}{2}(s - t) = s - m^2 - \mu^2 + \frac{1}{2}u = -t + m^2 + \mu^2 - \frac{1}{2}u \quad (3.9a)$$

In terms of X, u we can express (3.9) as

$$\text{Re } \Delta^{(\pm)}(X, u) = \frac{1}{\pi} \int_{s=(m+\mu)^2}^{s=s_0} \frac{dm' \Delta^{(\pm)}(X', u)}{X' - X} dX' + \frac{1}{\pi} \int_{t=\mu^2}^{t=t_0} \frac{dm' \Delta^{(\pm)}(X', u)}{X' - X} dX' \quad (3.10)$$

Now choose values for  $s_0$ ,  $t_0$  so that the range of integration with respect to X is symmetric about zero. This implies that only one of the quantities

$s_0$ ,  $t_0$  can be arbitrarily chosen and, as we shall see, the value of  $s_0$  is rather well limited by available phase shifts to be  $s_0 = 4.8 \text{ GeV}^2$  which fixes  $t_0$  to be  $4.8 \text{ GeV}^2$  as well, considerable above the 2-nucleon threshold  $4m^2 = 3.52 \text{ GeV}^2$ . These values correspond to the limits  $X = \pm(3.9 \text{ GeV}^2 + \frac{1}{2}u) = \pm X_0$ . The fact that our choice of  $t_0$  has been 'forced' does not at the present time cause any glaring conflicts with data available on the process  $\pi\pi \rightarrow N\bar{N}$ . In terms of these explicit limits on  $X$  equation (3.10) can be written

$$R_0 \Delta^{(\alpha)}(X, u) = \frac{1}{\pi} \int_{-X_0}^{X_0} \frac{dm \Delta^{(\alpha)}(X', u)}{X' - X} dX' \quad (3.11)$$

Expanding the denominator for some value of  $X$  such that  $|X| \gg |X_0|$  gives

$$0 = \sum_{n=0}^{\infty} X^{-n-1} \int_{-X_0}^{X_0} X'^n dm \Delta^{(\alpha)}(X', u) dX'$$

which can be satisfied only if

$$\int_{-X_0}^{X_0} X'^n dm \Delta^{(\alpha)}(X', u) dX' = 0 ; \quad n \geq 0, \text{ an integer.} \quad (3.12)$$

If the Regge and non-Regge terms are separated the FESR can be put in the form

$$\int_{-X_0}^{X_0} X'^n dm F_{\text{Regge}}^{(\alpha)}(X', u) dX' = \int_{-X_0}^{X_0} X'^n dm F^{(\alpha)}(X', u) dX' \quad (3.13)$$

This is the form of the FESR as written down by Barger et.al.<sup>(16)</sup> which we wish to examine in terms of much more realistic spectral functions  $dm F^{(\alpha)}(X, u)$ .

It should be noted that while the spectral functions which entered into the Mandelstam representation vanished at points outside the physical region of a given channel, the Regge term in Eq. (3.13) will be seen to be

non-zero throughout the entire region -  $x_0 \leq x \leq x_0$ .

It should also be noted that while we write Eq. (3.13) in terms of the 'imaginary part' of the appropriate amplitude, the proper spectral function is the so-called 'Discontinuity' defined for some arbitrary amplitude  $f(x)$  as

$$'Disc' f(x) \equiv \lim_{\epsilon \rightarrow 0} (f(x+i\epsilon) - f(x-i\epsilon))/2i \quad (3.14)$$

Further, if  $f(x)$  is to be an analytic function of  $x$ , it must have the property that  $f(x)^* = f(x^*)$  so that  $Disc f(x) = Im f(x)$ . The fact that the variable  $X$  is defined in terms of  $-t$  in Eq. (3.9a) interchanges the two terms in (3.14), introducing an over all  $(-)$  sign into the contribution of the  $t$ -channel singularities in the FESR. These considerations do not affect the  $s$ -channel terms since  $X$  and  $s$  have the same sign. Nor is the Regge term affected since, as we shall see shortly, it is constructed in terms of  $u$ -channel singularities which are independent of  $X$ .

### C. The Concept(s) of Duality

'Duality' refers to the idea that the separate channels of a given reaction are not 'independent'. The word is (or has been) understood in a variety of ways variously categorized as 'Strong duality', 'Weak Duality', etc. The difference between the various uses of the word hinge on the degree to which the separate channels are or are not thought of as 'independent'.

In terms of the Mandelstam representation as expressed by Eq. (3.4), the separate channels contribute to the amplitude in an identical fashion (through a fixed momentum-transfer integral over the physical cut in energy). In this sense the separate channels are completely independent. Further, the spectral function on the energy cut in each channel is constructed solely from intermediate states occurring in the channel (i.e. the

spectral function is not constructed via exchange mechanisms). Exchanges appear when the Mandelstam representation is evaluated only because it is not possible to select values of  $s$ ,  $t$ ,  $u$  simultaneously in the physical region of each channel. As evaluated in the Mandelstam representation the real part of an amplitude appears as a superposition of direct-and crossed-channel contributions.

Now consider the situation as viewed in Regge theory. In the forward direction the  $s$ -channel amplitude is calculated in terms of  $t$ -channel Regge pole exchange, in the backward direction  $u$ -channel Regge exchange dominates the amplitude at high energies. It would be formally possible to write down a direct channel Regge pole contribution, but in fact this is never done. Admittedly a direct channel Regge pole would be highly singular if it were represented by the simplest form of the trajectory (real  $\alpha$ ). But, even if the imaginary part of space were included a direct channel Reggeon would not contribute appreciably to the amplitude at high energies. This is due to the fact that the recurrences at high energy couple weakly to the elastic channel, being intercepted far from the physical region (at large  $\ln u$ ).

The conflict implied by the co-existence of these two views on the structure of the scattering amplitude is heightened by the fact that in the Mandelstam representation the close-by singularities are thought of as being the greater contributors to the amplitude at some point, while in Regge theory it is just these direct-channel contributors which are eliminated.

The means by which this situation can be understood is the existence of Finite Energy Sum Rules in the context of Duality.

The work of Dolen, Horn, Schmid<sup>(17)</sup> is the first element in the

explanation of the relationship between Regge theory and the Mandelstam representation. These authors were able to show that in the case of charge-exchange the  $\rho$  trajectory extrapolated to low  $s$  was a good representation of the average scattering amplitude as a function of energy along lines of fixed  $t$  corresponding to forward  $\pi N$  scattering. Such a statement is equivalent to an FESR. A function and its average have identical moments. This is the simplest sense in which Eq. (3.13) can be understood and the weakest statement of Duality. However, Dolen, Horn, Schmid noticed an even more interesting character of the amplitudes. It was unnecessary to integrate over the entire low-energy spectrum in order to get the scattering amplitude to 'average out' to the Regge trajectory; the  $\rho$  trajectory appeared to average the scattering amplitude over much smaller regions of energy. Thus the Regge exchange contributions could be said to represent the 'local' average of the scattering amplitude. Subsequently Dolen et.al. attempted to ascertain the validity of the local average concept in the backward direction. Although they found the concept to be valid near the point at which the amplitude becomes 'pure' Regge, this is to be expected. We shall show that the local average idea cannot be maintained convincingly at lower energies.

The ideas of Dolen et.al. were further elaborated by Schmid<sup>(18)</sup>, who observed that it was possible to extract 'resonant' partial waves from the  $\rho$ -Regge charge exchange amplitude which agreed surprisingly well with three established resonances. That is, the Regge amplitude corresponded to a  $90^\circ$  phase shift at C.M. energies 1920 MeV, 2190 MeV, 2420 MeV, the positions of three 'well-established'  $\pi N$  resonances (The 1920 and 2420 are listed at 1990 and 2650 ( $j=?$ ) in the January 1970 data tables). This simple Regge parameterization coincided so well with available data



that Schmid's work could be interpreted as suggesting that a sufficiently well elaborated Regge model might be able to supplant the direct-channel resonance model, even at low energies. This is Duality in its strongest form.

While the successes of Schmid's calculation have not been achieved in other cases and might be laid aside as coincidence, the equivalence of Regge and resonance models can be demonstrated in the so-called 'Regge' region even more convincingly than in the low or intermediate energy range. This demonstration has been carried out by Lichtenberg<sup>(19)</sup> et.al. These authors were able to show that the backward  $\pi N$  differential cross section in the energy range  $2.24 \text{ GeV} \leq W_{\text{c.m.}} \leq 3.2 \text{ GeV}$  could be fitted in a direct-channel resonance model as well as with u-channel Regge exchange<sup>(20)</sup>. While not all of the resonances required can be said to be well established, the authors demonstrated conclusively that the resonance model could be extended a considerable distance into the region in which the Regge model has been considered the only way to fit data. In this form Duality appears in a way stronger than the requirement that the FESR be satisfied, but weaker than the requirement of absolute interchangeability suggested by Schmid's work.

In the FESR written down by Barger et.al. the Regge term is constructed from u-channel Reggeons, the N and  $\Delta$  trajectories. The FESR are evaluated for  $0 \leq u \leq 10 \text{ GeV}^2$ . Referring to Figure 1, it can be seen that for  $X$  approaching  $X_0$  these  $u$  values correspond to backward scattering in the s-channel and for  $X$  approaching  $-X_0$  backward t-channel scattering. Meson Regge Trajectories ( $\sim s^{\alpha(t)-1}$ ) are suppressed because either  $s$  is small or, for large  $s$ ,  $\alpha(t)-1$  is large and negative. Therefore, there is no u-channel contribution to Eq. (3.9) and (3.13) (a u-channel amplitude

would asymptotically approach a  $t$ -channel Regge amplitude in the forward direction (along a line of fixed  $t$ ) or an  $s$ -channel Regge amplitude in the backward direction (along a line of fixed  $s$ )).

# IV

## THE SPECTRAL FUNCTIONS

### A. The Regge Amplitudes

The FESR are written down in terms of the amplitudes.

$$F_{\pm}^{N,\Delta}(\chi, u) = \mp A^{N,\Delta}(\chi, u) - (\sqrt{u} \pm m) B^{N,\Delta}(\chi, u) \quad (4.1)$$

The subscripts  $\pm$  should not be confused with the superscripts used to denote t-channel isotopic spin. The superscripts  $N, \Delta$  refer to u-channel isotopic spin 1/2, 3/2 respectively which are related to s- and t-channel isotopic spin by <sup>(21)</sup>

$$\begin{aligned} F^N &= -\frac{1}{3}F^{(1/2)} + \frac{2}{3}F^{(3/2)} = F^{(+)} - \frac{1}{2}F^{(-)} \\ F^{\Delta} &= \frac{2}{3}F^{(1/2)} + \frac{1}{3}F^{(3/2)} = F^{(+)} + F^{(-)} \end{aligned} \quad (4.2)$$

Thus, for a given moment number,  $n$ , in Eq. (3.13) there are four FESR, one for each of  $F_+^N$ ,  $F_-^N$ ,  $F_+$ ,  $F_-$ .

The amplitudes  $F_{\pm}^{N,\Delta}$  can be related to the s-channel spin-flip, no spin-flip amplitudes by applying the crossing relations (2.17) to the amplitudes  $F_{\mp}^{(\pm)}(s, t) \equiv 8\pi W/(E \pm m) f_{1,2}^{(\pm)}(s, t)$ , related to  $A^{(\pm)}$ ,  $B^{(\pm)}$  by Eq. (2.15).

One finds

$$\begin{aligned} F_-^{(\pm)}(s, t, u) &= \pm F_+^{(\pm)}(u, t, s) \\ F_+^{(\pm)}(s, t, u) &= \pm F_-^{(\pm)}(u, t, s) \end{aligned} \quad (4.3)$$

Singh <sup>(22)</sup> has shown that the amplitudes  $f_1$  and  $f_2$  are the appropriate

ones to Reggeize. The factor  $W$  is introduced to avoid a kinematic singularity at  $s(\text{or } u)=0$ . Eliminating the factor  $(E \pm m)$  simplifies the crossing relations (4.2) and avoids the possibility of suppressing low-lying Regge recurrences.

The subscripts refer to the  $\tau P$  values (signature  $\times$  parity) of the trajectories which contribute to each amplitude at high energies. The eight possible trajectories, four for each isospin value corresponding to the various choices  $(\tau, P) = (\pm, \pm)$ , are listed in Table 1 along with the labels customarily used to refer to them.

Regge analysis of the existing data are consistent with the assumption of zero residue for the  $N_{\tau}, N_{\delta}, \Delta_{\alpha}, \Delta_{\beta}$  trajectories<sup>(23)</sup>. Thus the number of trajectories we need consider are reduced by half.

The Regge amplitudes are parameterized as

$$F_{\pm}^{N, \Delta}(\chi, u) = R_{\pm}^{N, \Delta} (1 + z e^{-i\pi(\alpha(\sqrt{u}) - 1/2)}) \chi^{\alpha(\sqrt{u}) - 1/2} \quad (4.4)$$

where

$$R_{\pm}^{N, \Delta} = \gamma_{\pm}^{N, \Delta}(\sqrt{u}) / (\Gamma(\alpha + 1/2) \cos \pi \alpha)$$

$$\gamma_{+}^N(\sqrt{u}) = 8\pi((u - m^2)a + (\sqrt{u} + m)b)$$

$$\gamma_{-}^{\Delta}(\sqrt{u}) = 8\pi(d_0 + \sqrt{u}f_0)(1 + \sqrt{u}/M_{\pi\pi})e^{-g_0 u}$$

$$a = a_0 e^{c_0 u}, \quad b = b_0 e^{c_0 u}$$

$$\alpha_{+}^N(\sqrt{u}) = -0.38 + .91u$$

$$\alpha_{-}^{\Delta}(\sqrt{u}) = 0.21 + .84u$$

An explicit parameterization is necessary for only one of the residues

$\gamma_{\pm}(\sqrt{u})$  for each isospin since the other can be determined by McDowell Symmetry<sup>(24)</sup> which requires that

$$\gamma_{\pm}(-\sqrt{u}) = -\gamma_{\pm}(\sqrt{u})$$

This is simply an expression of the content of Eq. (2.15) under the condition of allowing  $A^{(\pm)}(s,t,u)$  and  $B^{(\pm)}(s,t,u)$  to be defined for negative energies ( $\sqrt{u}$  is the C.M. energy in the u-channel).

The constants  $a_0, b_0, c_0, d_0, f_0, g_0$  introduced above are assigned the values 0.8, 1.8, 0.5, 0.2, 0.09, -0.7 respectively ( $u$  is measured in  $\text{GeV}^2$ ). It can be seen from (4.4) that the Regge spectral function have well defined X-parity for real  $u > 0$ , namely

$$\text{Im} F_{\pm}(x, u) = -\tau \text{Im} F_{\pm}(-x, u)$$

The well-defined parity of the Reggeons allows them to be isolated in the FESR. The  $N_{\alpha}, N_{\beta}$  trajectories contribute only to odd-n moments of the FESR, the  $\Delta_S, \Delta_M$  to even-n moments only. Thus the even-n 'N' FESR and odd-n ' $\Delta$ ' FESR have the form of finite energy superconvergence relations for the total amplitude. However, we are not surprised to discover that the amplitudes do not exactly satisfy these superconvergence conditions. While the residues of the corresponding Reggeons are consistent with zero residue, it is likely that they are non-zero although they are apparently much smaller than the other Regge residues. This contention is supported by the fact that the 'zero' moments of the FESR are always very much smaller than the corresponding non-zero ones.

Our FESR calculations are limited by the above consideration to real  $u \gg 0$ . Further, since the Regge fits are done for real  $\alpha(u)$ , we are limited to values of  $u$  below the u-channel threshold (the Regge recurrences have zero width and hence correspond to singularities in the u-channel physical region). Thus we limit our calculations to the interval  $0 \leq u \leq 1 \text{ GeV}^2$ . This region in the Mandelstam plane is shown in Figure 3.

Isospin	$\tau P$	$(\tau, P)$	Label	$n$
$I = \frac{1}{2} (N)$	+	+ +	$N_\alpha$	odd
		- -	$N_\beta$	
	-	+ -	$N_\beta$	odd
		- +	$N_\delta$	
$I = \frac{3}{2} (\Delta)$	+	+ +	$\Delta_\alpha$	
		- -	$\Delta_\beta$	even
	-	+ -	$\Delta_\beta$	
		- +	$\Delta_\delta$	even

Table 1. The Baryon trajectories and their quantum numbers. The second column lists the subscripts of the u-channel helicity amplitudes to which a given trajectory contributes. The last column lists the values of the moment number  $n$  for which the corresponding Regge amplitude yields a non-zero contribution to the FESR.

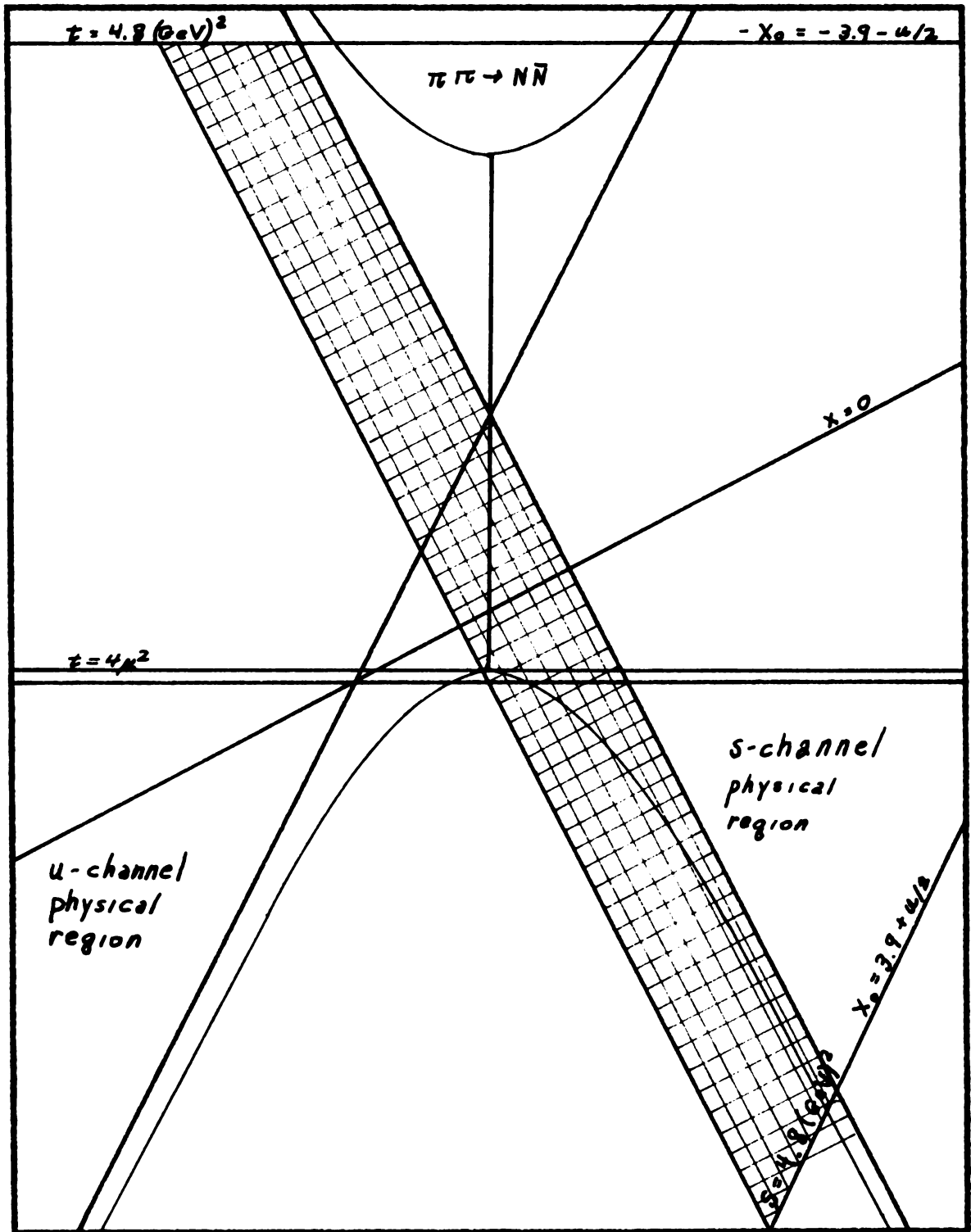


Figure 3. The region of integration associated with the FESR. The cross-hatching corresponds to lines of fixed  $u$  and  $X$ .

## B. The s-channel Spectral Functions

In order to determine  $F^{N, \Delta}(X, u)$  on the cut  $s \geq (m + \mu)^2$ , it is necessary to specify the partial wave amplitudes  $f_{\ell s}^j$  over the range  $(m + \mu)^2 \leq s \leq s_{\max} = 4.8 \text{ GeV}^2$ . Then equations (2.14), (2.15) and (4.1) determine the spectral functions  $\text{Im } F_j^N(X, u)$ . The partial wave amplitudes are specified by the (real) phase shift,  $\delta$ , and the (real) inelasticity,  $\eta$ , as in (1.14). Unitarity limits the inelasticity to be in the range  $0 \leq \eta \leq 1$ . Each partial wave state of good  $J, L, I$  is specified by a separate phase shift and inelasticity, thought of as functions of energy, although  $\eta$  is identically one below the limit of pion production (1.218 GeV). In practice only a relatively few low- $L$  partial waves are assumed to be significant.

Phase shift analysis is commonly done by one or both of two methods. In the first method a set of values are chosen for the phase shift (including the inelasticity) for each state at each energy and these values are used to 'predict' the measured cross sections and angular distributions at various energies. Discrepancies between the predictions and measurements are then minimized by varying the phases and performing subsequent predictions. This process is iterated until some error criterion (typically a Chi-square test) is satisfactorily minimized. A 'smooth' curve connecting the final values of each phase shift and inelasticity then represents the energy-dependence of that particular parameter. In fact, the initial choice of values is not so arbitrary as it might appear from this discussion. Available knowledge of the known resonances can be used to fix rather accurately both the phase shift and inelasticity of some states over a wide energy range. It would be difficult to rationalize arbitrary choices for the  $P_{33}$  phase in the range  $W \leq 1.3 \text{ GeV}$  for example. Some ambiguities can be resolved by imposing dispersion relation



constraints. The Chew-Low ambiguity was resolved in this fashion. Phase shift analyses which extend to high energies also have the existing low energy analyses available to minimize these initial choices. This approach is often characterized as 'model-independent' or phenomenological phase shift analysis.

The second approach is to predict cross sections and angular distributions as a means of fitting the phenomenological constants of some model of the  $\pi N$  interaction from which phase shift and inelasticity information can be extracted. The resonance model is the major one of these 'model dependent' phase shift analyses. The parameters to be fitted in this approach are the masses, widths, and inelasticities of various hypothetical Baryon resonances. The 'Roper resonance' ( $N(1520)$ ) is the earliest example of a resonance 'discovered' by phase shift analysis. The use of dispersion relations as additional constraints can lead to the simultaneous determination of meson resonance parameters.

While we have discussed model-dependent and phenomenological phase shift analyses as separate approaches, they are frequently used as parts of the same analysis. This is the case with the phase shifts we use - - the CERN PIP phases of Donnachie, Kirsopp, and Lovelace<sup>(25)</sup>. This analysis resulted in two separate sets of phases and inelasticities, the 'TH' and 'EXP' solutions respectively.

The EXP phases are the model-independent set. They provide a good fit to  $\pi N$  data in the range  $1.078 \text{ GeV} \leq W \leq 2.190 \text{ GeV}$  (chi-square of  $\sim 1000$  for  $\sim 4000$  data points) and provide the 'data' for the model-dependent TH solution. The reasons for attempting a second solution in the face of such a good fit to data are that the EXP phases do not possess very smooth energy dependence and also do not provide a meaningful

theoretical model for the  $\pi N$  interaction (it is virtually impossible to extract resonance parameters, etc. from such phases, even though they do fit the data). The TH solution is extracted from a resonance model by fitting the EXP phases as data and imposing dispersion relation constraints; i.e., the dispersion relations were saturated by the EXP phases. The resonances which figure in the TH solution are supplied only if an acceptable solution (the EXP phases are the guide here) cannot be found for a particular partial wave state without one. This raises the problem of distinguishing resonances from uncorrelated 'phase space' or 'background' effects. The phase shift associated with the 'background' can not only be quite large but can also vary quite rapidly with energy while its associated inelasticity is a (presumably) slowly-varying function of energy. Thus Lovelace et.al. identify a resonance by a minimum in the inelasticity rather than a phase passing through  $90^\circ$ . By this criterion nine new Baryon resonances were identified. Coupling constants were also determined for the  $\rho(I = 1)$  and  $\sigma(I = 0)$  mesons. Energy-dependent phase shifts and inelasticity parameters were determined for 22 partial wave states,  $S_{1/2}$  through  $H_{3/2}$ , throughout the energy range  $1.078 \text{ GeV.} \leq W \leq 2.190 \text{ GeV.}$

The TH phases describe partial wave amplitudes which are smooth functions of energy with a tabulated resonance structure. In this respect these phases are an admittedly significant improvement over competing phases produced at Berkeley and Saclay. However, the TH phases are markedly inferior to the EXP set in reproducing experimental data, particularly for  $\pi p$  elastic scattering. This was to be expected since the TH phases were fitted to the EXP phases as 'data' and therefore cannot be expected to fit cross sections and angular distributions as well as a

set fitted directly. The recent rediscovery of this fact has caused some comment as to which set is 'better' <sup>(26)</sup>. The result of this discussion is that while the TH phases are superior in terms of interpreting  $\pi N$  interactions, the EXP phases are more desirable for purposes of calculation.

Nonetheless, the TH phases were commonly used to generate  $\pi N$  amplitudes until quite recently. We have examined the TH and EXP amplitudes and find that the EXP amplitudes possess better convergence properties, i.e., they more closely approximate the Regge amplitudes near  $X = X_0$  ( $s = 4.8 \text{ GeV}^2$ ) than do the TH amplitudes. The TH, EXP, and Regge amplitudes in the region near  $X = X_0$  are shown in Figure 4 and 5. The contributions of the TH and EXP amplitudes to the FESR are virtually identical, as we shall see, despite the evident discrepancies.

In addition to the physical cut  $s \geq (m + \mu)^2$  one must also include the Nucleon 'Born term' which contributes a singularity of the form  $g^2 / (s - m^2)$  whose imaginary part is just a delta function. We choose the value of the coupling constant so that  $g^2/4 = 14.6$ . <sup>(27)</sup>

### C. The t-channel Spectral Function

In the region  $t \geq 4\mu^2$  the spectral function is constructed through Eq. (2.19), which exhibits the amplitudes  $A^{(\pm)}(s, t, u)$ ,  $B^{(\pm)}(s, t, u)$  as a sum of states of good (t-channel) total angular momentum and like or unlike  $N\bar{N}$  helicity.

Contrary to the case of the s-channel cut, little direct information is available about the t-channel amplitudes. The region  $4\mu^2 \leq t < 4m^2$  is experimentally inaccessible. Little information is available above the physical nucleon threshold. However, the relationship between the process  $\pi\pi \rightarrow N\bar{N}$  and elastic  $\pi\pi$  scattering provides something of a guide to the determination of the amplitude near  $t = 4\mu^2$ . Further, Barger and Cline <sup>(28)</sup> have shown that a Regge model using  $N_{\alpha}$  and  $\Delta_8$  trajectories

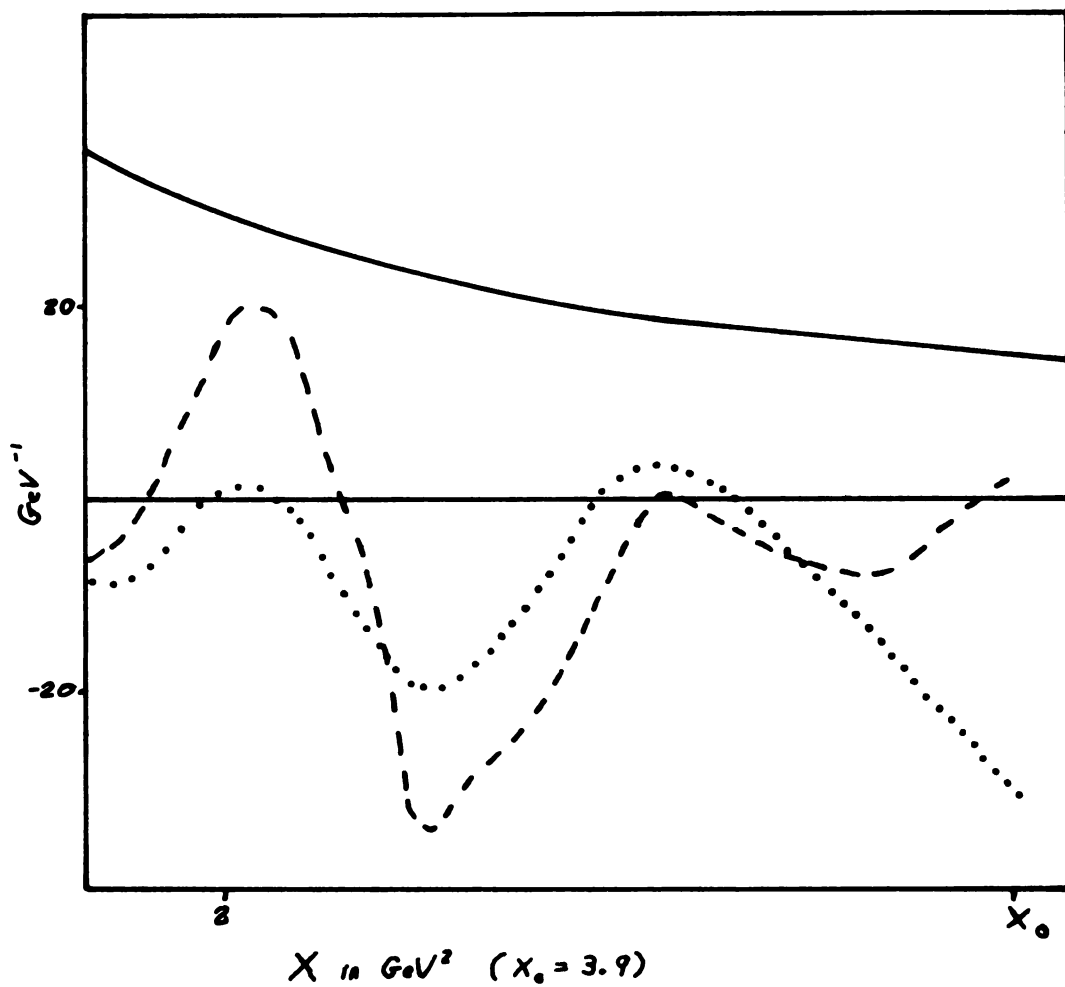


Figure 4. The spectral function for the state described by  $F_+^N(X, u)$  at  $u=0$ . The region of  $X$  near  $X_0$  is shown. The solid curve is the Regge spectral function. The low energy amplitudes generated by the TH and EXP phase shifts are shown as dotted and dashed curves respectively.

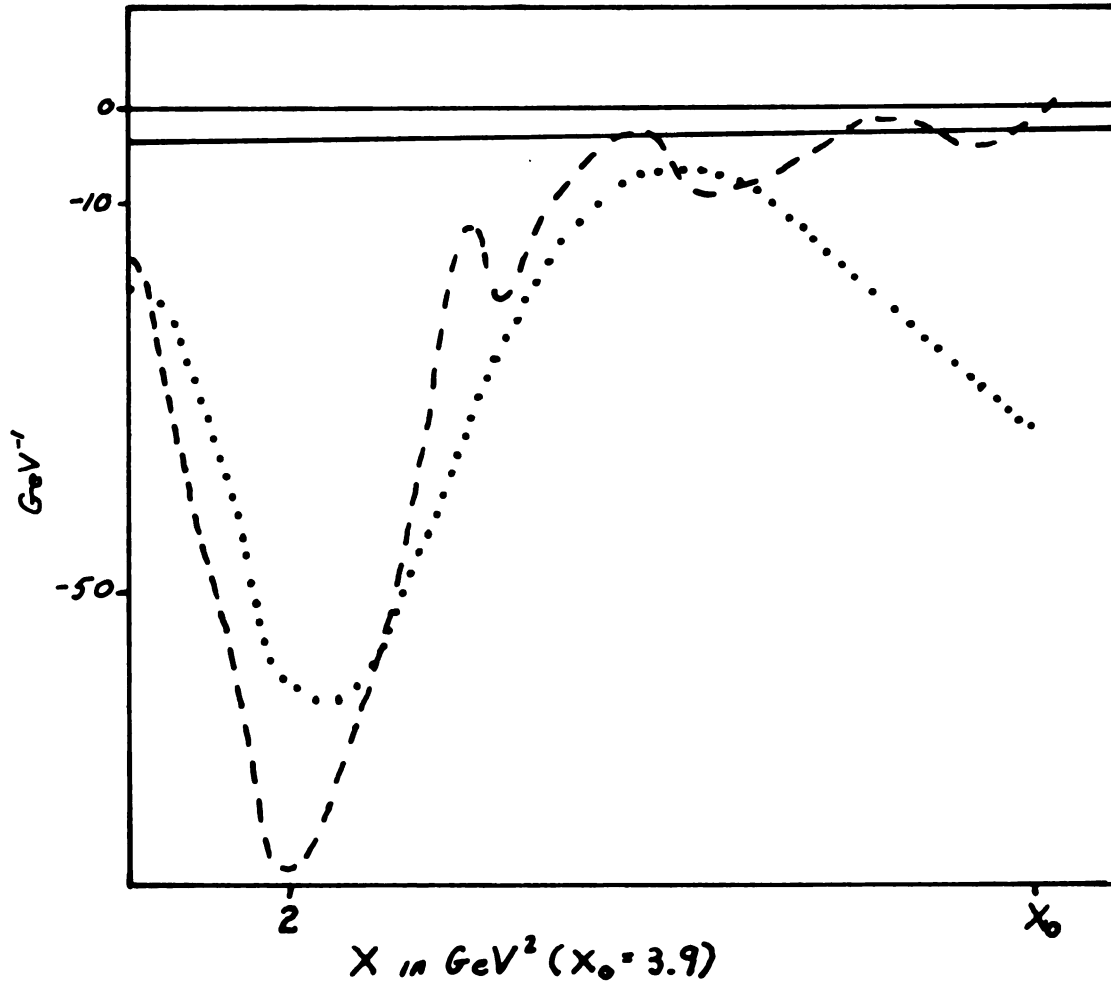


Figure 5. The spectral functions for the state described by  $F_+^{\Delta}(X,u)$  at  $u=0$ . The region of  $X$  near  $X_0$  is shown. The solid curve is the Regge spectral function. The low energy amplitudes generated by the TH and EXP phase shifts are shown as dotted and dashed curves respectively.

is consistent with early data on  $\rho\bar{\rho} \rightarrow \pi\bar{\pi}$  at backward angles (small  $u$ ). A reasonable  $t$ -channel spectral function should therefore be expected to converge to the corresponding Regge amplitude near  $t=4\text{GeV}^2$ . The spectral functions developed in this chapter show rather good convergence properties, especially at small  $u$ .

The  $t$ -channel spectral functions are constructed as follows. Beginning with Eq. (2.19)

$$A^{(\pm)}(t, u, \phi) = \frac{8\pi}{p} \sum_j (j + \frac{1}{2})(pq)^j \left\{ \frac{m}{\sqrt{j(j+1)}} f_{-}^{(\pm)j}(t) \cos\phi P'_j(\cos\phi) - f_{+}^{(\pm)j}(t) P_j(\cos\phi) \right\}$$

$$B^{(\pm)}(t, u, \phi) = 8\pi \sum_j \frac{(j + \frac{1}{2})}{\sqrt{j(j+1)}} (pq)^{j-1} f_{-}^{(\pm)j}(t) P'_j(\cos\phi)$$

one needs to specify the set of amplitudes  $f_{\pm}^{(\pm)j}(t)$  to determine  $A^{(\pm)}$ ,  $B^{(\pm)}$  and hence the spectral functions  $F_{\pm}^{N,\Delta}(X, u)$ .

The simplest approximation which is used to generate spectral functions is to saturate the amplitudes with zero-width meson resonances, parameterized by a mass-square and a coupling constant for each of the  $N\bar{N}$  helicity states. Notice that the system cannot couple to an intermediate state Baryon.

In this approximation each resonance would be accounted for by a 'Born' pole of the form

$$f_{\pm}(t) = \frac{C_{\pm}}{t_0 - t}$$

corresponding to a mass  $m = \sqrt{t_0}$  and two free parameters  $C_{\pm}$ . Spin and isospin labels on  $f_{\pm}(t)$  will be the quantum numbers of the resonance. This is the approach used by Barger. He included four mesons;  $\epsilon, \rho, f_0, \eta$ . Coupling constants for the  $\rho$  and  $\epsilon$  were available from the work of Lovelace. Barger fixed the coupling constants of the  $f_0$  and  $\eta$  by

requiring that the FESR which isolated the  $N_\gamma$ ,  $N_f$ ,  $\Delta_\omega$ , and  $\Delta_\rho$  trajectories be small compared to the  $N_\omega$  FESR for low moment number  $n$  (see Table 1). A complete list of Barger's resonance parameters is presented in Table 2. Notice that the  $I=0$ ,  $J=0$  member is here labelled ' $\epsilon$ ' rather than ' $\sigma$ '. Also, by inspection of Eq. (2.19) it is clear that the units of the coupling constants  $C_\pm$  must depend on  $J$ . Also, the  $\rho$  is listed at an admittedly low mass. As Lovelace points out<sup>(29)</sup> this is a consequence of attempting to represent all the weight of the low energy  $J=1$ ,  $I=1$  state by a simple pole. This part of the cut is sufficiently near the s-channel threshold that the distribution along the cut is as important as the total weight. We will shortly adjust the masses of both the  $\rho$  and  $\epsilon$  to more meaningful values.

The FESR calculations of Barger, et.al., using the zero-width mesons listed in Table 2 (along with the CERN-TH phases to generate the s-channel spectral function) produced remarkably good agreement for the lowest moment ( $n=1$ )  $N_\omega$  and  $N_\rho$  FESR. However, since the imaginary part of a Born pole is a delta-function the t-channel spectral function is not continuous and therefore cannot converge to the corresponding Regge amplitude in any meaningful fashion. Thus, without a continuous spectral function the FESR are not as meaningful as they might be - - if Regge convergence could be explicitly demonstrated. For this reason we determined to replace the zero-width spectral functions by continuous ones and see if the FESR could still be satisfied. The continuous spectral functions arrived at not only satisfied the FESR but also show good convergence behavior although not constrained in any way in this respect.

The new spectral functions were constructed as follows. First, the Born poles were replaced by Breit-Wigner poles of the form

	Mass	I-spin	Spin	$C_+$	$C_-$
$\epsilon$	.437 GeV.	0	0	.37 GeV <sup>3</sup>	.....
$\rho$	.591 GeV.	1	1	1.5 GeV.	8.1
$f_0$	1.250 GeV.	0	2	11.5 GeV. <sup>-1</sup>	10.7 GeV <sup>-2</sup>
$g$	1.660 GeV.	1	3	4.2 GeV <sup>-3</sup>	6.4 GeV <sup>-4</sup>

Table 2. Quantum numbers and coupling constants for the zero-width mesons used in Barger's FESR calculations. Note that there is no  $C_-$  for the  $I=0, J=0$  state since only like helicity  $N\bar{N}$  pairs can occur in this state.



$$f_{\pm}(t) = \frac{g_{\pm}}{t_0 - t - iM\Gamma}$$

The values of  $M$  and  $\Gamma$  corresponding to each meson in Barger's list were selected from the data tables. This involved a considerable change in the masses of the  $\rho$  and  $\epsilon$ . To fix the coupling constants  $g_{\pm}$  it was required that the overall weight of each t-channel amplitude remain unchanged. That is, that

$$\frac{1}{4\mu^2} \int_{-\infty}^{\infty} \pi C_{\pm} \delta(t-t_0) dt = \int_{-\infty}^{\infty} \frac{M\Gamma g_{\pm}}{(t-t_0)^2 + M^2\Gamma^2} dt$$

This reduces to

$$g_{\pm} = \frac{C_{\pm}}{1/2 + (1/\pi) \tan^{-1}((t_0 - 1/2)/M\Gamma)} \quad (4.5)$$

Notice that  $g_{\pm}$  approaches  $C_{\pm}$  in the limit of zero width. The singularities associated with the zero width parameterization of the intermediate states have now been eliminated. No new arbitrary parameters were introduced in the process.

The spectral function associated with the Breit-Wigner resonance form is still not completely adequate to allow the convergence properties to be thoroughly examined since  $A^{(\pm)}(t, \cos\phi)$  is singular at the  $N\bar{N}$  threshold. To see this observe that  $\cos\phi$  diverges as  $(pq)^{-1}$  at  $p=0$ . Thus, while the terms  $(pq)^J P_J'(\cos\phi)$  and  $(pq)^J P_J(\cos\phi)$  are finite at  $p=0$ , the over all factor  $1/p^2$  produces a divergence. To remove this singularity we must take into account the threshold properties of the amplitude  $f_{\pm}^{(2)}(s)$ .

For the spinless pions, orbital and angular momentum are identical so that  $\lim_{s \rightarrow 0} f_{\pm}^{(2)}(s)$  must behave like  $q^{2J+1}$  as  $q$  approaches zero. Similarly the absorptive part of any amplitude corresponding to good orbital angular momentum of the  $N\bar{N}$  system must behave like  $p^{2L+1}$  as  $p$

approaches zero. In Appendix D the amplitudes  $f_{\pm}^{(\pm)j}(\epsilon)$  are decomposed into contributions from states of good  $\mathbf{l}(=\mathbf{j}\pm 1)$  for the  $N\bar{N}$  system. The results, expressed in Eq. (2.22) are

$$\begin{aligned} f_{+}^{(\pm)j} &= \frac{1}{\sqrt{2}} \left( \frac{j}{2j+1} \right)^{1/2} f_{j-1}^{(\pm)j} - \frac{1}{\sqrt{2}} \left( \frac{j+1}{2j+1} \right)^{1/2} f_{j+1}^{(\pm)j} \\ f_{-}^{(\pm)j} &= \frac{1}{\sqrt{2}} \left( \frac{j+1}{2j+1} \right)^{1/2} f_{j-1}^{(\pm)j} + \frac{1}{\sqrt{2}} \left( \frac{j}{2j+1} \right)^{1/2} f_{j+1}^{(\pm)j} \end{aligned}$$

The subscripts  $j\pm 1$  denote the orbital angular momentum  $\mathbf{l}$  of the  $N\bar{N}$  system.

In each of the amplitudes  $f_{\pm}^{(\pm)j}(\epsilon)$  we replace the fixed width  $M\Gamma$  by the  $t$ -dependent term  $\gamma_{\pm}^j / p^{2l+1} q^{2j+1}$ , defining  $\gamma_{\pm}^j$  such that

$$M\Gamma = \gamma_{\pm}^j / p^{2l+1} q^{2j+1} \Big|_{\epsilon=M^2}$$

The absorptive part of each amplitude  $f_{\pm}(\epsilon)$  now has the form

$$\text{Im } f_{\pm}^{(\pm)j}(\epsilon) = \frac{g_{\pm}^j \gamma_{\pm}^j / p^{2l+1} q^{2j+1}}{(t - t_0)^2 + (\gamma_{\pm}^j / p^{2l+1} q^{2j+1})^2} \quad (4.6)$$

The coupling constants  $g_{\pm}^j$  are determined by inverting Eq. (2.22) at  $t_0 = M^2$ , which yields

$$\begin{aligned} g_{j+1}^j &= \left( \frac{2j}{2j+1} \right)^{1/2} g_{-} - \left( \frac{2j+2}{2j+1} \right)^{1/2} g_{+} \\ g_{j-1}^j &= \left( \frac{2j+2}{2j+1} \right)^{1/2} g_{-} + \left( \frac{2j}{2j+1} \right)^{1/2} g_{+} \end{aligned} \quad (4.7)$$

There is still another difficulty to be overcome at the  $N\bar{N}$  threshold.

The  $j=1, l=0$  state  $f_0^{(\pm)1}(\epsilon)$  behaves like  $q^3 p$  as  $p$  approaches zero, which will not overcome the  $1/p^2$  term in  $A^{(\pm)}(t, \cos\phi)$ , although all the other states will be finite at  $p=0$ . This difficulty can easily be overcome by momentarily reverting to the Mandelstam representation. In this case Frazer and Fulco<sup>(30)</sup> have shown that the partial waves of the amplitudes  $A^{(\pm)}(t, \cos\phi)$ ,  $B^{(\pm)}(t, \cos\phi)$  converge at least as rapidly as  $(pq)^j +$

$\mathcal{O}(pq)^{1/2}$ ...etc. as either  $p$  or  $q$  approaches zero. Combining this requirement with the  $N\bar{N}$  angular momentum barrier factor  $p^{2\ell+1}$ , it can be shown that the  $J=1$  amplitude must converge at least as rapidly as  $p^2$  as  $p$  approaches zero.

To do this first invert Eq. (2.19) giving

$$f_{\pm}^{(\pm)J} = \frac{1}{8\pi} \left\{ -\frac{p^2}{(pq)^2} A_J^{(\pm)} + \frac{mv}{2J+1} \frac{1}{(pq)^{J+1}} [(J+1)B_{J+1}^{(\pm)} + J B_{J-1}^{(\pm)}] \right\} \quad (4.8)$$

$$f_{\pm}^{(\pm)J} = \frac{1}{8\pi} \frac{\sqrt{2(J+1)}}{2J+1} \frac{1}{(pq)^{J+1}} \{ B_{J+1}^{(\pm)} - B_{J-1}^{(\pm)} \}$$

The amplitude we are concerned with is the  $J=1, \ell=0$  state. In this case the threshold properties deduced by Frazer and Fulco reduce to

$$f_{\pm}^{(\pm)1} \sim \text{Const} + \mathcal{O}(p^2)$$

However, this state is composed of  $\ell=0, 2$   $N\bar{N}$  states which guarantees that  $f_{\pm}^{(\pm)1}$  converges at least as rapidly as  $p^1$ . Thus the constant must be zero and so the first non-zero term is at least quadratic in nucleon momentum. This behavior is guaranteed by adding an additional factor of  $p$  in the  $t$ -dependence of the width of the  $J=1, \ell=0$  amplitude  $f_{\pm}^{(\pm)1}$ . Thus no term in Eq. (2.19) converges slower than  $p^2$  at the  $N\bar{N}$  threshold and the apparent singularity in  $A^{(\pm)}(t, \cos\phi)$  at this point is removed.

#### D. The Preliminary Spectral Functions

The spectral functions constructed according to the specifications of the preceding sections of this chapter are presented in Figures 6 through 11. Even or odd moments of these functions generate the corresponding FESR.

The parameters of the mesons used to construct the  $t$ -channel amplitude are listed in Table 3 along with their coupling constants. In order to compare these values with those in Table 2 we quote the coupling

	$I$	$J$	Mass (GeV)	Width (GeV)	$g_+$	$g_-$
$\epsilon$	0	0	.725	.400	$1.39 \text{ GeV}^3$	....
$\rho$	1	1	.765	.125	$2.67 \text{ GeV}$	$14.42 \text{ GeV}^0$
$f_0$	0	2	1.253	.145	$11.96 \text{ GeV}^{-1}$	$11.13 \text{ GeV}^{-2}$
$g$	1	3	1.660	.120	$4.28 \text{ GeV}^3$	$6.53 \text{ GeV}^{-1}$
$\rho'$	1	3	2.120	.250	$2.31 \text{ GeV}^5$	$3.01 \text{ GeV}^6$

Table 3. Parameters for the meson states used to construct the t-channel amplitude.

Figure 6. The spectral functions for the state described by the amplitude  $F_-^N(X,u)$ . Moments of this function generate the  $N_-$  FESR. The spectral functions are shown for  $u=0$ . The solid curve is the Regge spectral function. The dashed curve is the low energy spectrum.

Figure 7. The  $F_-^A(X,u)$  spectral functions  $u=0$ . As in Fig. 5 the solid and dashed curves represent the Regge and low energy spectral functions respectively.

Figure 8. The  $F_-^N(X,u)$  spectral functions at  $u=1.0 \text{ GeV}^2$ .

Figure 9. The  $F_+^N(X,u)$  spectral functions at  $u=1.0 \text{ GeV}^2$ .

Figure 10. The  $F_-^A(X,u)$  spectral functions at  $u=1.0 \text{ GeV}^2$ . The Regge term is essentially zero in this case.

Figure 11. The  $F_+^A(X,u)$  spectral functions at  $u=1.0 \text{ GeV}^2$ . Again, the Regge term is essentially zero.

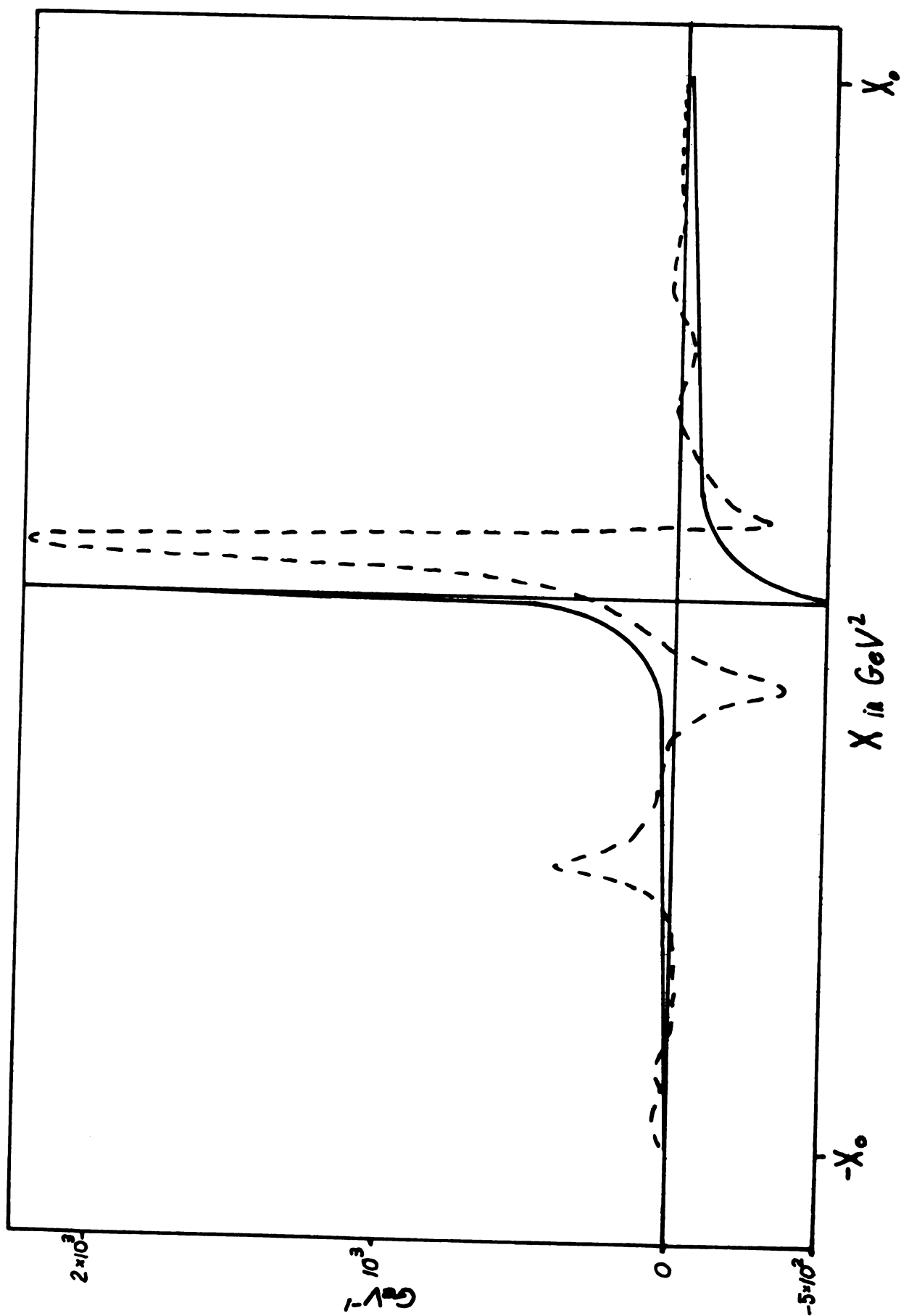


FIGURE 6

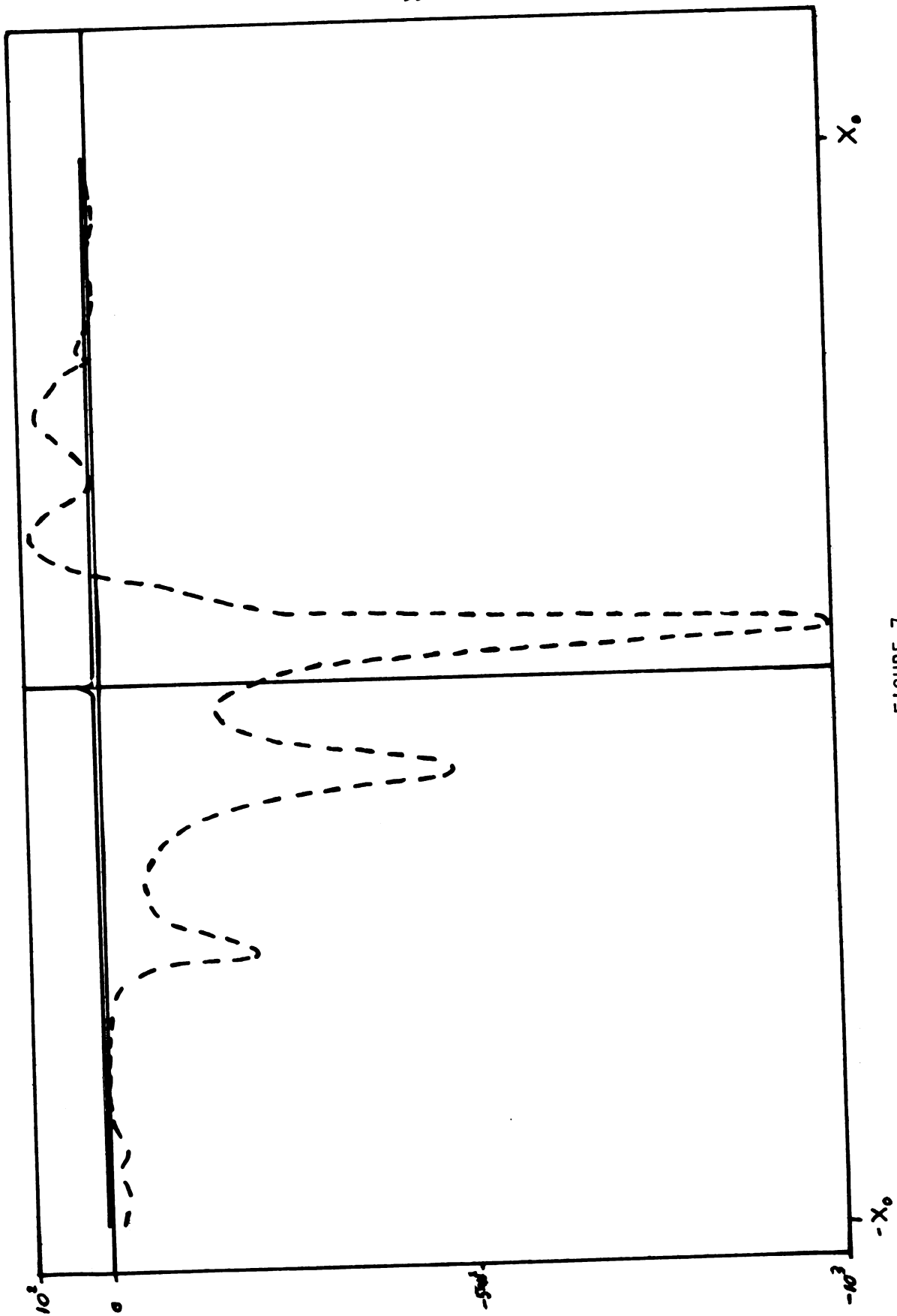


FIGURE 7

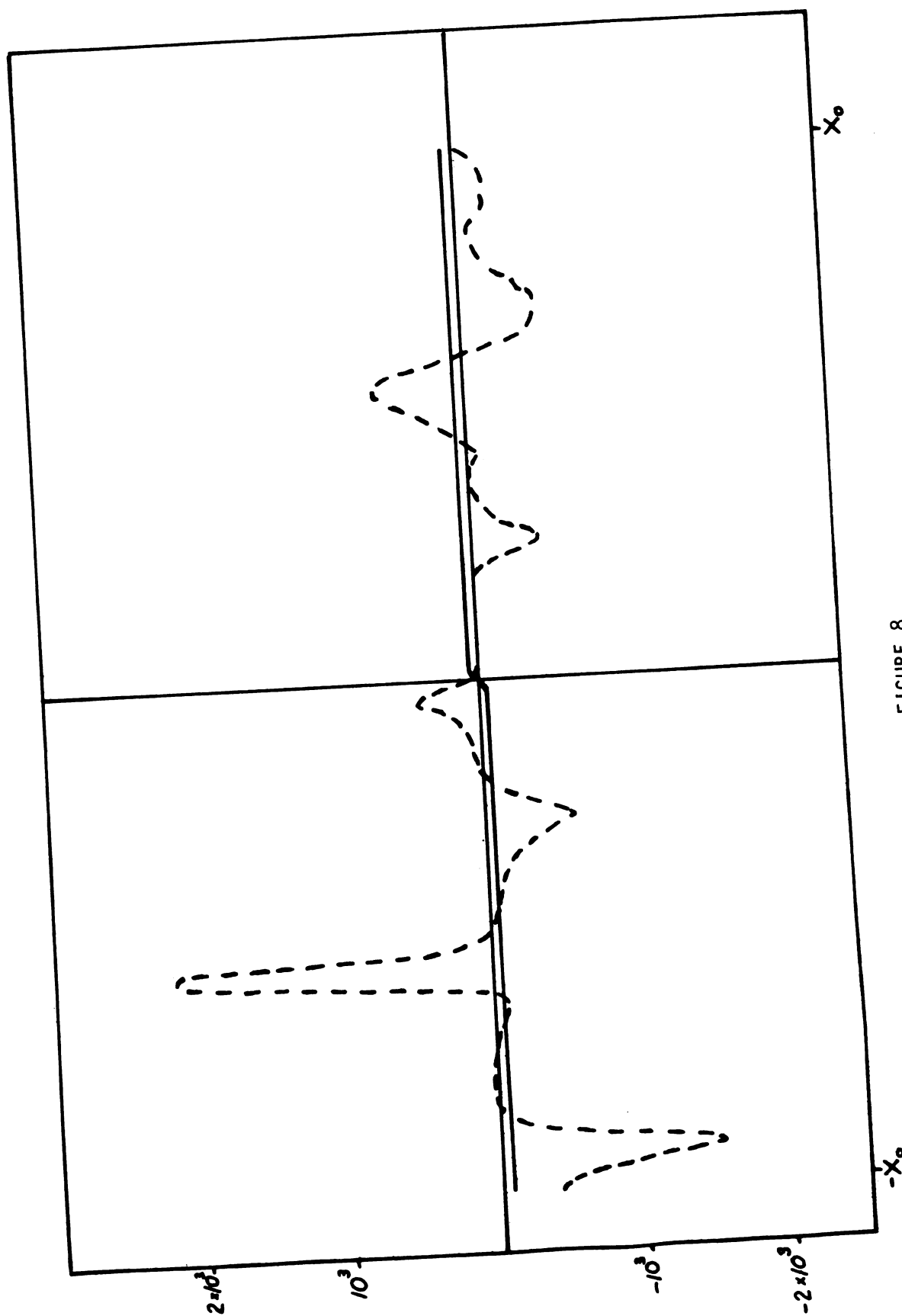


FIGURE 8



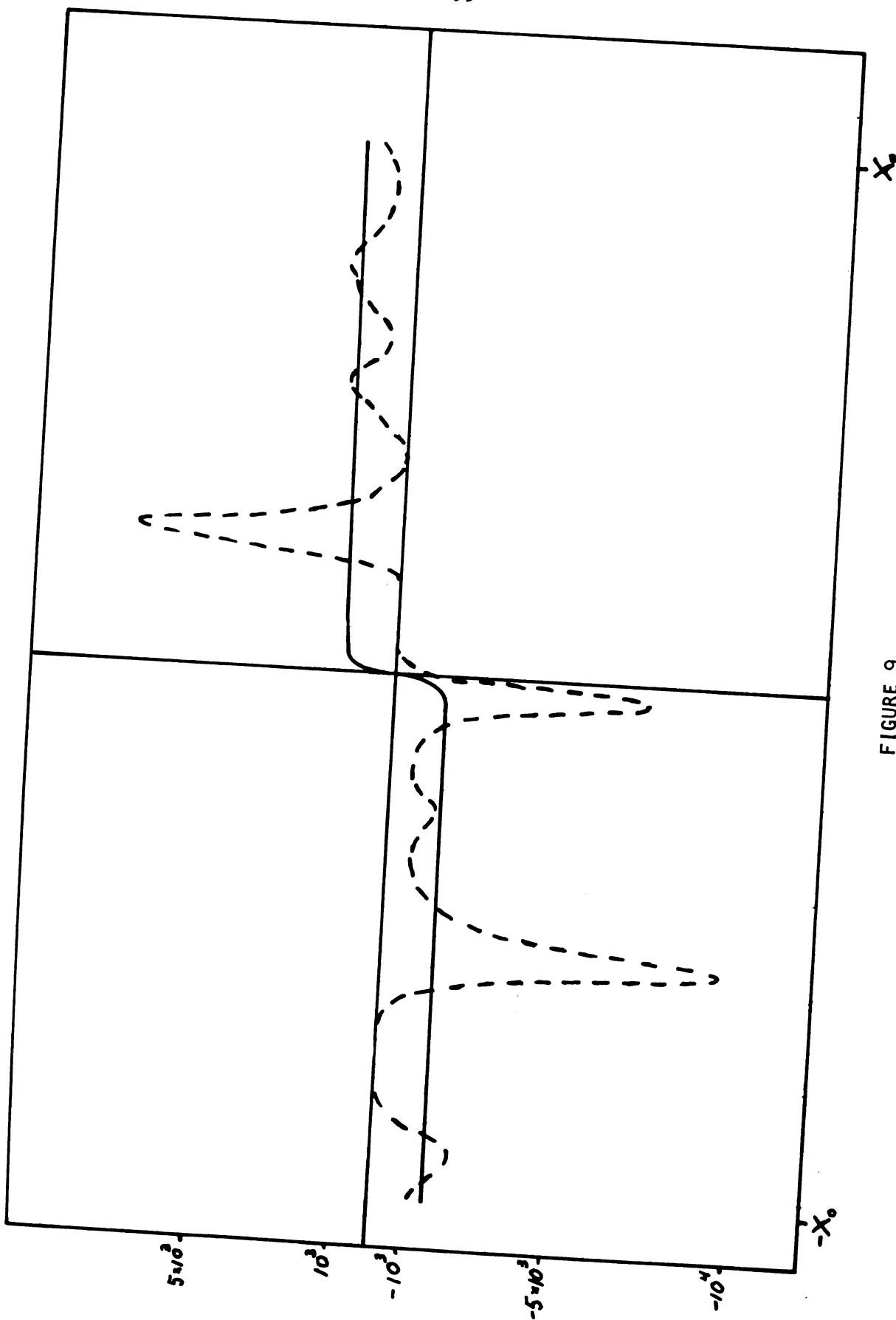


FIGURE 9

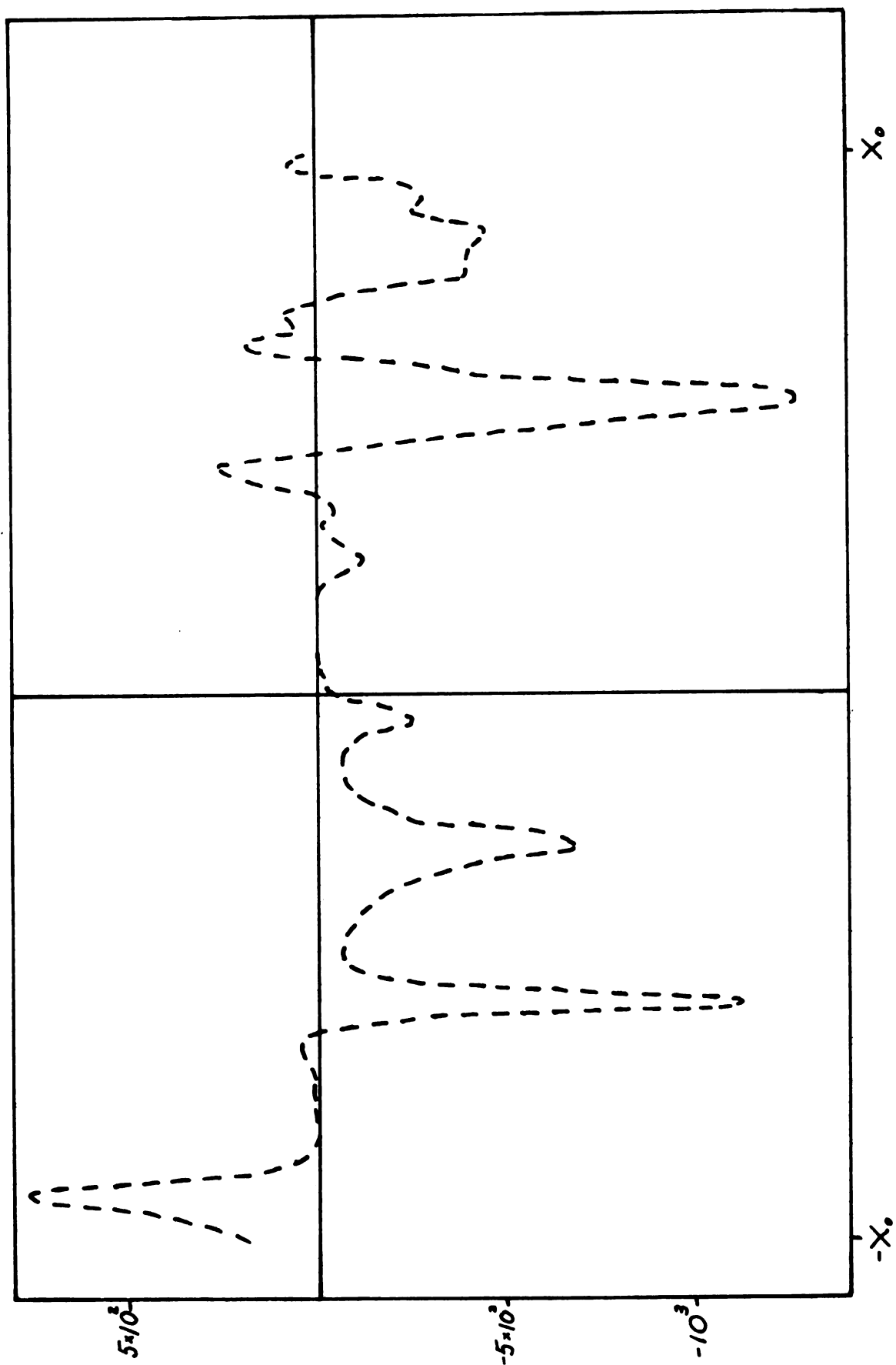


FIGURE 10

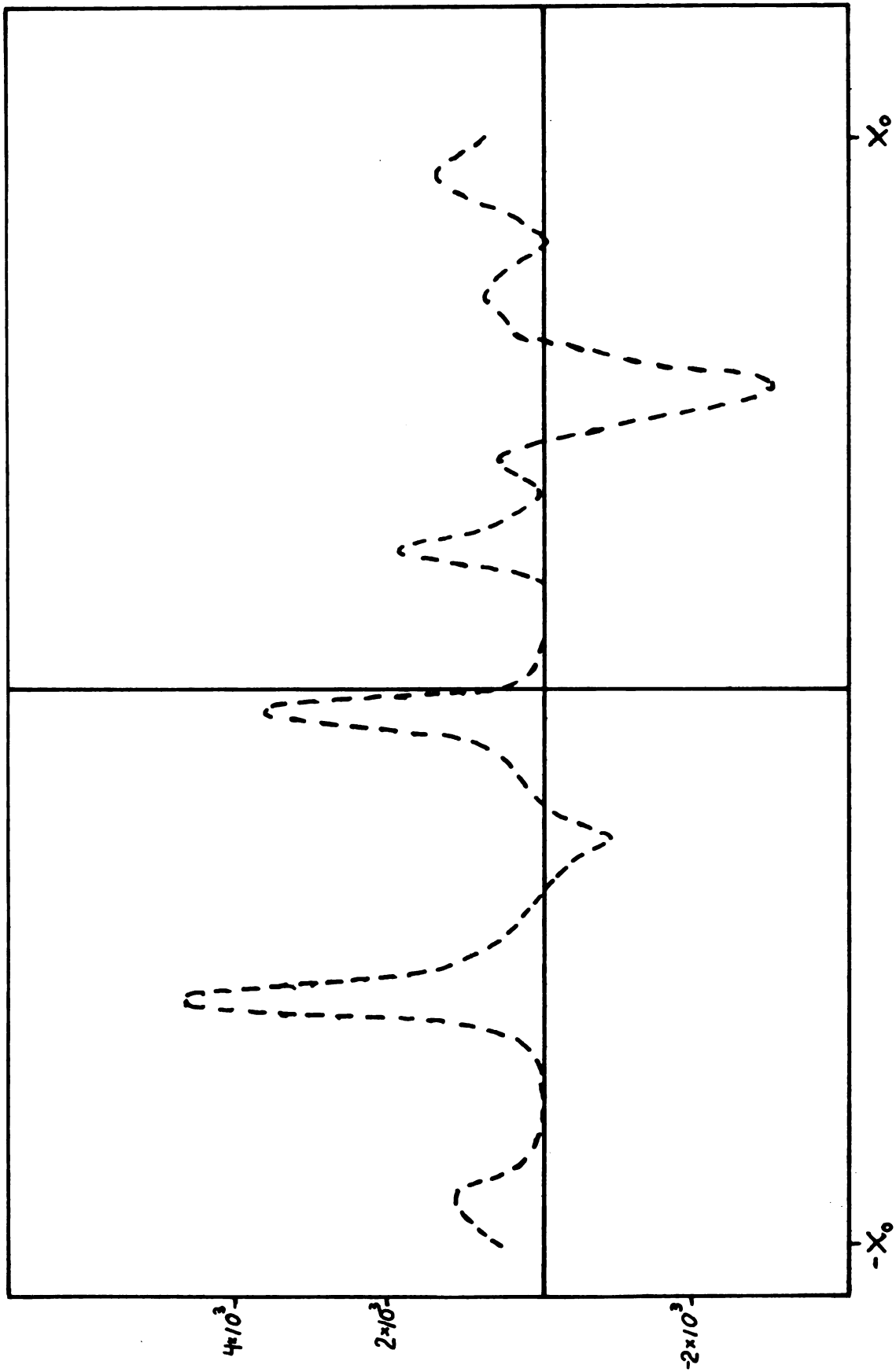


FIGURE 11

constants  $g_{\pi}$  rather than  $g_{\pi}'$ . In addition we have added one more meson in order to extend the t-channel spectrum to  $-X_0$ . This state, labelled  $\rho'$ , is known to couple to both  $2\pi$  and  $N\bar{N}$  states and was selected from the list of high mass suspected mesons for this reason. The coupling constants of the  $\rho'$  were selected to enhance the agreement of the  $N_{\pi}$  and  $N_{\rho}$   $n=1$  FESR near  $u=1.0 \text{ GeV}^2$ .

Including the  $\rho$  and  $\epsilon$  at their proper masses produced rather large changes in their coupling constants, although the other refinements we have made affected them little as can be seen by comparing the  $f_0$  and  $g$  coupling constants in Tables 2 and 3.

The s-channel spectral function were generated from the EXP phases to take advantage of their better convergence properties (see Figures 4 and 5).

Before examining the spectral function in detail note that at  $u=0$  the amplitudes  $F_{\pm}$  are simply the negative of one another. In this case Eq. (4.1) reduces to  $F_{\pm} = \mp (A + mB)$ . Thus at  $u=0$  we plot only  $F_{-}^{N\Delta}$ . These amplitudes have units of inverse energy; we plot them in units of  $\text{GeV}^{-1}$ . Figures 6 and 7 are the  $u=0$  spectral functions, Figures 8 through 11 show the  $u=1.0 \text{ GeV}^2$  spectral functions.

Some general features can be seen in Figure 6 showing the spectral function for the state described by  $F_{-}^N(X,u)$ . First, the divergence at the  $N\bar{N}$  threshold (near  $-X_0$ ) has been eliminated. The large peak just to the right of  $X=0$  is the  $\rho$ . The  $f_0$  and  $g$  are well resolved peaks on the negative  $X$  axis. The  $\epsilon$  lies under the  $\rho$  and can be seen only as a shoulder to the left of the  $\rho$ . The  $N_{33}^*$  overlaps the  $\rho$  on the right and appears as a somewhat attenuated dip. The Regge amplitude is singular at  $X=0$  since, for  $u=0$ ,  $\alpha_{-1/2} = -.88$  so that the amplitude diverges as  $X^{-.88}$ .

The convergence properties of the low energy spectral function is particularly good at  $u=0$ . The amplitude is dominated by the resonances occurring at low  $X$  and the higher resonances damp out monotonically as  $X$  approaches  $\pm X_0$ . This behavior is also evident in  $F_-$  at  $u=0$  (Figure 7). However, good convergence properties alone do not guarantee that the FESR will be satisfied (In fact the  $\Delta$ FESR are not nearly so well satisfied as the N FESR).

The spectral functions at  $u=1.0 \text{ GeV}^2$  are plotted in Figures 8 through 11. Unlike the  $u=0$  case the oscillations in the low energy amplitude do not damp out as  $X$  approaches  $\pm X_0$  but in some cases even increase, although a few of the amplitudes still show relatively good convergence.

This distortion is due to the fact that  $\cos\phi$  and  $\cos\theta$  are larger in magnitude along the line  $u=1.0 \text{ GeV}^2$  than at the corresponding value of  $X$  along  $u=0$ . The higher terms in each partial wave series (the high energy contributors) are beginning to dominate the lower terms. This is the situation mentioned previously in Chapter 2. The partial wave series deteriorates, as any polynomial approximation does, if extrapolated too far from the region in which the successive coefficients (in this case the s- and t-channel partial wave amplitudes) were fitted to actual data. In the next section we shall examine some attempts to deal with this situation.

#### E. Transforming the Partial Wave Series

Before considering how the approximation of fitting a scattering amplitude to a few partial waves can be improved we will first consider some of the basic limitations of the Legendre series itself.

If we consider energy and angle as basic independent variables to describe the scattering amplitude in some channel it is clear that cross-

channel singularities appear as poles in the  $x = \cos\theta$  plane. At a fixed energy the partial wave series has the form of a Taylor expansion about  $x=0$ . The series converges for  $-\mathcal{N}_0 \leq x \leq \mathcal{N}_0$ , where  $\mathcal{N}_0$  is the magnitude of  $\cos\theta$  at the pole nearest to  $x=0$ .

In the s-channel the nearest singularity in the  $\cos\theta$  plane is encountered at the t-channel threshold  $t = 4\mu^2$ . To see this note that

$$\cos\theta|_{t=4\mu^2} = 1 + 2\mu^2/k^2$$

If we now evaluate  $u$  at  $\cos\theta = -(1 + \frac{2\mu^2}{k^2})$  we find

$$u = (m^2 - \mu^2)^2/\Delta + 4\mu^2$$

These values are only  $4\mu^2$  larger than the value of  $u$  in the backward direction. Hence the region of convergence of the Legendre series falls far short of the u-channel threshold. This can be seen in Figure 12.

In the t-channel the cross-channel thresholds are symmetric, since  $\cos\phi$  can be expressed as

$$\cos\phi = \frac{s - u}{4pq}$$

Thus the values of  $\cos\phi$  at the s and u-channel thresholds for fixed  $t$  are the negative of one another and the t-channel Legendre series converges throughout the region between the cross-channel cuts.

In the context of the Mandelstam representation it can be shown that the Legendre expansion converges not only along  $-\mathcal{N}_0 \leq x \leq \mathcal{N}_0$  but throughout an ellipse in the  $x = \cos\theta$  complex plane. The semi-major and semi-minor axes are  $\mathcal{N}_0$  and  $\sqrt{\mathcal{N}_0^2 - 1}$  with foci at  $x = \pm 1$ . This is the so-called Lehmann ellipse<sup>(31)</sup>. Figure 12 indicates the intersection of the Lehmann ellipse with the region throughout which the spectral functions are calculated in the present case.

The finite extent of the region of convergence of the Legendre

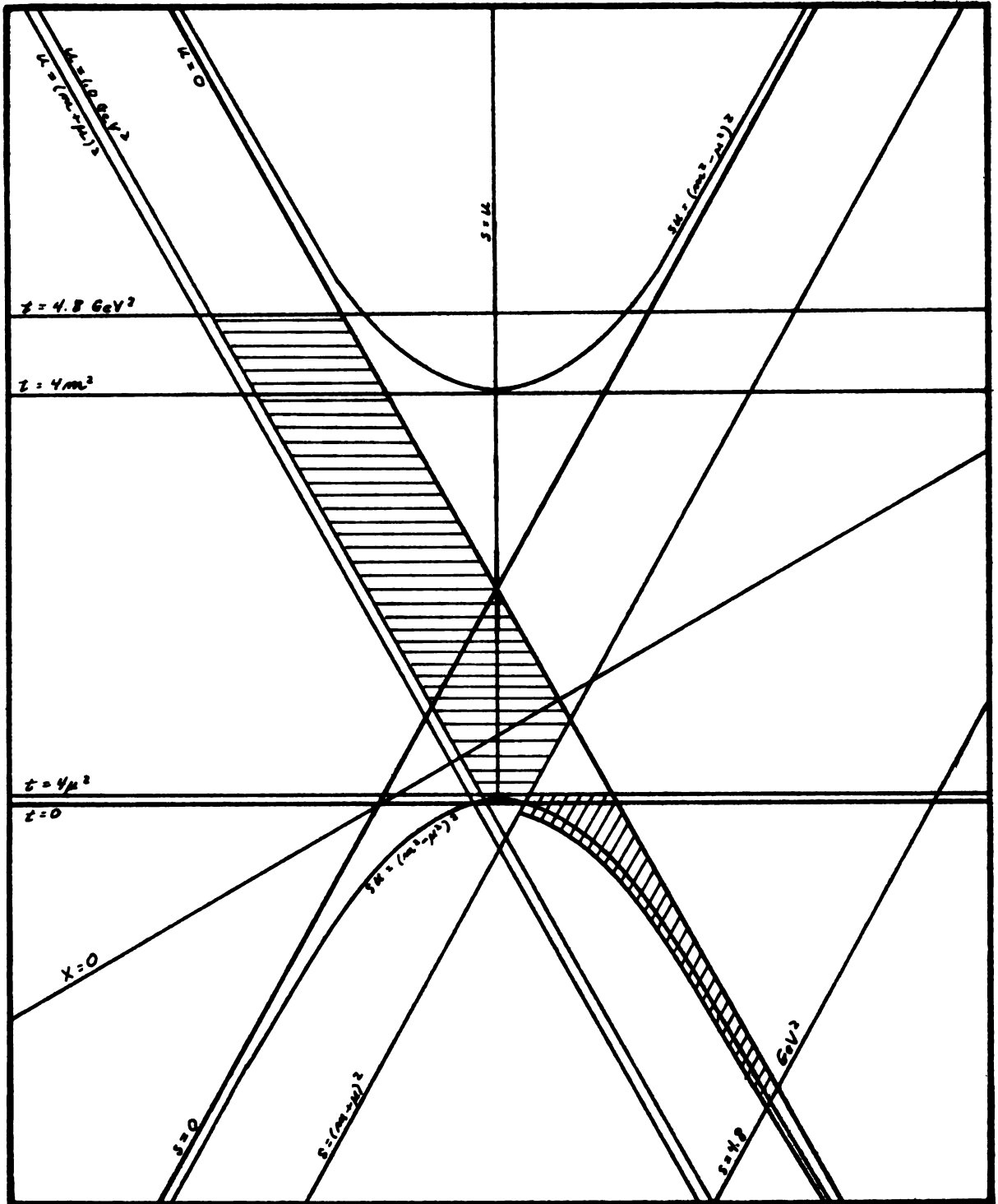


Figure 12. The intersection of the regions of convergence of the s-channel and t-channel Legendre series with the region in which the FESR are calculated.

series is a serious obstacle to applying any technique which requires extrapolating the scattering amplitudes outside the physical region. In the present case the s-channel spectral function has to be extrapolated beyond the Lehmann ellipse in the forward direction for small  $u$  and in the backward direction for large  $u$ . For  $u \geq \frac{(m^2 - \mu^2)^2}{2} + 4\mu^2$  the entire s-channel cut lies outside the region of convergence of the Legendre series.

Extrapolating a finite approximation to the Legendre series (constructed from a few low- $l$  partial waves) beyond the limits of convergence will obviously produce a finite result. Further, although the procedure is not mathematically justified, a comparison of corresponding  $u=0$  and  $u=1 \text{ GeV}^2$  spectral functions makes it clear that some of the information content of the physical region is preserved in the process. One could reasonably hope to improve this situation in two respects. In the s- and u-channel the region of convergence could be extended to include the entire region between the cross-channel cuts as in the t-channel case. Also it is evident that one can never fit more than a finite number of partial waves to data in the physical region. Such a finite approximation to the full Legendre series cannot reproduce the analyticity properties of the amplitudes in the  $\cos\theta$  plane. One cure for this situation is to replace  $x$  by a coordinate which itself is an analytic function in the  $\cos\theta$  plane with cuts corresponding to the cross-channel singularities.

A transformation possessing the desired properties has been constructed by Cutkosky and Deo<sup>(32)</sup>. In our problem this transformation has been useful in reducing somewhat the unsatisfactory features of  $u = 1.0 \text{ GeV}^2$  spectral functions.

This transformation is effected in two stages. First the cuts  $(-\infty, -1_-)$ ,  $(1_+, \infty)$  in the  $\cos\theta$  plane are mapped into the symmetric



cuts  $(-\infty, -W)$ ,  $(W, \infty)$  in the  $w$  plane by the mapping

$$w = (x - y_0) / (1 - x y_0) \quad (4.9)$$

where

$$y_0 \equiv (x_- - x_+) / (x_+ x_- + Z_+ Z_- - 1)$$

$$Z_{\pm} \equiv \sqrt{x_{\pm}^2 - 1}$$

$$W \equiv -w(-x_-) = w(x_+)$$

Note first that this transformation maps the physical region into itself.

In the  $t$ -channel  $x_+ = x_-$  so that  $y_0 = 0$ . Then of course  $w = x$ . In the  $s$ -channel however this transformation extends the region of convergence of the Legendre series (in  $w$ ) to include the entire region between the  $t$ - and  $u$ -channel branch points. However a finite expansion in place of  $x$  would not explicitly exhibit the analytic structure of a  $\pi N$  scattering amplitude since  $w$  has only a simple pole at  $x = 1/y_0$ .

The second stage of the Cutkosky-Deo transformation is to map  $w$  into the  $z$ -plane by the transformation

$$z = \sin(\Phi(w, \beta)) \quad (4.10)$$

where

$$\beta \equiv 1/W$$

$$\Phi(w, \beta) = (\pi/2) F(\sin^{-1} w, \beta) / K(\beta)$$

$$F(b, a) \equiv \int_0^b \frac{dx}{\sqrt{1 - a^2 \sin^2 x}}$$

$$K(a) \equiv \int_0^{\pi/2} \frac{dx}{\sqrt{1 - a^2 \sin^2 x}} = F(\pi/2, a)$$

The functions  $K(a)$  and  $F(b, a)$  are respectively the complete and incomplete Elliptic Integrals of the first kind<sup>(33)</sup>. This transformation maps  $x = \pm 1$  into  $z = \pm 1$  (to see this substitute  $w = \pm 1$  into 4.10). The coordinate  $z$  is an analytic function of  $w$  with branch cuts  $(-\infty, -W)$  and  $(W, \infty)$  in the

w-plane. As a function of  $x$ , then  $z$  possesses the analytic structure of the cross-channel cuts. To see this note that the denominator of  $F(\sin^{-1} \lambda, \beta)$  will be singular for  $|w| > W$ , i.e., for  $x$  outside the range  $-W \leq x \leq W$ . If we now consider a  $\pi N$  scattering amplitude approximated by a finite power series in  $z$ , even this finite approximation contains information regarding the cross-channel cuts which was absent from a finite Legendre series in  $x$ .

At any energy one can calculate  $z$  as a function of  $x$  or  $x$  in terms of  $z$  very efficiently by means of the Landen transformation<sup>(34)</sup>. The Landen transformation is a set of recursion relations which allows the values  $b_0, a_0$  of the arguments of  $F(b, a)$  to be replaced by a pair of values  $b_1, a_1$  such that

$$F(b_1, a_1)/K(a_1) = F(b_0, a_0)/K(a_0)$$

Writing the incomplete elliptic integral of the first kind as

$$F(\sin^{-1} \lambda, \beta) = \int_0^{\sin^{-1} \lambda} \frac{dx}{\sqrt{1 - \beta^2 \sin^2 x}} \quad (4.11)$$

the recursion relations take the form

$$\beta_1 = (1 - \sqrt{1 - \beta_0^2}) / (1 + \sqrt{1 - \beta_0^2}) \quad (4.12)$$

$$\lambda_1 = \lambda_0 (1 + \sqrt{1 - \beta_0^2}) / (1 + \sqrt{1 - \lambda_0^2 \beta_0^2})$$

Since  $\beta_0 \equiv 1/W$  is less than unity,  $\beta_{m+1} < \beta_m$ . If we apply these relations repeatedly the parameter  $\beta$  will eventually be reduced to zero. From (4.10) and (4.11) we see that  $z$  will be equal to the corresponding value of  $\lambda$ . Since the successive values of  $\beta$  are independent of  $\lambda$  one can use them to recover  $x$  if  $z$  is known, simply by inverting (4.12). Details of the procedure are presented in the work cited in reference 33.

This mapping also preserves the threshold properties of the partial wave expansion. This is apparent since  $W$  approaches infinity as either  $p$ ,  $q$ , or  $k$  vanishes. Equation (4.10) then gives  $z = x$ . This guarantees that the  $t$ -channel amplitudes will be well-behaved as functions of  $z$ . Figures 13 and 14 illustrate the behavior of  $z$  as a function of  $x$  in the  $s$ -channel. Figure 15 shows  $z$  and  $x$  at a representative value of  $t$ .

The Cutkosky-Deo transformation does not specify the form of the scattering amplitude as a function of  $z$  which is to replace the Legendre series in  $x$ . One approach would be to replace  $x$  by  $z$  in the partial wave expansions (2.14) and (2.19), replacing the partial wave amplitudes themselves by a set of 'transformed' partial waves.

We have investigated this approach in detail for the  $s$ -channel amplitudes. In this case the 'transformed' partial waves are defined by

$$f_1(k, \cos \theta) = \sum_{l=0} \tilde{f}_{l+}(k) P'_{l+}(z) - \sum_{l=2} \tilde{f}_{l-}(k) P'_{l-}(z)$$

$$f_2(k, \cos \theta) = \sum_{l=1} \{ \tilde{f}_{l-}(k) - \tilde{f}_{l+}(k) \} P'_l(z)$$

$$\tilde{f}_{l\pm}(k) \equiv \frac{1}{2} \int_{-1}^{+1} \{ f_1(k, \cos \theta) P_l(z) + f_2(k, \cos \theta) P'_{l\pm}(z) \} dz$$

The transformed partial waves  $\tilde{f}_{l\pm}(k)$  no longer correspond to good  $L$  and  $J$  except at threshold; however this nomenclature is more than simply a convenience. One would expect that the improved analyticity properties of the transformed partial wave series would allow an equally good description of  $\pi N$  scattering with fewer terms in the series. Thus we might hope to eliminate the "small" G and H waves from the expansion. This led us to attempt two expansions of the form of Eq. (4.13), the first containing only S, P, D, F transformed partial waves, a total of

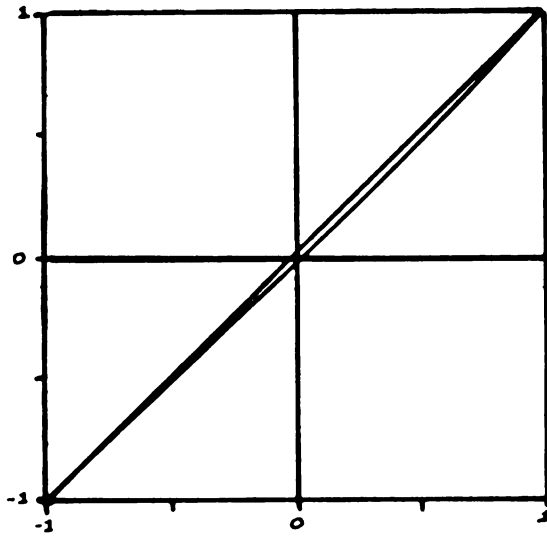


Figure 13. Graphs of  $x$  and  $z$  in the physical region just above the  $s$ -channel threshold, ( $W=1.1$  GeV).

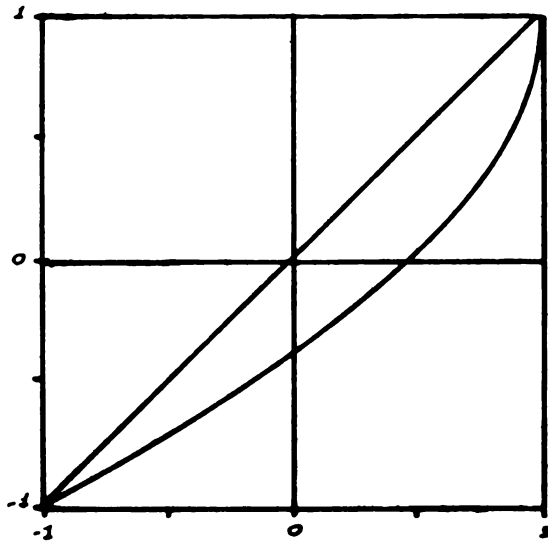


Figure 14. Graphs of  $x$  and  $z$  in the physical region well above the  $s$ -channel threshold, ( $W=1.8$  GeV).

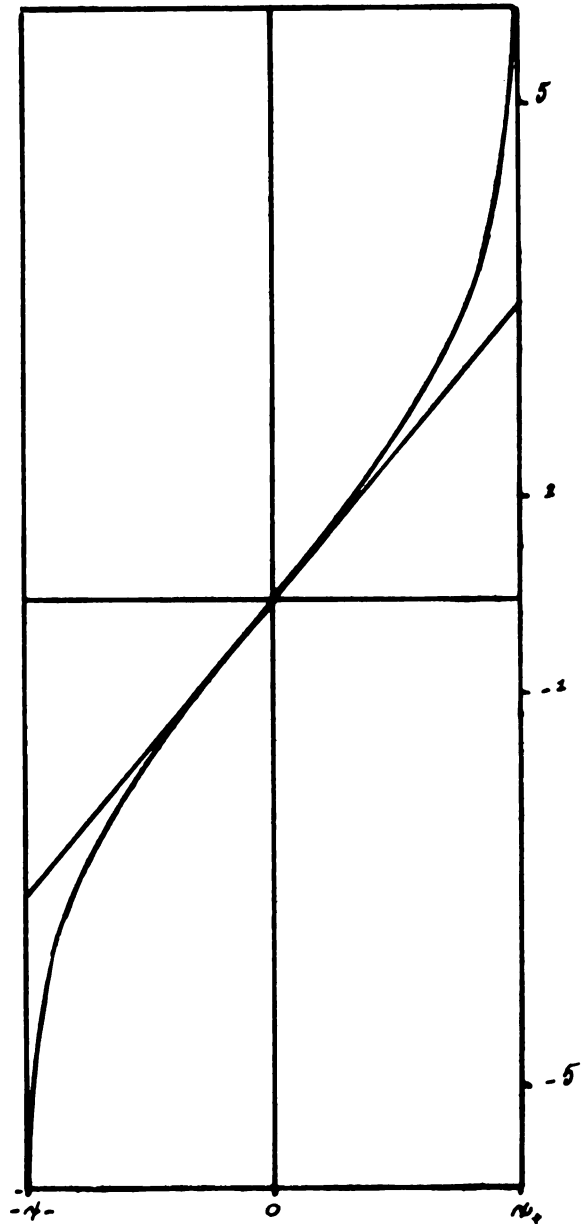


Figure 15. Graphs of  $x$  and  $z$  in the  $t$ -channel covering the region  $(-x, x+)$ . These graphs were plotted at  $t=4.125$  GeV<sup>2</sup>.

14 terms, and the second containing S through H waves, 22 terms in all, the same number of terms as the CERN phases used as 'data'.

The results of this calculation are presented in part in Figure 16 which shows the  $F_+^N$  spectral function in the s-channel for  $u=1.0 \text{ GeV}^2$ . The 14 term and 22 term transformed partial wave expansions easily reproduce the lower energy structure of the partial wave expansion. However, the 14 term transformed expansion fails completely to reproduce the high energy behavior of the amplitude while the 22 term expansion wildly exaggerates that structure. Further, neither transformed expansion possesses acceptable Regge convergence properties. From Figure 16 it is apparent that some transformed partial wave expansion of more than 14 terms but less than 22 terms might very well be able to reproduce the content of the partial wave expansion but it would be unlikely to represent any real improvement in general as a means of performing the extrapolation from the physical region.

An alternative procedure is to preserve the form of equations (2.14) and (2.19) in their respective physical regions, expanding  $x$  in orthogonal polynomials in  $z$ . We have chosen to write

$$N = \sum_m a_m P_m(z) \quad (4.14)$$

$$a_m = (m+1/2) \int_{-1}^{+1} N P_m(z) dz$$

Since  $x = \pm 1$  map into  $z = \pm 1$  we have the constraints

$$\sum_m a_m = 1 \quad ; \quad \sum_m (-)^m a_m = -1 \quad (4.15)$$

In order to preserve the information content of the partial wave expansions in their respective physical regions we require that the constraints be satisfied to 1 part in  $10^6$ . The resultant spectral functions reproduce the partial wave expansions exactly within their respective physical

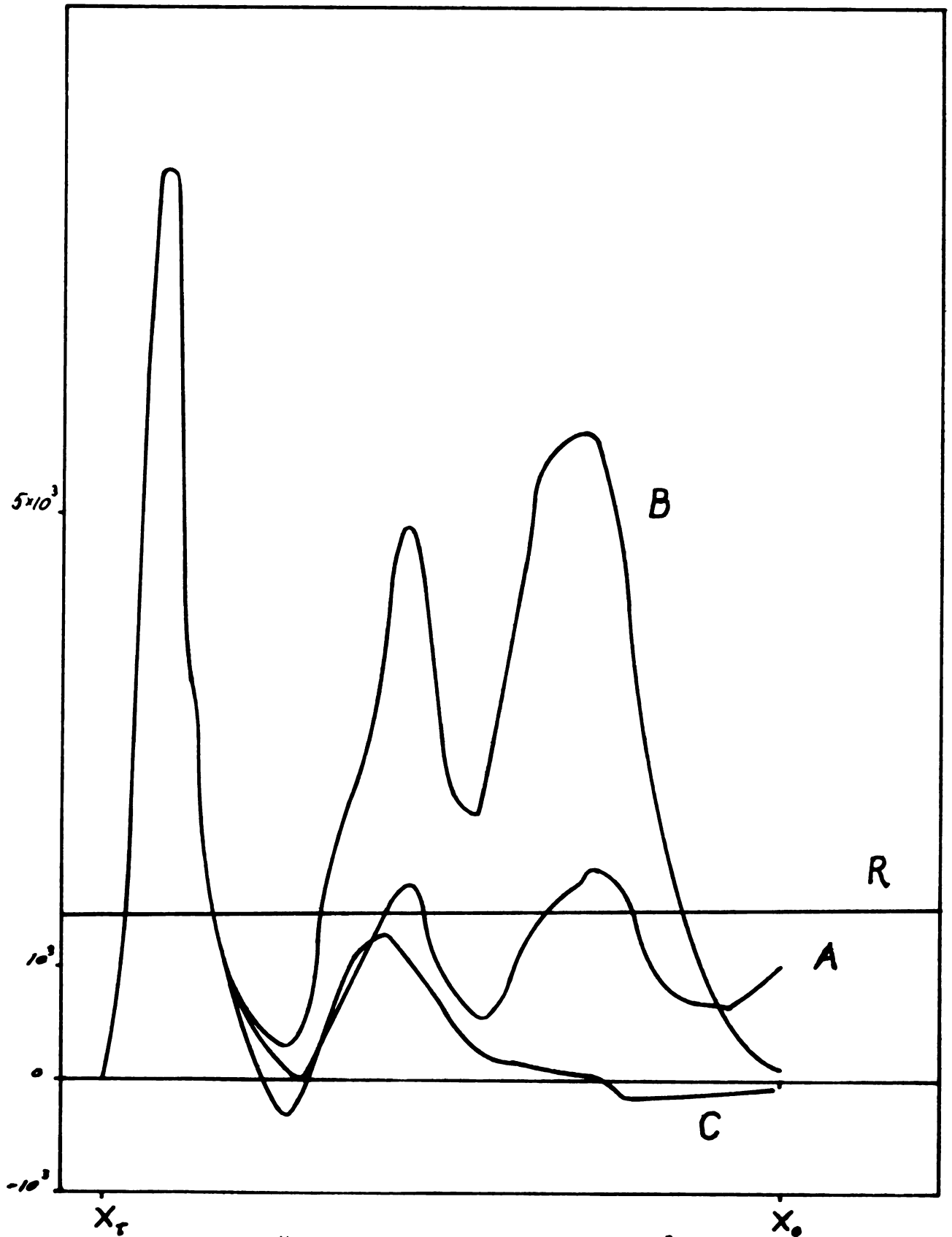


Figure 16. The  $F_+^N$  spectral function at  $u=1.0 \text{ GeV}^2$  near  $X=X_0$ . A, B, C, R label the amplitudes generated using 22 partial waves, 22 transformed partial waves, 14 transformed partial waves, and the Regge amplitude respectively. The value of  $X$  at the  $s$ -channel threshold  $X_t$  is  $.78 \text{ GeV}^2$ .

regions but will differ outside.

The criterion we have used to determine when to truncate the expansion of  $x$  in terms of  $z$  means that the number of expansion coefficients required in Eq. (4.14) differs at various energies. In general the higher the energy the greater the number of coefficients required. Thus this technique does not produce a spectral function of fixed order in  $z$  at all energies. The higher-ordered partial waves are small at low energies but dominate the amplitude at high energies and large unphysical angles. Hence at high energies for large  $u$  the expansion in  $z$  generates significant contributions from very high ordered polynomials in  $z$  - - much higher than the original expansion in terms of  $x$ . Yet, the resultant expansion preserves the information content of the partial wave expansion well outside the physical region. Figure 17 shows the  $F_+^N$  spectral function generated at  $u=1.0 \text{ GeV}^2$  by this method. The expansion in  $z$  differs appreciably from the partial wave Legendre series in  $x$  only at high energies. As we shall see in the next section these small changes will have noticeable effects on the FESR, although they have only a slight effect on Regge convergence properties.

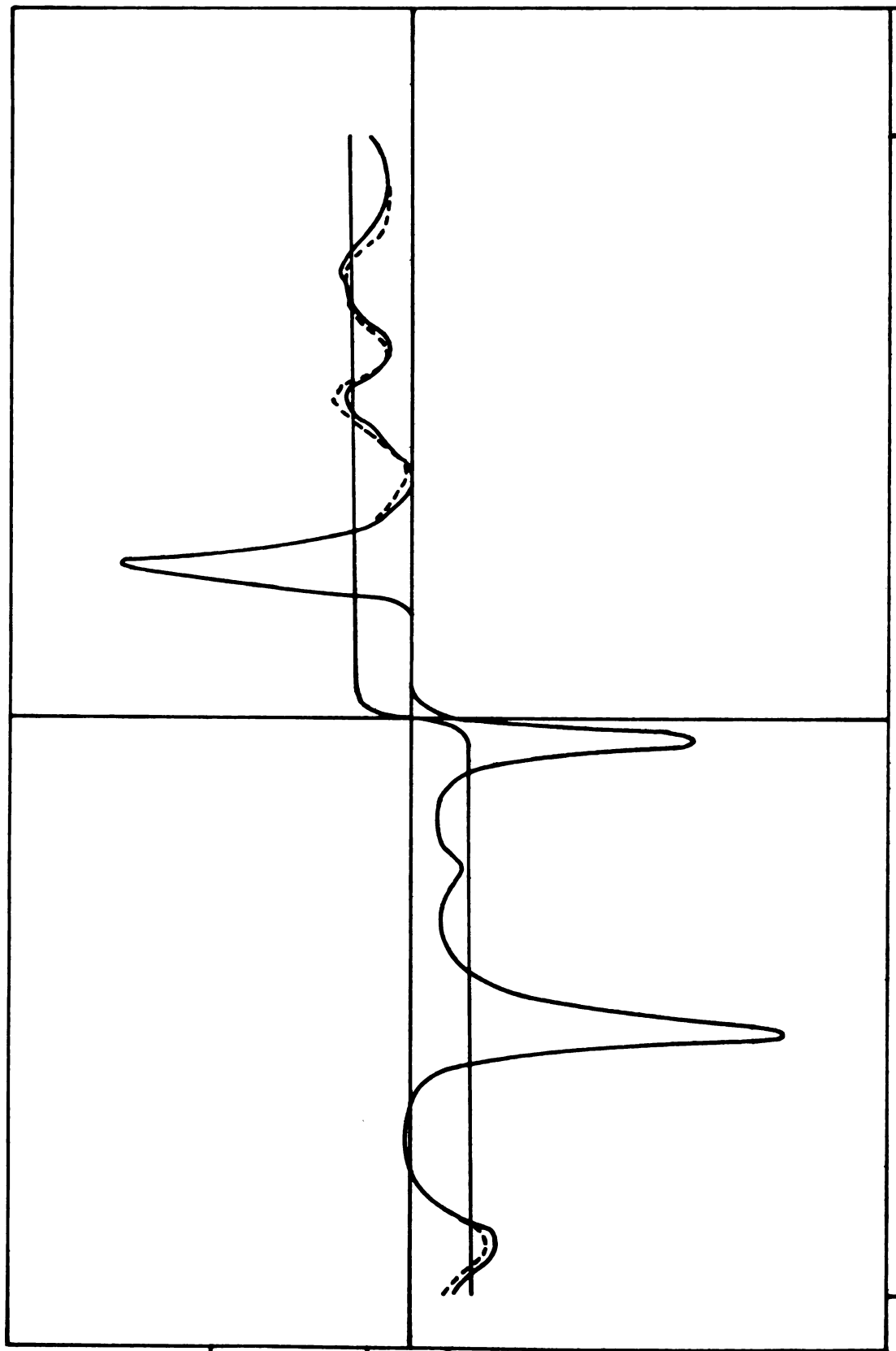


Figure 17. The  $F_+^N$  spectral function at  $u=1.0 \text{ GeV}^2$ . The solid curves are the Regge and low-energy spectral functions from Figure 9. The  $F_+^N$  spectral function generated by expanding  $x$  directly in terms of powers of  $z$  is shown by a dashed curve. Note that this curve diverges from the solid curve only for high energies ( $x$  near  $\pm x_0$ ).



## RESULTS AND DISCUSSION

A. The Finite Energy Sum Rules

The form of the FESR is given by Eq. (3.13). For the sake of comparing with Barger's results we introduce his normalization factor  $1/16\pi$ . The FESR now have the form

$$\frac{1}{16\pi} \int X^n \Im_{\text{Regge}} F(X, u) dX = \frac{1}{16\pi} \int X^n \Im F(X, u) dX \quad (5.1)$$

Isotopic spin and signature-parity indices have been suppressed for simplicity. Since  $n$  is unrestricted except that it be a non-negative integer Eq. (5.1) lists an infinite number of relations between the low-energy and Regge spectral functions for each of the four choices of isospin and signature-parity labels. The limited state of present knowledge of the singularities occurring on the  $t$ -channel cut make it unreasonable to expect that more than a few of the lower moments be meaningful. Further, our experience suggests that it is unnecessary to examine a large number of moments since any improvement in the lowest moment is always apparent in the higher moments. We have calculated moments up to  $n=5$  for each of the spectral functions using the standard Legendre series in  $\cos\theta$  and partial wave amplitudes. Only  $n=1$   $N_\alpha$  and  $N_\beta$  FESR were calculated using the expansion of  $x$  in terms of Legendre polynomials in  $z$  according to Eq. (4.14). Limited availability of computer time made it impractical to calculate any more moments in this case since approx-

imately 45 minutes of 6500 CP time were required in each case. Calculating only a few such moments is not a serious limitation since it can be seen from Figure 17 that the spectral functions generated by the Cutkosky-Deo continuation do not differ significantly in either qualitative or quantitative aspects from those generated by standard partial wave expansion since it can be seen from Figure 16 that these spectral functions possess markedly inferior Regge convergence properties and do not represent a meaningful way of satisfying the FESR without further elaboration.

#### B. The $N_{\pi}$ and $N_{\rho}$ FESR

The  $N_{\pi}$  FESR are more well satisfied than any other. The  $n = 1, 3, 5$  FESR are shown in Figures 18, 19 and 20 respectively. The real significance of these results is apparent only with reference to Figures 6 and 9 which demonstrate that the corresponding spectral functions possess good Regge convergence properties in addition to rather good agreement in the sum rules. As expected the FESR are progressively less well satisfied with increasing moment number. This is caused by not weighting the higher-mass states heavily enough. The confusion regarding the high-mass meson states made it impossible to include many of them. One would also have to include some higher partial waves in the s-channel and extend phase shift analysis to a somewhat higher energy before any marked improvement could be seen in the higher moments.

Note that the rather small high-energy variations between the spectral functions continued to  $u = 1.0 \text{ GeV}^2$  in x and z (Figure 17) produces a noticeable difference in their respective contributions to the  $n = 1$   $N_{\pi}$  FESR (Figure 18).

The  $N_{\rho}$  FESR is not so well satisfied as the  $N_{\pi}$  sum rules, at least qualitatively in that the low energy term does not reproduce the

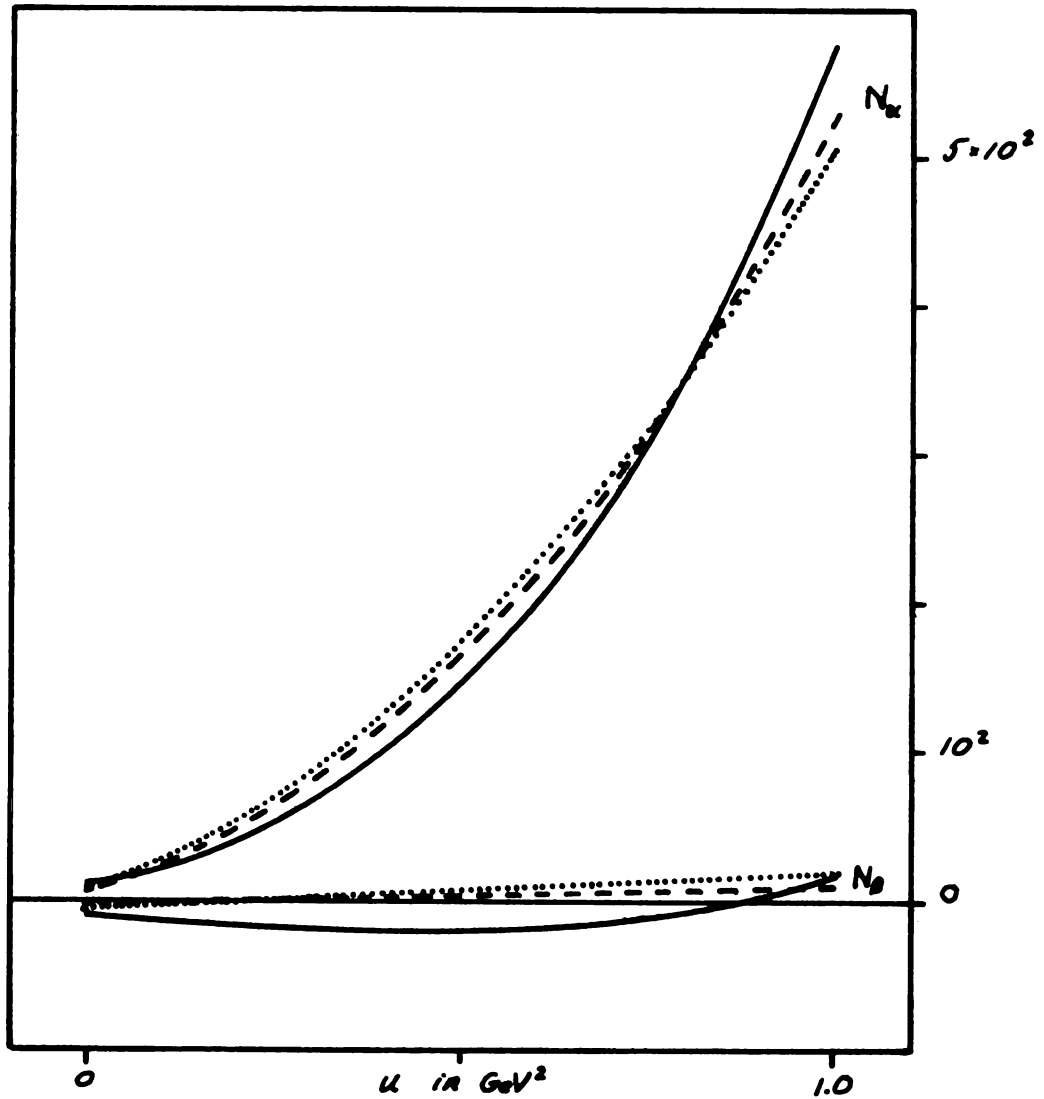


Figure 18. The  $n=1$   $N_+$  and  $N_0$  FESR. The Regge terms are indicated by solid lines. The low energy terms generated by the Legendre series in  $x$  are shown as dashed lines. Terms generated by the Cutkosky-Deo scheme are shown as dotted lines. If either sum rule were exactly satisfied the solid curve and the dashed or dotted curves would coincide.

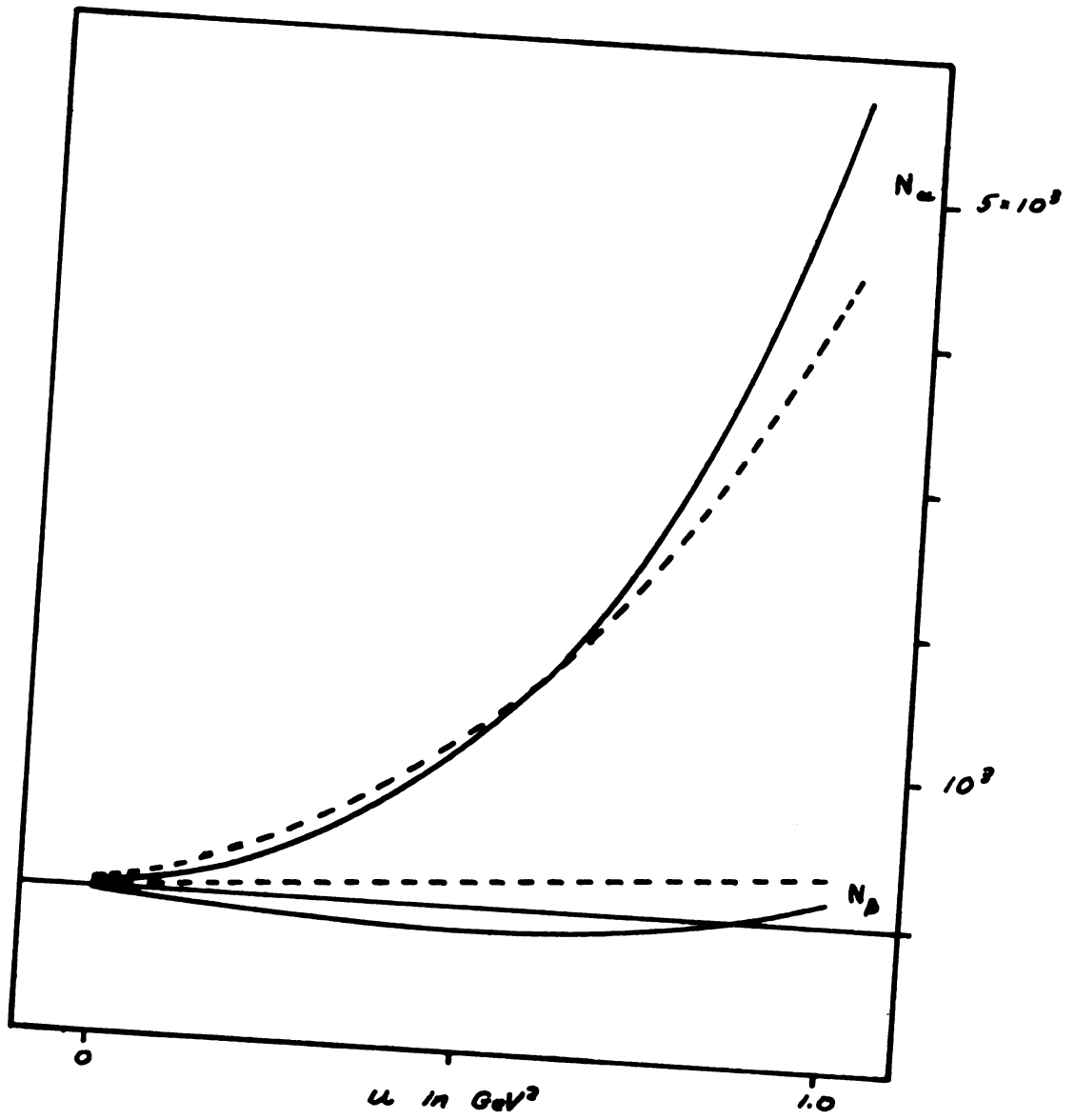


Figure 19. The  $n=3$   $N_\alpha$  and  $N_\beta$  FSR, indicated as in the preceding graphs.

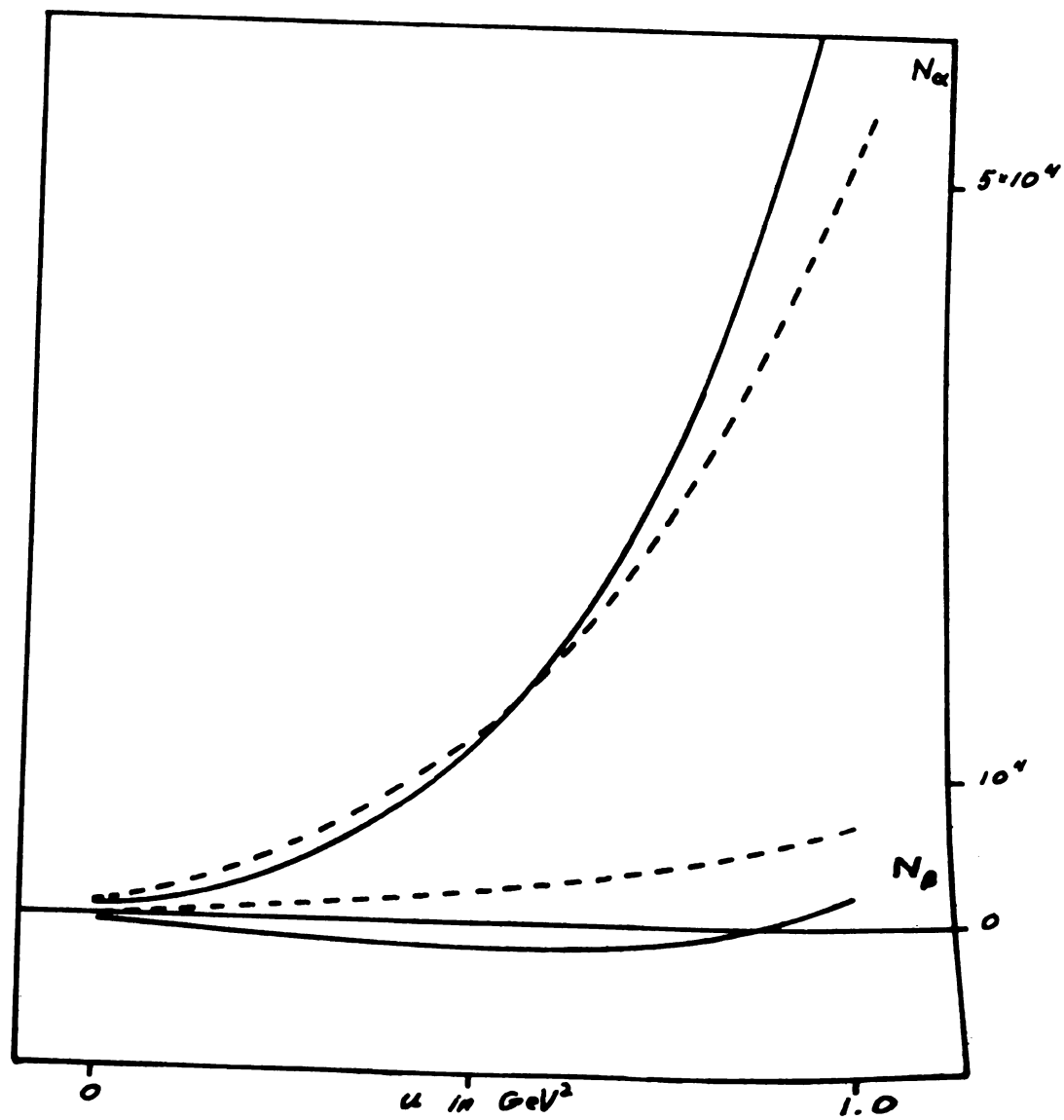


Figure 20. The  $n=5$   $N_\alpha$  and  $N_\beta$  FESR.

zero at  $u = m^2$  in the Regge term. This node is required in order to eliminate an  $N_{\rho}$  Regge recurrence at  $u = m^2$ , corresponding to a negative-parity nucleon. No such 'parity partner' to the  $N$  nucleon has been observed. Since the need for including parity partners in Regge parameterizations is not a well established matter of necessity we do not consider it a serious deficiency to be unable to reproduce this feature in the low energy term.

It was mentioned earlier that the coupling constants of the  $\rho'$  were chosen so as to enhance the agreement of the  $n = 1$   $N_{\alpha}$  and  $N_{\rho}$  FESR near  $u = 1.0 \text{ GeV}^2$ . In fact these coupling constants were chosen so as to require that the  $n = 1$   $N_{\alpha}$  and  $N_{\rho}$  FESR be exactly satisfied at  $u = 1.0 \text{ GeV}^2$  using a less sophisticated  $t$ -channel spectral function than that used to generate the final results. Since this procedure masks the effects of other high-mass mesons and high  $s$ -channel partial waves we did not impose such a rigid criterion on the final calculations. Close inspection of Figures 18, 19 and 20 shows that the Regge term diverges more rapidly than the low energy term in each case as  $u$  increases. This is further evidence that higher partial waves are required in both the  $s$ - and  $t$ -channels to fit the FESR over any very wide range of  $u$ .

The connection between the rate of increase of the FESR as a function of  $u$  and the mass and angular momentum of the states used to generate the spectral functions is illustrated in Figure 21 which shows the contribution of each of Barger's zero width mesons to the low energy term in the  $n = 1$   $N_{\alpha}$  FESR. Note that the high-mass, high-angular momentum states  $f_0$  and  $g$  completely dominate the low-mass, low-angular momentum states  $\sigma$  and  $\rho$  for large  $u$ . This is due to the fact that higher-ordered Legendre polynomials diverge faster as functions of  $u$ .

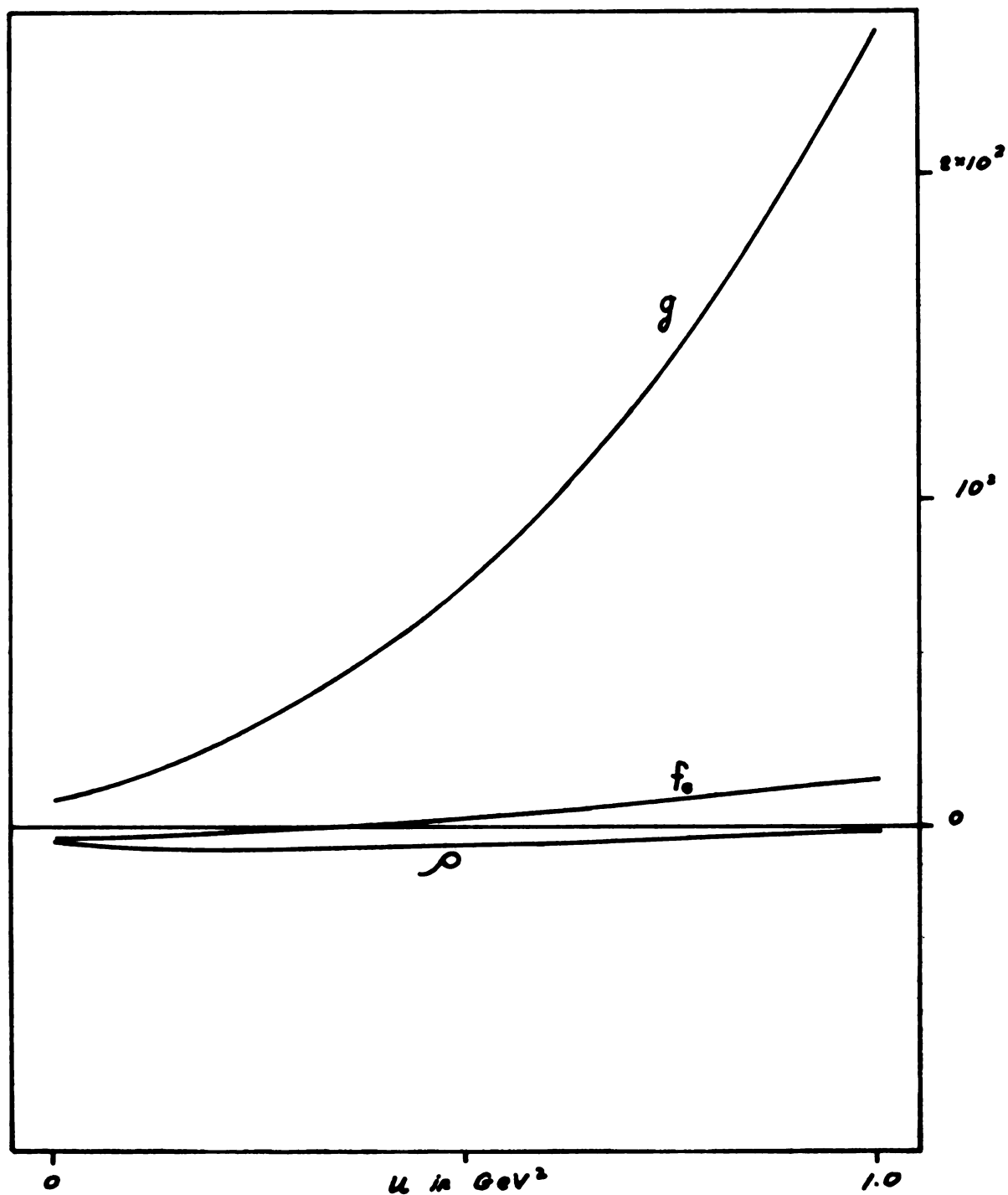


Figure 21. The contributions of each of Barger's zero-width mesons to the  $n=1$   $N_u$  FESR. The contribution of the  $\sigma$  (not shown) is essentially zero.

Also, higher mass states are intercepted at large values of  $x$  than lower-lying ones. Thus the rate of change of the low-energy terms with  $n$  is an indication of the weight of higher-mass states while the rate of increase as a function of  $u$  measures the effect of higher partial waves.

The fact that high-mass, high angular momentum states dominate the FESR is important in that it offers the possibility of discriminating between these states, a difficult task in the typical approach via dispersion relations which tend to be sensitive only to low-mass, low-angular momentum states.

#### C. The $\Delta$ FESR

Figures 22 and 23 show the low-energy contributions to the  $\Delta$  FESR for  $n = 0, 1, 2, 3, 4$ , and 5. Note that these terms are of the same order of magnitude as the errors in the corresponding  $N$  FESR. As a consequence the 'zero' and 'non-zero' FESR are not well resolved. The Regge terms are extremely small in this case as well and can all be regarded as zero. Thus it is impossible to regard these sum rules as particularly significant. One could attempt meaningful solutions in these cases only to resolve very minute features of otherwise very well determined spectral functions. Such a task is far beyond the scope of the present work.

#### D. The Cutkosky-Deo Scheme

While we have chosen to calculate the FESR in the context of the Cutkosky-Deo scheme by the method of expanding  $x$  directly in terms of polynomial in  $z$  it is clear that the transformed partial wave approach is the definitive test of this idea. The expansion of  $x$  in powers of  $z$  produces a  $u = 1.0 \text{ GeV}^2$  spectral function which differs from the standard continuation only as a function of the criterion used to truncate



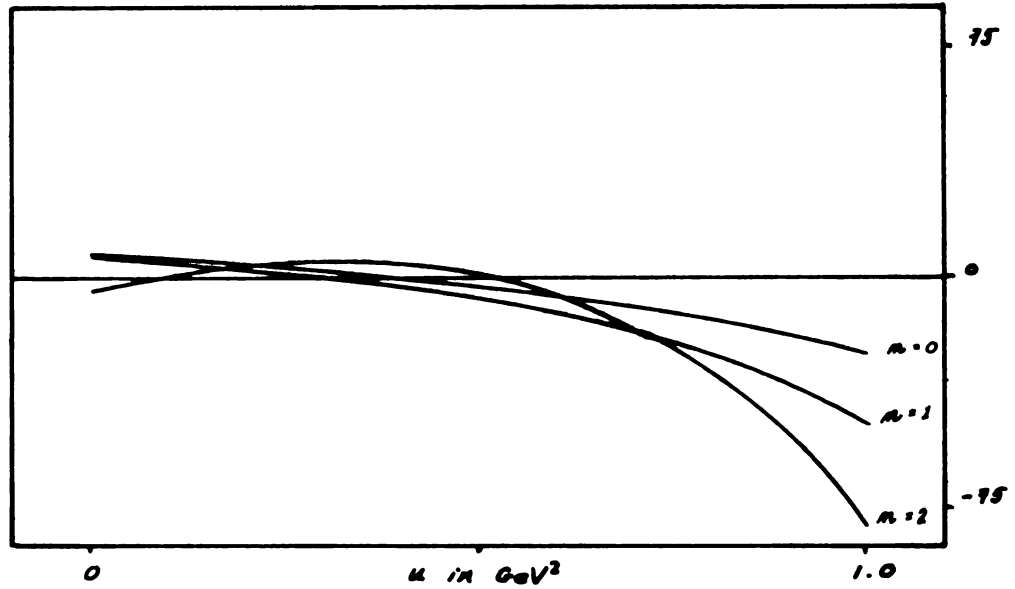


Figure 22. The low-energy terms for the  $n=0, 1, 2 \Delta_s$  FESR. The Regge terms, vanishingly small for both 'zero' and 'non-zero' moments, are not shown.

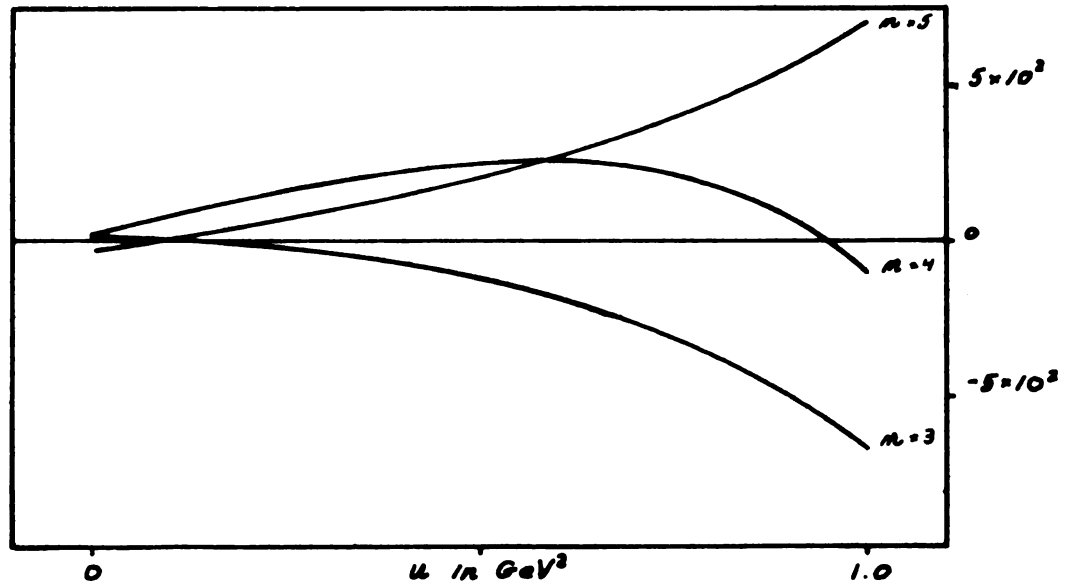


Figure 23. The low-energy terms for the  $n=3, 4, 5 \Delta_s$  FESR. The  $n=5$  term have been scaled down by a factor of 10. Again the Regge terms are all essentially zero.

the expansion. Had we been in a position to double or triple the number of expansion coefficients for example the spectral functions in  $x$  and  $z$  could obviously have been made to agree to within any desired accuracy at  $u = 1.0 \text{ GeV}^2$ . Hence this way of using the Cutkosky-Deo scheme has little to add to any attempt at improving the qualitative features of spectral functions.

However, the lack of good Regge convergence properties in the case of the transformed partial wave expansion can be interpreted as suggesting that the  $G$  and  $H$  waves of the CERN phases are not well determined. This applies particularly to the case of the 22 term transformed partial wave expansion. Imposing good Regge convergence on the transformed partial wave spectral functions might be a means of determining the higher phases much more exactly than can be done in the context of dispersion relations. If this calculation were to prove feasible, the FESR could then be used solely to determine the higher-mass  $t$ -channel spectrum. In connection with improved data on cross-sections, etc. this could be a powerful tool in determining the detailed features of the meson spectrum at high energies.

## APPENDICES

## APPENDIX A

### GENERALIZED SPINOR INVARIANTS FOR $\pi N$ SCATTERING

## APPENDIX A

### GENERALIZED SPINOR INVARIANTS FOR $\pi N$ SCATTERING

To construct the most general spinor invariant to describe the interaction of a spin zero particle with a spin- $\frac{1}{2}$  particle described by the Dirac Equation

$$(i \gamma \cdot \hat{p} + m) u(\hat{p}) = 0$$

we could begin by adding all possible invariants which can be constructed from the  $\gamma$ -matrices and the four 4-momentum vectors  $p_1, p_2, q_1, q_2$ . Such a function would have the form;

$$\begin{aligned} F = & F_0(k, \cos \theta) + \sum_i \{ \gamma \cdot p_i F_i(k, \cos \theta) \\ & + \gamma \cdot q_i G_i(k, \cos \theta) \} \\ & + \sum_{i,j} \gamma \cdot p_i \gamma \cdot q_j F_{ij}(k, \cos \theta) \\ & + \sum_{i,j,k} \gamma \cdot p_i \gamma \cdot q_j \gamma \cdot p_k F_{ijk}(k, \cos \theta) \\ & + \dots \end{aligned}$$

where  $F_0, F_i, G_i, F_{ik}, F_{ijk}$  are simply functions of  $k$  and  $\cos \theta$  or  $s, t, u$ . First, we observe that a matrix element

$\bar{u}(\hat{p}_4) \gamma \cdot p u(\hat{p}_1) \times F_i(k, \cos \theta)$  can be reduced by the Dirac Equation to  $i m \bar{u}(\hat{p}_4) u(\hat{p}_1) F_i(k, \cos \theta)$  by operating to the right or left on  $\bar{u}(\hat{p}_4)$  or  $u(\hat{p}_1)$  whichever is appropriate. Thus, terms linear in Nucleon momenta are equivalent to terms containing no  $\gamma$ -matrices at all (i.e.,  $F_0$ ), and can be eliminated. Second, the terms  $\gamma \cdot q_1$  and  $\gamma \cdot q_2$  are not independent since

$$q_2 = q_1 + p_1 - p_2$$

and then

$$\begin{aligned}\gamma \cdot q_2 &= \gamma \cdot q_1 + \gamma \cdot p_1 - \gamma \cdot p_2 \\ &= \gamma \cdot q_1 + \text{'const'}\end{aligned}$$

the last term again following from the Dirac equation.

Now we can replace all terms up to those linear in any 4-momentum by the sum of a spinor-independent term plus a term linear in Pion 4-momentum.

Terms quadratic in  $\gamma$ -matrices can be shown to be spinor-independent directly from the anti-commutation and normalization properties<sup>(35)</sup> of the  $\gamma$ -matrices;

$$[\gamma_\mu, \gamma_\nu]_+ = 2\delta_{\mu\nu} \quad (A1)$$

$$\gamma_\mu^2 = 1 \quad (A2)$$

where  $\delta_{\mu\nu}$  are the elements of the  $4 \times 4$  unit matrix. Write the quadratic term,  $\mathcal{O}_2$ , as;

$$\begin{aligned}\mathcal{O}_2 &= \sum_{i,j} \gamma \cdot p_2 \gamma \cdot q_1 F_{ij}(k, \omega, \theta) \\ &= + \sum_{i,j} F_{ij}(k, \omega, \theta) \left[ \sum_{\mu, \nu} [\gamma_\mu, \gamma_\nu]_+ p_i^\mu q_j^\nu + \sum_\lambda \gamma_\lambda^2 p_i^\lambda q_j^\lambda \right]\end{aligned}$$

In the bracketed factor substitute (A1) and (A2) in the first and second term respectively. Then;

$$\mathcal{O}_2 = \sum_{i,j} F_{ij}(k, \omega, \theta) \left[ \sum_{\mu, \nu} 2\delta_{\mu\nu} p_i^\mu q_j^\nu + \sum_\lambda p_i^\lambda q_j^\lambda \right]$$

or, simplifying the  $\delta$ -function:

$$\mathcal{O}_2 = \sum_{i,j} F_{ij}(k, \omega, \theta) \sum_\lambda p_i^\lambda q_j^\lambda$$

an explicit spinor-independent.

To reduce any higher-ordered term with an odd number of  $\gamma$ -matrix indices one can first perform the simplification above on any pair of indices as many times as necessary to reduce it to a linear form. That linear form will then be equivalent to a spinor-independent plus a term linear in Pion 4-momentum as we have shown.

Any higher-ordered terms even in  $\gamma$ -matrix indices can be reduced to a spinor-independent form simply by repetition of the operation performed on the quadratic term for arbitrary pairs of indices.

The conventional choice of spinor-independent<sup>(36,37)</sup> plus Pion 4-momentum is,

$$F = -F_0(k, \cos \theta) + \frac{1}{2} \not{Q} F_1(k, \cos \theta)$$

where

$$\not{Q} \equiv \gamma \cdot q_1 + \gamma \cdot q_2$$

## APPENDIX B

### ISOTOPOLOGY OF $\pi$ N SCATTERING



## APPENDIX B

### ISOTOPOLOGY OF $\pi N$ SCATTERING

The possible isotopic spins of the  $\pi(I = 1)^{\pm} N(I = \frac{1}{2})$  state are  $I = 1/2, 3/2$ . In terms of a set of projection operators  $\mathcal{A}_I$  the most general form of any operator in  $\pi N$  isotopic spin space is:

$$\mathcal{O} = \mathcal{A}_{\frac{1}{2}} \mathcal{O}^{\frac{1}{2}} + \mathcal{A}_{\frac{3}{2}} \mathcal{O}^{\frac{3}{2}} \quad (B1)$$

where  $\mathcal{O}_{\frac{1}{2}}, \mathcal{O}_{\frac{3}{2}}$  are the respective eigenamplitudes. The projection operators can be constructed using the identity,

$$\vec{I} = \frac{1}{2} \vec{\tau} + \vec{T} \quad (B2)$$

where;  $\vec{\tau}$  is the 2 X 2 Nucleon isospin 'Pauli matrix', identical in form to the familiar  $\vec{\sigma}$ -matrix.

$\vec{T}$  is the corresponding Pion isotopic spin operator.

The Nucleon isotopic-spin operator is well known. In the charged Pion basis the Pion isospin-matrix<sup>(38)</sup> is,

$$T_1 = \frac{1}{\sqrt{2}} \begin{bmatrix} 0 & 1 & 0 \\ 1 & 0 & 1 \\ 0 & 1 & 0 \end{bmatrix}, T_2 = \frac{1}{\sqrt{2}} \begin{bmatrix} 0 & -i & 0 \\ i & 0 & -i \\ 0 & i & 0 \end{bmatrix}, T_3 = \frac{1}{\sqrt{2}} \begin{bmatrix} 1 & 0 & 0 \\ 0 & 0 & 0 \\ 0 & 0 & -1 \end{bmatrix} \quad (B3)$$

The Pion isospinors are,

$$|\pi^+\rangle = \begin{bmatrix} 1 \\ 0 \\ 0 \end{bmatrix}, |\pi^-\rangle = \begin{bmatrix} 0 \\ 0 \\ 1 \end{bmatrix}, |\pi^0\rangle = \begin{bmatrix} 0 \\ 1 \\ 0 \end{bmatrix} \quad (B4)$$

Forming  $I^2$  we have, from (B2);

$$I^2 = \vec{\tau} \cdot \vec{T} + \frac{1}{4} \tau^2 + T^2$$

But;

$$\tau^2 = 3$$

$$T^2 = 2$$

Or:  $\vec{\tau} \cdot \vec{T} = I^2 - 11/4$

Finally;  $\vec{\tau} \cdot \vec{T} = -2, 1 \text{ for } I = \frac{1}{2}, \frac{3}{2}$

]

Thus,  $\Lambda_{\frac{1}{2}}, \Lambda_{\frac{3}{2}}$  can be written<sup>( )</sup> as;

$$\begin{aligned}\Lambda_{\frac{1}{2}} &= \frac{1}{3}[1 - \vec{\tau} \cdot \vec{T}] \\ \Lambda_{\frac{3}{2}} &= \frac{1}{3}[2 + \vec{\tau} \cdot \vec{T}]\end{aligned}\quad (B5)$$

We have now made explicit the content of equation (B1). The next step is to define the numbered Pion basis<sup>(39)</sup>;

$$\begin{aligned}|\pi_1\rangle &= \frac{1}{\sqrt{2}}(|\pi^+\rangle + |\pi^-\rangle), \quad |\pi_2\rangle = \frac{1}{\sqrt{2}}(|\pi^-\rangle - |\pi^+\rangle) \\ |\pi_3\rangle &= |\pi^0\rangle\end{aligned}$$

To show that (B2) has the form (1.8) with  $\Lambda_{\frac{1}{2}}, \Lambda_{\frac{3}{2}}$  defined as in (B5) note that in the numbered Pion basis

$$T_{\alpha, \beta}^{\delta} = -i \varepsilon_{\delta \alpha \beta} \quad (B7)$$

Where;  $T^{\delta}$  is any component of the Pion isospin matrix.

$\alpha, \beta$  are labels of charged pions.

$\varepsilon_{\delta \alpha \beta}$  is the customary Levi-Civita symbol.

Then we can write;

$$(\vec{\tau} \cdot \vec{T})_{\alpha \beta} = \sum_{\delta} \tau_{\delta} T_{\alpha \beta}^{\delta}$$

where  $\tau_{\delta}$  is still a Nucleon isospin operator while  $T_{\alpha \beta}^{\delta}$  indicates the matrix element of the  $\delta$ -component of the Pion isospin between states  $\alpha, \beta$ .

Substituting (B7) into (B8) gives;

$$\begin{aligned}(\vec{\tau} \cdot \vec{T})_{\alpha \beta} &= \sum_{\delta} -i \tau_{\delta} \varepsilon_{\delta \alpha \beta} \\ &= -i \tau_{\gamma}\end{aligned}$$

Where  $\delta$  does not equal  $\alpha$  or  $\beta$ .  $\tau_{\delta}$  can be expressed in terms of

$\tau_{\alpha}$  and  $\tau_{\beta}$  by the commutation relation;

$$[\tau_{\alpha}, \tau_{\beta}] = 2i \tau_{\gamma}$$

Where  $(\alpha, \beta, \gamma)$  is a circular permutation on  $(1, 2, 3)$ . Then,

$$(\vec{\tau} \cdot \vec{\tau})_{\alpha\beta} = -\frac{1}{2} [\tau_\alpha, \tau_\beta]$$

Then from (B5) we have;

$$\left(\Lambda_{\frac{1}{2}}\right)_{\alpha\beta} = \frac{1}{3} \{ \delta_{\alpha\beta} + \frac{1}{2} [\tau_\alpha, \tau_\beta] \}$$

$$\left(\Lambda_{\frac{2}{3}}\right)_{\alpha\beta} = \frac{1}{3} \{ 2\delta_{\alpha\beta} - \frac{1}{2} [\tau_\alpha, \tau_\beta] \}$$

Then an operator of the form;

$$\Theta = \Lambda_{\frac{1}{2}} \Theta^{\frac{1}{2}} + \Lambda_{\frac{2}{3}} \Theta^{\frac{2}{3}}$$

can be written;

$$\begin{aligned} (\Theta)_{\alpha\beta} &= \Theta^{\frac{1}{2}} \left\{ \frac{1}{3} \delta_{\alpha\beta} + \frac{1}{6} [\tau_\alpha, \tau_\beta] \right\} \\ &\quad + \Theta^{\frac{2}{3}} \left\{ \frac{2}{3} \delta_{\alpha\beta} - \frac{1}{6} [\tau_\alpha, \tau_\beta] \right\} \\ &= \frac{1}{3} \{ \Theta^{\frac{1}{2}} + 2\Theta^{\frac{2}{3}} \} \delta_{\alpha\beta} \\ &\quad + \frac{1}{3} \{ -\Theta^{\frac{2}{3}} + \Theta^{\frac{1}{2}} \} \frac{1}{2} [\tau_\alpha, \tau_\beta] \end{aligned}$$

Comparing this equation with (1.8) yields

$$A^{(\prime\prime)} = \frac{1}{3} (A^{\frac{1}{2}} + 2A^{\frac{2}{3}})$$

$$A^{(\prime)} = \frac{1}{3} (A^{\frac{1}{2}} - A^{\frac{2}{3}})$$

The same relations hold for B.

Inverting these relations yields,

$$A^{\frac{2}{3}} = A^{(\prime\prime)} + A^{(\prime)}$$

$$A^{\frac{1}{2}} = A^{(\prime\prime)} + 2A^{(\prime)}$$

which is just equation (1.9).

To relate good isotopic spin amplitudes to the amplitudes for physical processes we first expand:

$$|\pi^- p\rangle = \frac{1}{\sqrt{2}}|\frac{3}{2}, \frac{1}{2}\rangle - \sqrt{\frac{2}{3}}|\frac{1}{2}, \frac{1}{2}\rangle$$

$$|\pi^0 n\rangle = \sqrt{\frac{2}{3}}|\frac{3}{2}, -\frac{1}{2}\rangle + \frac{1}{\sqrt{2}}|\frac{1}{2}, -\frac{1}{2}\rangle$$

$$|\pi^+ p\rangle = |\frac{3}{2}, \frac{3}{2}\rangle$$

$$|\pi^- n\rangle = |\frac{3}{2}, -\frac{3}{2}\rangle$$

Then simply taking matrix elements of (B1)

$$\begin{aligned}\mathcal{O}^{\pi n} &= \langle \pi^0 n | \Lambda_{\frac{1}{2}} \mathcal{O}^{\frac{1}{2}} + \Lambda_{\frac{3}{2}} \mathcal{O}^{\frac{1}{2}} | \pi^+ p \rangle \\ &= \frac{\sqrt{2}}{3} \mathcal{O}^{\frac{3}{2}} - \frac{\sqrt{2}}{3} \mathcal{O}^{\frac{1}{2}} \\ &= -\sqrt{2} \mathcal{O}^{(-)}\end{aligned}$$

$$\begin{aligned}\mathcal{O}^{\pi^+ p} &= \langle \pi^+ p | \Lambda_{\frac{1}{2}} \mathcal{O}^{\frac{1}{2}} + \Lambda_{\frac{3}{2}} \mathcal{O}^{\frac{1}{2}} | \pi^+ p \rangle \\ &= \mathcal{O}^{\frac{3}{2}}\end{aligned}$$

$$\begin{aligned}\mathcal{O}^{\pi p} &= \langle \pi^0 p | \Lambda_{\frac{1}{2}} \mathcal{O}^{\frac{1}{2}} + \Lambda_{\frac{3}{2}} \mathcal{O}^{\frac{1}{2}} | \pi^0 p \rangle \\ &= \frac{1}{3} \mathcal{O}^{\frac{1}{2}} + \frac{2}{3} \mathcal{O}^{\frac{3}{2}} \\ &= \mathcal{O}^{(+)} + \mathcal{O}^{(-)}\end{aligned}$$

These relations hold for both A and B, as well as any other amplitude with isospin labels.

## APPENDIX C

### INVARIANTS IN TERMS OF PARTIAL WAVES

# APPENDIX C

## INVARIANTS IN TERMS OF PARTIAL WAVES

The T-matrix operator has the form

$$T = -A + \frac{i}{2} B \quad (C1)$$

Also, the scattering amplitude can be written<sup>(40)</sup> in terms of projection operators  $P_{j=l+1/2}$ ,  $P_{j=l-1/2}$  as,

$$F(k, \cos \theta) = \sum_{l=0}^{\infty} (2l+1) \{ P_{j=l+1/2} f_l(k) + P_{j=l-1/2} f_l(k) \} \quad (C2)$$

To determine  $P_{j=l \pm 1/2}$  write,

$$\vec{J} = \vec{L} + \frac{1}{2} \vec{\sigma}$$

$$J^2 = L^2 + \frac{1}{4} \sigma^2 + \vec{\sigma} \cdot \vec{L}$$

Then

$$\vec{\sigma} \cdot \vec{L} = J^2 - L^2 - \frac{1}{4} \sigma^2$$

$$= j(j+1) - l(l+1) - 3/4$$

So that

$$\vec{\sigma} \cdot \vec{L} = l, -(l+1) \text{ for } j=l+\frac{1}{2}, j=l-\frac{1}{2}$$

Then

$$P_{j=l+\frac{1}{2}} = \frac{\vec{\sigma} \cdot \vec{L} + l + 1}{2l + 1}$$

$$P_{j=l-\frac{1}{2}} = \frac{1 - \vec{\sigma} \cdot \vec{L}}{2l + 1}$$

Now evaluate

$$\vec{\sigma} \cdot \vec{L} P_l(\cos \theta) = \vec{\sigma} \cdot \vec{L} P_l(\hat{q} \cdot \hat{q}')$$

$$= \vec{\sigma} \cdot \hat{q}' \times i \vec{\nabla}_q P_l(\hat{q} \cdot \hat{q}')$$

$$= i \vec{\sigma} \cdot \hat{q}' \times \hat{q} \frac{1}{q} P'_l(\hat{q} \cdot \hat{q}')$$

$$= i \vec{\sigma} \cdot \vec{q} \times \vec{q}' P'(\vec{q}, \vec{q}') \\ \equiv i \vec{\sigma} \cdot \hat{n} P'(\vec{q}, \vec{q}')$$

So that (C2) has the form;

$$F(k, \omega, \theta) = \sum_{l=0}^{\infty} \{ (l+1) f_l(k) + l f_{l-1}(k) \} P_l(\omega, \theta) \\ + i \vec{\sigma} \cdot \hat{n} \sum_{l=0}^{\infty} \{ f_l(k) - f_{l-1}(k) \} P'_l(\omega, \theta) \quad (C3)$$

The operator  $\vec{\sigma}$  is the spin operator in the space of Pauli spinors.

To reduce (C1) note that the Nucleon spinors  $u^{(2)}(\vec{p})$  can be expressed in Pauli form as;

$$u^{(2)}(\vec{p}) = (2m(m+E))^{-1/2} (i\vec{p} + m) u^{(1)}(0) \quad (C4)$$

where

$$u^{(1)}(0) = \begin{bmatrix} 1 \\ 0 \\ 0 \\ 0 \end{bmatrix} \quad u^{(2)}(0) = \begin{bmatrix} 0 \\ 1 \\ 0 \\ 0 \end{bmatrix}$$

A convenient form of the  $\gamma$ -matrices is

$$\gamma_0 = \rho_3 \otimes \mathbb{1} \quad \vec{\gamma} = \rho_2 \otimes \vec{\sigma}$$

The 2 X 2 matrices  $\rho_i$  are formally identical to the Pauli matrices

$\sigma_i$ . In this representation,

$$-\bar{u}(\vec{p}') A u(\vec{p}) = -(2m(m+E))^{1/2} A u^{(1)}(0) [ \rho_3 (m + \rho_3 E \\ + i \rho_2 \vec{\sigma} \cdot \vec{q}' \chi_{m+\rho_3 E} + i \rho_2 \vec{\sigma} \cdot \vec{q} ) ] u(0)$$

$$B \bar{u}(\vec{p}') \frac{1}{2} \not{q} u(\vec{p}) = (4m(m+E))^{1/2} B u^{(1)}(0) [ \rho_3 (2m\omega\rho_1 - i\rho_2 \vec{\sigma} \cdot$$



$$\begin{aligned}
& (\vec{q} + \vec{q}')m + 2E\omega - i\rho_3\rho_2 E \vec{\sigma} \cdot (\vec{q} + \vec{q}') \\
& + 2\omega i\rho_3\rho_2 \vec{\sigma} \cdot \vec{q}' + \vec{\sigma} \cdot \vec{q}' \vec{\sigma} \cdot (\vec{q} + \vec{q}') \\
& (m + \rho_3 E + i\rho_2 \vec{\sigma} \cdot \vec{q})] u(0)
\end{aligned}$$

The operators standing between 2-component spinors reduce to

$$\left\{ \frac{m+E - (E-m)\cos\theta}{2m} - i\vec{\sigma} \cdot \hat{n} \frac{E-m}{2m} \right\} A \quad (C5)$$

and

$$\begin{aligned}
& \left\{ \frac{(E+m)(W-m)}{2m} + \frac{(E-m)(W+m)}{2m} \cos\theta \right. \\
& \left. - i\vec{\sigma} \cdot \hat{n} \frac{(E-m)(W+m)}{2m} \cos\theta \right\} B
\end{aligned} \quad (C6)$$

respectively.

Comparing (C5), (C6) and (C3) yields,

$$\begin{aligned}
& \left\{ \frac{m+E + (E-m)\cos\theta}{2m} A \right. \\
& \left. \frac{(E+m)(W-m) + \frac{(W+m)}{(E-m)} \cos\theta}{2m} B \right\} \\
& = \frac{-W}{16\pi m} \sum \{ (l+1) f_l(k) + l f_{l-1}(k) \} P_l(\cos\theta)
\end{aligned} \quad (C7)$$

The recurrence relations

$$\begin{aligned}
l P_l(\cos\theta) &= \cos\theta P'_l(\cos\theta) - P'_{l-1}(\cos\theta) \\
(l+1) P_{l+1}(\cos\theta) &= P'_{l+1}(\cos\theta) - \cos\theta P'_l(\cos\theta)
\end{aligned}$$

can be used to put the sum on the right-hand side of (C7) in the form

$$\sum_{l=0}^{\infty} f_l(\cos\theta) (P'_l(\cos\theta) - P'_{l-1}(\cos\theta))$$

$$\begin{aligned}
& + \sum_{l=0}^{\infty} f_{l+} (-\cos \theta P'_l(\cos \theta) + P'_{l+1}(\cos \theta)) \\
& = \cos \theta \sum_{l=0}^{\infty} \{f_l - f_{l+}\} P'_l(\cos \theta) \\
& \quad + \sum_{l=0}^{\infty} f_{l-} P'_{l+1}(\cos \theta) - f_{l+} P'_{l+1}(\cos \theta) \\
& = f_1(k, \cos \theta) + \cos \theta f_2(k, \cos \theta)
\end{aligned}$$

Or, from (C7)

$$\begin{aligned}
f_1(k, \cos \theta) &= \frac{E+m}{8\pi W} \{A - (W-m)B\} \\
f_2(k, \cos \theta) &= \frac{E-m}{8\pi W} \{A + (W+m)B\}
\end{aligned} \tag{C8}$$

These relations could also have been extracted by comparing coefficients of the operator  $\vec{\sigma} \cdot \vec{n}$  in (C3), (C5) and (C6).

Note that  $F(k, \cos \theta)$  has the form;

$$\begin{aligned}
F(k, \cos \theta) &= f_1(k, \cos \theta) + \cos \theta f_2(k, \cos \theta) \\
&\quad - i \vec{\sigma} \cdot \vec{n} \sin \theta f_2(k, \cos \theta)
\end{aligned}$$

In the forward direction  $\cos \theta = 1$  and,

$$F(k, \cos \theta = 1) = f_1(k, \cos \theta = 1) + f_2(k, \cos \theta = 1)$$

so that the optical theorem has the form

$$\begin{aligned}
\sigma_{\text{tot}} &= \frac{4\pi}{k} \text{Im} F(k, \cos \theta = 1) \\
&= \frac{4\pi}{k} \text{Im} \{f_1(k, \cos \theta = 1) + f_2(k, \cos \theta = 1)\} \\
&= \frac{2\pi}{k^2} \sum_{l=0}^{\infty} (l+1) (1 - \eta_{l+} \cos 2\delta_{l+}) + l (1 - \eta_{l-} \cos 2\delta_{l-})
\end{aligned}$$

Below the inelastic limit the expression has the familiar form <sup>(41)</sup>,

$$\sigma_{\ell 0 \ell} = \frac{\pi}{k^2} \sum_{l=0}^{\infty} (l+1) \sin^2 \delta_{\ell+} + l \sin^2 \delta_{\ell-}$$

## APPENDIX D

PARTIAL WAVE AMPLITUDES FOR  $\pi\pi \rightarrow \bar{N}N$

## APPENDIX D

### PARTIAL WAVE AMPLITUDES FOR $\pi\pi \rightarrow N\bar{N}$

The partial wave amplitudes we wish to define can be conveniently extracted from the helicity formalism. Jacob and Wick<sup>(42)</sup> express the helicity amplitude  $f_{\lambda_a \lambda_b \lambda_c \lambda_d}$  which describes a two particle reaction  $a + b \rightarrow c + d$  in terms of T-matrix elements as

$$(D1) \quad f_{\lambda_a \lambda_b \lambda_c \lambda_d} = \frac{1}{p} \sum_j (j + \frac{1}{2}) \langle j m \lambda_a \lambda_b | T | j m \lambda_c \lambda_d \rangle e^{i(\lambda - \mu)\phi} d_{\lambda\mu}^j(\theta)$$

where  $\lambda_i$  = helicity of particles  $i$ .

$$\lambda = \lambda_a - \lambda_b$$

$$\mu = \lambda_c - \lambda_d$$

$$\lambda_a = \lambda_b = 0 \text{ for spinless mesons}$$

$$\lambda_c, \lambda_d = \pm \frac{1}{2} \text{ for spin-}\frac{1}{2}\text{fermeons}$$

$d_{\lambda\mu}^j(\theta)$  are the standard reduced rotation operators.

In terms of  $f_{\lambda_a \lambda_b \lambda_c \lambda_d}$ ,

$$\frac{d\sigma}{d\Omega} = \sum_{\substack{\lambda_a, \lambda_b, \\ \lambda_c, \lambda_d}} |f_{\lambda_a \lambda_b \lambda_c \lambda_d}|^2$$

For the process  $\pi\pi \rightarrow N\bar{N}$  there are only two non-trivial helicity labels -- those of the  $N$  and  $\bar{N}$  -- which have values of  $\lambda_c, \lambda_d = \pm \frac{1}{2}$ .

The helicity amplitudes and cross-section relations then take on the form

$$f_{\lambda_c \lambda_d} = \frac{1}{P} \sum_j (j + \frac{1}{2}) \langle j m \lambda_c \lambda_d | T | j m 0 0 \rangle e^{-i\mu\phi} d_{0\mu}^j(\theta)$$

$$\frac{d\sigma}{d\Omega} = |f_{\frac{1}{2}\frac{1}{2}}|^2 + |f_{\frac{1}{2}-\frac{1}{2}}|^2 + |f_{-\frac{1}{2}-\frac{1}{2}}|^2 + |f_{-\frac{1}{2}\frac{1}{2}}|^2$$

Noting that the states  $|j m \lambda_1 \lambda_2\rangle$  for  $s_1 = s_2 = \frac{1}{2}$  have the symmetry property<sup>(43)</sup>

$$P_{12} |j m \lambda_1 \lambda_2\rangle = (-)^{j-1} |j m -\lambda_1 -\lambda_2\rangle$$

one can write

$$\langle j m \lambda_c \lambda_d | T | j m \lambda_a \lambda_b \rangle = \langle j m -\lambda_c -j | T | j m -\lambda_a -\lambda_b \rangle$$

So that,

$$\langle j m \frac{1}{2} \frac{1}{2} | T | j m 0 0 \rangle = \langle j m -\frac{1}{2} -\frac{1}{2} | T | j m 0 0 \rangle \equiv T_+^j$$

$$\langle j m \frac{1}{2} -\frac{1}{2} | T | j m 0 0 \rangle = \langle j m -\frac{1}{2} \frac{1}{2} | T | j m 0 0 \rangle \equiv T_-^j$$

i.e., the subscripts  $\pm$  refer to states of like or opposite helicity.

If we also note that the reduced rotation operators  $d_{0\mu}^j(\theta)$

have the symmetry

$$d_{0\mu}^j(\theta) = -d_{\mu 0}^j(\theta)$$

the helicity amplitudes and cross-sections can be written

$$f_+ \equiv f_{\frac{1}{2}\frac{1}{2}} = f_{-\frac{1}{2}-\frac{1}{2}} = \frac{1}{P} \sum_j (j + \frac{1}{2}) \langle j m \frac{1}{2} \frac{1}{2} | T | j m 0 0 \rangle d_{00}^j(\theta)$$

$$f_- \equiv f_{\frac{1}{2}-\frac{1}{2}} = -f_{-\frac{1}{2}\frac{1}{2}} = \frac{1}{P} \sum_j (j + \frac{1}{2}) \langle j m \frac{1}{2} -\frac{1}{2} | T | j m 0 0 \rangle d_{01}^j(\theta)$$

$$\frac{d\sigma}{d\Omega} = 2|f_+|^2 + 2|f_-|^2$$

where the  $\phi$ -dependence, which cancels out in  $\frac{d\sigma}{d\Omega}$  has been neglected.

We can now construct partial wave amplitudes whose relation to measurable quantities is clear by expanding the matrix elements  $T_+^j$  and  $T_-^j$  in terms of  $\langle j m \lambda \lambda | T | j m j 0 \rangle$ .

Since only NN states with  $j = l \pm 1$  contributes we have:

(D2)

$$\langle j m \lambda_c \lambda_d | T | j m 00 \rangle =$$

$$\langle j m j 0 | j m 00 \rangle \sum_{\substack{l=j-1 \\ l \neq j}}^{l=j+1} \langle j m \lambda_c \lambda_d | j m l 1 \rangle \langle j m l 1 | T | j m j 0 \rangle$$

In this case, the coupling coefficients take the form <sup>(44)</sup>

(D3)

$$\langle j m l 1 | j m \lambda_1 \lambda_2 \rangle = \left( \frac{2l+1}{2j+1} \right)^{1/2} C(l 1 j; 0, \lambda_1) C(\frac{1}{2} \frac{1}{2} 1; \lambda_1, -\lambda_2)$$

It is clear that  $|j m j 0\rangle = |j m 00\rangle$  so that

$$\langle j m j 0 | j m 00 \rangle = 1$$

Then

(D4)

$$T_{\pm}^j = \sum_{\substack{l=j-1 \\ l \neq j}}^{l=j+1} \langle j m \lambda_a \lambda_b | j m l 1 \rangle T_l^j$$

Where  $T_l^j$  are just the partial wave amplitudes we seek.

The general expression for  $C(j \pm 1, 1, j; 0, \pm 1)$  appear in Rose <sup>(45)</sup>.

The required results are;

$$C(j+1, 1, j; 00) = \left[ \frac{j+1}{2j+1} \right]^{1/2}$$

$$C(j-1, 1, j; 00) = \left[ \frac{j}{2j+1} \right]^{1/2}$$

$$C(j+1, 1, j; 01) = \left[ \frac{j}{2(j+3)} \right]^{1/2}$$

$$C(j-1, 1, j; 01) = \left[ \frac{j+1}{2(j-1)} \right]^{1/2}$$

The Clebsch-Gordon constants  $C(\frac{1}{2} \frac{1}{2} 1; \pm \frac{1}{2} \frac{1}{2})$  are trivial.

Substituting these results in Equation (D4) yields

$$\langle j m; \frac{1}{2} \frac{1}{2} | j m; j+1, 1 \rangle = -\frac{1}{\sqrt{2}} \left[ \frac{j+1}{2j+1} \right]^{1/2}$$

$$\langle j m; \frac{1}{2} \frac{1}{2} | j m; j-1, 1 \rangle = \frac{1}{\sqrt{2}} \left[ \frac{j}{2j+1} \right]^{1/2}$$

$$\langle j m; \frac{1}{2} - \frac{1}{2} | j m; j+1, 1 \rangle = \frac{1}{\sqrt{2}} \left( \frac{j}{2j+1} \right)^{\frac{1}{2}}$$

$$\langle j m; \frac{1}{2} - \frac{1}{2} | j m; j-1, 1 \rangle = \frac{1}{\sqrt{2}} \left( \frac{j+1}{2j+1} \right)^{\frac{1}{2}}$$

So that,

$$(D5) \quad \begin{aligned} T_+^j &= \frac{1}{\sqrt{2}} \left( \frac{j}{2j+1} \right)^{\frac{1}{2}} T_{j-1}^j - \frac{1}{\sqrt{2}} \left( \frac{j+1}{2j+1} \right)^{\frac{1}{2}} T_{j+1}^j \\ T_-^j &= \frac{1}{\sqrt{2}} \left( \frac{j+1}{2j+1} \right)^{\frac{1}{2}} T_{j-1}^j + \frac{1}{\sqrt{2}} \left( \frac{j}{2j+1} \right)^{\frac{1}{2}} T_{j+1}^j \end{aligned}$$

which serves to allow us to shuttle between the helicity formalism and partial waves as needed.

Further, since  $S_z^j = i \left( \frac{P}{q} \right)^{\frac{1}{2}} T_z^j$  (there is no elastic scattering in this case) we can apply the above results to S-matrix elements. In particular we will use these results to expand the amplitudes

$$\begin{aligned} f_+^j(t) &\equiv (P/q) \frac{E}{(pq)^{\frac{1}{2}}} T_+^j \\ f_-^j(t) &\equiv (P/q) \frac{1}{(pq)^{\frac{1}{2}}} T_-^j \end{aligned}$$

which appears in equation (1.19).



## REFERENCES

## REFERENCES

1. These values, taken from the work of J. Durso, correspond to the charged member of each multiplet.
2. G. F. Chew, M. L. Goldberger, F. E. Low, and Y. Nambu, Phys. Rev., 106, 1337 (1957).
3. Stephen Gasiorowicz, Elementary Particle Physics, John Wiley & Sons, New York (1966), Chap. 23.
4. V. Singh, Phys. Rev., 129, p. 1889 (1963).
5. M. L. Goldberger and K. M. Watson, Collision Theory, John Wiley & Sons, New York (1964) p. 647.
6. J. Bowcock, W. N. Cottingham, and D. Lurie, Nuovo Cimento, X 16, p. 918 (1960).
7. S. Mandelstam, Phys. Rev., 115, p. 1741, p. 1752 (1959).
8. C. Lovelace, CERN Report TH-838.
9. J. Durso, Private communication.
10. J. Hamilton and T. D. Spearman, Annals of Physics, 12, p. 172 (1961).
11. Op. Cit. // 6.
12. One can obviously write FESR not only for  $A^{(\pm)}$  and  $B^{(\pm)}$  but also for linear combinations of these amplitudes provided the coefficients are not too pathological.
13. V. Barger, et.al., Phys. Rev., 185, p. 1852 (1969).
14. R. Dolen, D. Horn, C. Schmid, Phys. Rev. Lett., 19, p. 402 (1967).
15. C. B. Chiu & M. DerSarkissian, Nuovo Cimento, 55, p. 396 (1968).
16. Op. Cit. # 13. See Eq. (7).
17. R. Dolen, et.al., Phys. Rev., 166, p. 1768 (1968).
18. C. Schmid, Phys. Rev. Lett., 20, p. 689 (1968).

19. D. R. Crittenden, R. M. Heinz, D. B. Lichtenberg, E. Predazzi, Phys. Rev. D, 1, p. 169 (1970).
20. Op. Cit. # 13.
21. P. A. Carruthers & J. Kirsch, Annals of Physics, 33, p. 1 (1965).
22. Op. Cit. # 4.
23. V. Barger and D. Cline, Phys. Rev. Lett., 21, p. 392 (1968).
24. S. W. McDowell, Phys. Rev., 116, p. 774 (1960).
25. A. Donnachie, R. G. Kirsopp, and C. Lovelace, CERN Report TH-838 and Addendum (1967).
26. A. D. Brody et.al., SLAC-PUB-709 (1970). See especially the bibliography.
27. This is the value quoted by Barger et.al. We use it for purposes of comparison.
28. V. Barger and D. Cline, Physics Letters, 25B, p. 415 (1967).
29. C. Lovelace, CERN Report TH-839 (1968).
30. W. Frazer and J. Fulco, Phys. Rev., 117, p. 1603 (1960).
31. A complete discussion of the convergence properties of the Legendre expansion can be found in J. Hamilton and W. S. Woolcock, Rev. Mod. Phys., 35, p. 737 (1963).
32. R. E. Cutkosky and B. B. Deo, Phys. Rev., 174, p. 1859 (1968).
33. M. Abramowitz and I. A. Stegun, "Handbook of Mathematical Functions", Nat. Bureau of Standards AMS 55 (1964).
34. I am indebted to Dr. Y. A. Chao for supplying me a copy of his FORTRAN program for generating the Landen Transformation.
35. Op. Cit. # 3. p. 32.
36. Op. Cit. # 6.
37. Op. Cit. # 10.
38. R. Levi-Setti, Elementary Particles, Univ. of Chicago Press (1963) pp. 26f.
39. H. Muirhead, The Physics of Elementary Particles, Oxford, Pergamon Press (1965) p. 388.
40. Op. Cit. # 3. p. 379.

41. Ibid. p. 373.
42. M. Jacob and G. C. Wick, Annals of Physics, 7, p. 404 (1959).
43. Ibid, p. 417.
44. Ibid, p. 427.
45. M. E. Rose, Elementary Theory of Angular Momentum, New York, John Wiley & Sons (1957) p. 225.

MICHIGAN STATE UNIVERSITY LIBRARIES



3 1293 03177 5533